A 3.15 GHz Digital Class E Load-Modulated Balanced Amplifier

Master Thesis

David Denekamp

Delft University of Technology

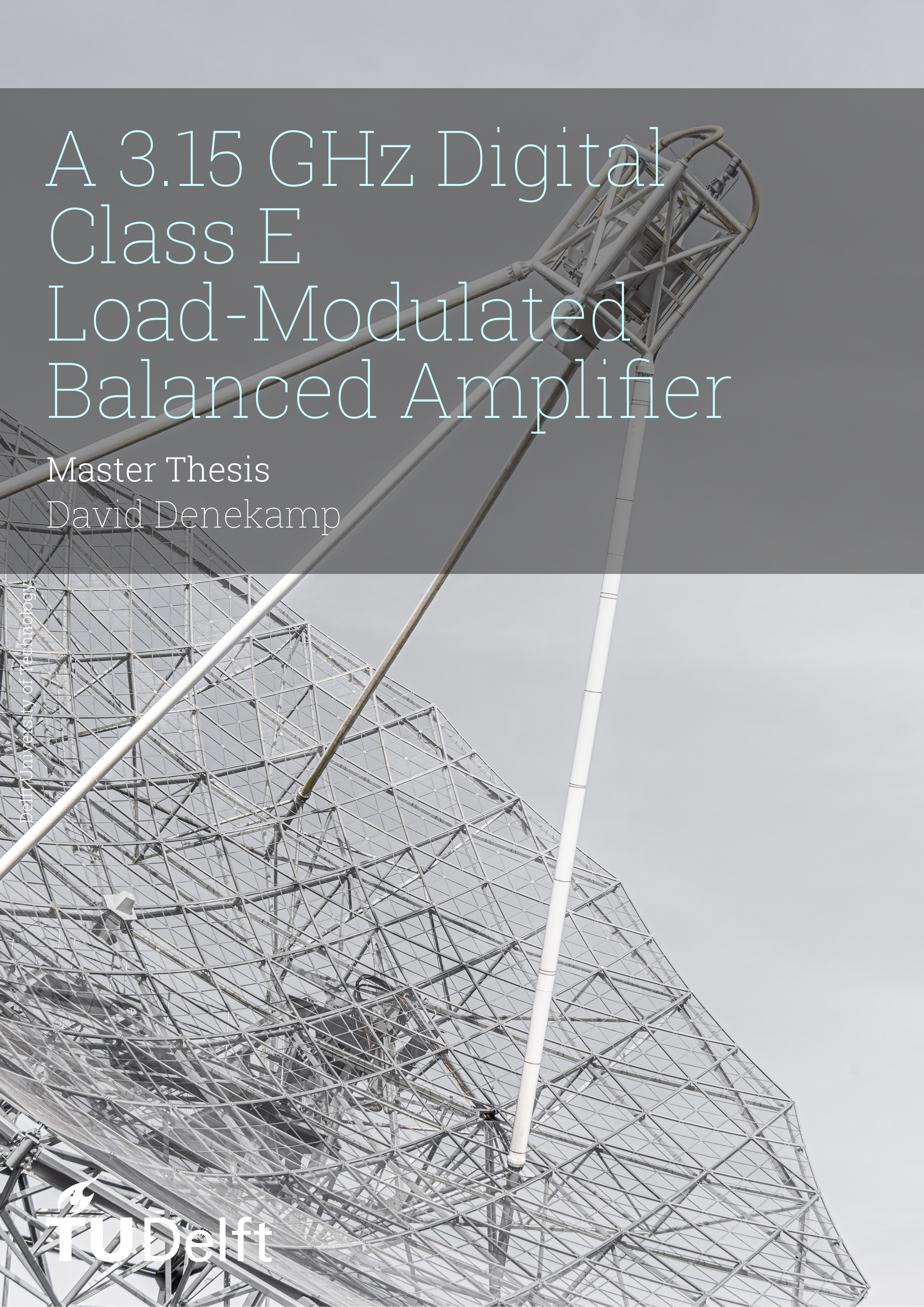

A 3.15 GHz Digital Class E Load-Modulated Balanced Amplifier

by

David Denekamp

in partial fulfilment of the requirements for the degree of

Master of Science
in Microelectronics

Department of Electrical Engineering,
Delft University of Technology,
July 2024

TU Delft supervisor:	dr. Morteza Alavi
TNO supervisor:	dr. Gijs van der Bent
Thesis committee:	dr. Marco Spirito dr. Maria Alonso-delPino

Student Number: 4900561

Photo: By Julian Steenbergen on Unsplash.
Style: TU Delft Report Style, with modifications by Daan Zwaneveld.

TU Delft

Acknowledgement

I would like to thank my supervisor at TU Delft, Morteza Alavi, for his endless advice and encouragement. His steering of the project helped to bring it to a successful end.

Thanks also to my supervisor at TNO, Gijs van der Bent, who always found time to help me. His always positive encouragement and his insights into technology were extremely valuable. He, together with the company TNO, made this thesis possible.

In addition, a thank you to Ph.D. student Anil Kumar Kumaran and postdoctoral researcher Mohammad Reza Beikmirza for their sometimes critical questions and insightful comments.

Finally, I would like to thank my family and friends for their encouragement and love.

David Denekamp
Delft, June 2024

Abstract

Radar technology requires high efficiency and wide bandwidth performance at high output powers. However, new developments like using Joint Communication and Radar Sensing (JCRS), pulse shaping, and amplitude tapering provides an additional requirement: amplitude modulation. To satisfy all of these requirements, a Load-Modulated Balanced Amplifier (LMBA) using a wideband Class E is designed for 2.9–3.4 GHz using GaN transistors. First, an accurate linear model for the transistor is presented. After this, a new state-space solution for a Class-E LMBA is derived. And lastly, a LMBA using a wideband Class E is presented. Using a lossless matching network, the GaN-based amplifier has an average drain efficiency of 81% over the full 10 dB power back-off. However, the final design has an average drain efficiency of 45% with a peak output power of 44 dBm.

Contents

1 Introduction

New developments in radar technology require higher efficiency and more flexible power amplifiers (PA). Most of the time single technologies, such as Gallium-Nitride (GaN) or Gallium-Arsenide (GaAs), were used. However, due to the development of computing technology, Complementary-Metal-Oxide- Semiconductor (CMOS) transistors are becoming applicable in the GHz range. Driving the PA directly by digital logic instead of using a digital-to-analog converter (DAC) is the final frontier, these PAs are called Digital Power Amplifiers (DPA).

Due to the miniaturisation of the CMOS transistor the f_T of the transistor goes up, and since the power consumption of CMOS is also scaled down with the size they can be used to design low power circuits at high frequencies. This make CMOS a highly efficient cost effective technology compared to other technologies. In S-band however, output powers of 100W or more at high efficiencies (80% or more) using CMOS have not been reported. Therefore for high power applications other technologies such as GaN are still necessary. Combining these two technologies have great promise but also severe difficulties to overcome. Such as the negative biasing required for GaN HEMT devices and the large dynamic driving range required.

In this master thesis, research is done the possibilities for the implementation of the DPA in radar applications in the range of 2.9–3.4 GHz. Radars require wide bandwidth signals and most of the time, use only constant output power, however, in this thesis I will look at efficiency enhancement techniques in the case of Amplitude modulation (AM). The goal was to design a digital Load-Modulated Balanced Amplifier(LMBA) in the GHz range using the technology that TNO had at their disposal. In the end a wideband LMBA Class-E matching network is designed.

2
Literature review

2.1. Power Amplifiers

Power Amplifiers (PAs) are essential in radars. They amplify a low-power signal into a high-power signal, which can be in the hundreds of watts. Any energy lost in amplifying the signal is converted into heat, which must be removed by active cooling systems, which consume energy by themselves and are expensive. Therefore, the PA in these applications must reach high efficiency. The radar also needs to fulfill spectral requirements so that it does not cause interference for others. This condition constrains the required linearity and noise of such a PA. A new requirement discussed in this thesis and rarely seen in pulse-Doppler radar applications is amplitude modulation. Amplitude control has multiple advantages, such as pulse shaping, amplitude tapering, and power control. This arrangement requires the PA to reach not just a constant output power but varying output power, and over this range, the efficiency should ideally stay constant. The linearity requirements are out of the scope of this thesis, and the main focus is on the efficiency and power back-off requirements. This section starts with some definitions and explains the basics of an amplifier. Most PA classes are discussed with a focus on the switch-mode classes D, E, and E/F. The focus is on comparing these different classes and their use cases, rather than necessarily designing one.

2.1.1. Basics of a Power Amplifier

We can categorize the PAs into various operational modes or classes. These classes are distinguished based on the voltage and current waves on and through the transistor. To analyze the voltage and current waveforms, we need to start with the basics of a transistor. In this thesis, FETs are only discussed, and BJT-like devices are out of scope. The most simplified version of a FET is a voltage-controlled current source (transconductance converter). As such, the voltage is applied between the gate and source of Figure 2.1, and the current is flowing from the drain to the source. The relation of this voltage to current dependency is highly non-linear but can be approximated by two lines, as shown in Figure 2.1. When the gate voltage is below the threshold voltage, the transistor is turned off, and the drain current is zero. When the gate voltage is higher than the threshold voltage, the transistor is turned on, and the drain current is approximated as a linear dependence on the applied gate voltage, functioning as a current source.

However, for a transistor to function as a voltage-controlled current source, the drain must be adequately biased by being connected to a voltage source and using some resistance or inductance. By utilizing a resistor for biasing, we can find a relationship between the drain-to-source current and drain-to-source voltage. When the drain current is large, the voltage drop over this biasing resistor is large, and therefore, the drain-to-source voltage is small. When the drain current is small, the voltage drop over the biasing resistor is small, and therefore, the drain-to-source voltage over the transistor is large. The value of this resistance together with the gain of the transistor, therefore, determines the voltage-in to voltage-out relationship; the optimal value depends on many variables but determines this ratio, which is called voltage gain. Although simplifying a voltage-controlled current source is often valid, it is not always the case. In [31], Earl McCune explains that a transistor can be better described as a 3-port device where the third input is the supply voltage. Depending on the drain voltage, the transistor can behave as a switchable resistor instead of a voltage-controlled current source. Suppose the FET is operating in its saturation region. In that case, it can be analyzed like a voltage-controlled current source, but if the FET is operating in the resistive region, it can be analyzed like a resistor switching between a high state and a low state.

In the more conventional analysis of an amplifier, we describe a different region where different I_D-V_{DS} curves are expected depending on the operation regime, where the dependency is on the gate-to-drain voltage and the threshold voltage of the transistor (V_t). The behavior is as follows:

$$\begin{cases} \text{Triode-region: Resistor} & \text{for } V_{DS} > V_{knee} \quad (V_{knee} = V_{GS} - V_t \texttt{ for MOSFET}) \\ \text{Linear-region: Voltage-controlled current source} & \text{for } V_{DS} < V_{knee} \end{cases} \tag{2.1}$$

Although this analysis is perfectly correct and very useful, we need to elaborate further on when to use the large-signal or small-signal models. In other words, whether the power device operates in the full range of the drain-to-source voltage or just a small range.

In the following sections, the thesis will continue discussing this voltage-current relationship and compare the different types of classes; however, to compare and discuss them, we need to start with a few definitions that are important to continue.

The drain efficiency is defined as the ratio of the output power to the DC power provided. This metric does not consider the input power but can provide insight into the amplifier's efficiency.

$$\eta_d = \frac{P_{OUT}}{P_{DC}} = \frac{P_{load}}{P_{load} + P_{switch}} \tag{2.2}$$

Where P_{load} is the power delivered to the load impedance and P_{switch} is the power dissipated in the transistor.

For example, if the drain efficiency is high but the transistor is large, a large signal needs to drive the input capacitor, lowering the overall efficiency. Therefore, Power Added Efficiency (PAE) is another essential type of efficiency. Thus, it is defined as follows:

$$PAE = \frac{P_{OUT} - P_{IN}}{P_{DC}} \tag{2.3}$$

The PAE is also more insightful than the drain efficiency due to the input power consideration.

Another efficiency that is often used is total efficiency, which is defined as follows:

$$\eta_{total} = \frac{P_{OUT}}{P_{DC} + P_{in}} \tag{2.4}$$

In this case, the input power is added to the DC power, and both are dissipated power. In literature, all definitions are used, but only sometimes are they all used in the same paper, which can be problematic when comparing results.

2.1.2. Current-mode classes A, AB, B and C

The current-mode class operates the transistor as a current source; this means that the gate-to-drain voltage will never be greater than the saturation voltage. In this case, the FET will not enter the triode region and will stay in the saturation region. The wave's shape depends on the applied gate voltage; this is usually a sine wave with a second harmonic or a square wave in the case of the digital domain. The change of the duty cycle for a DTX resembles changing the conduction angle in the analog case.

In this section, we will briefly discuss classes A, AB, and C. However, a more elaborate discussion can be found in [15] to keep the report's focus the same.

In the analog case, a voltage sine wave is applied at the gate; when looking at the V_{GS}-I_D curve, we can see that depending on the bias point, the size and shape of the drain-to-source current change. When the shape changes from an ideal sine-wave to a half sine-wave higher, even harmonics start to appear at the drain, and the dc voltage at the output changes. The circuit used is shown in Figure 2.1, where the conduction angle in the time domain and the biasing point in the voltage domain are illustrated. The conduction angle ϕ is in the figure at 90 degrees; however, it changes depending on the biasing point. The conduction angle ϕ indicates the proportion of RF-cycle that the transistor conducts and is in the figure at 90 degrees; however, it changes depending on the biasing point. The definition of conduction is different depending on the author. For now, I am going to use a conduction angle of $0 - \pi$, where 0 is no conduction and π is full conduction, and that is therefore what I am going to use to continue. The transistor is connected to a parallel RLC circuit, which resonates at the operation frequency and shorts higher harmonics; a DC feed is used to supply bias current. The AC-coupling capacitor is used to make sure that no DC current flows into the load resistor.

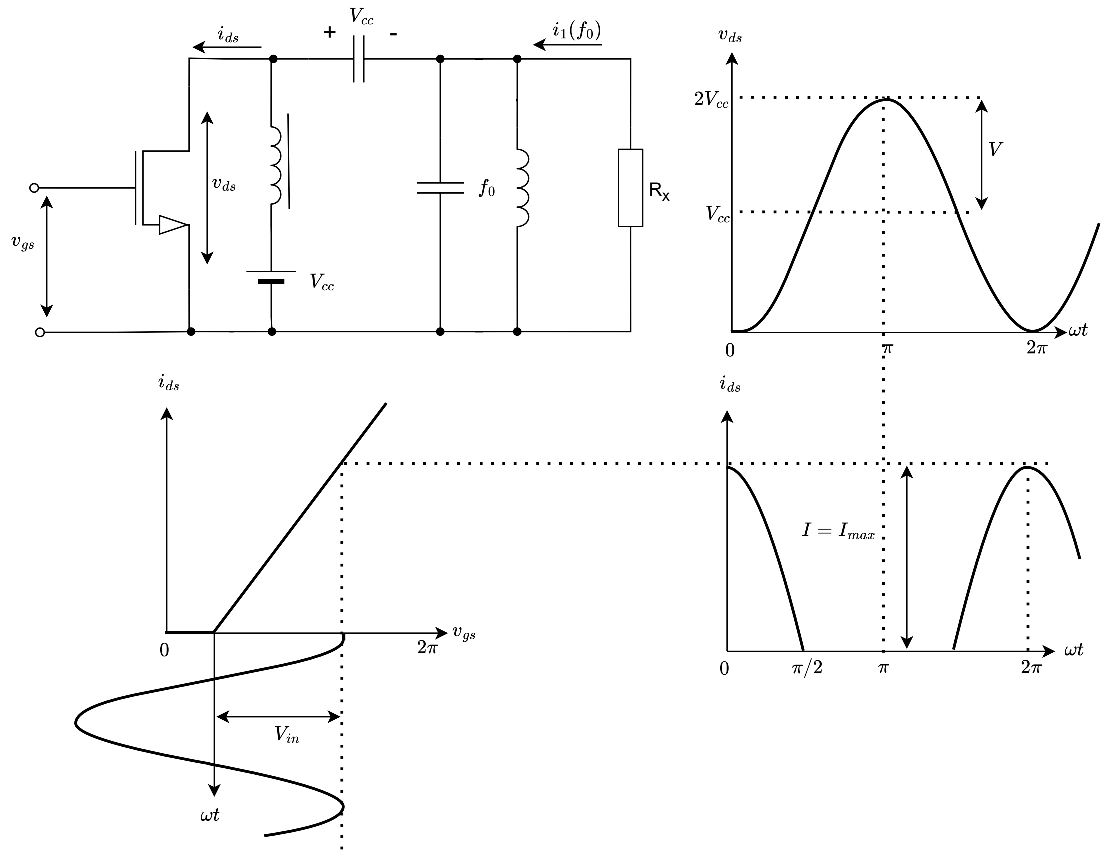

Figure 2.1: A Class-B configuration using an ideal transistor is described in [22]. At the top left, the circuit can be seen where the transistor is biased with a DC feed, and the higher harmonics are removed using a parallel LC filter. At the bottom, the I_ds–V_ds curve can be seen with the applied voltage sine at the gate. At the bottom right, the resulting drain current shape versus conduction angle can be seen, which is a half sine wave for ideal Class-B operation. At the top right, the drain-source voltage can be seen, which is a full sine wave with an amplitude of V_{cc}.

This thesis report does not contain the complete derivation of the efficiencies and output power because one can look it up in [15]. But what is important are the efficiency and output power as a function of changing the conduction angle for both the analog and digital cases. In the analog case, the biasing point changes, and in the digital companion, the duty cycle changes. In Figure 2.2, one can see that both the digital and analog variants could have a drain efficiency of 100%; however,

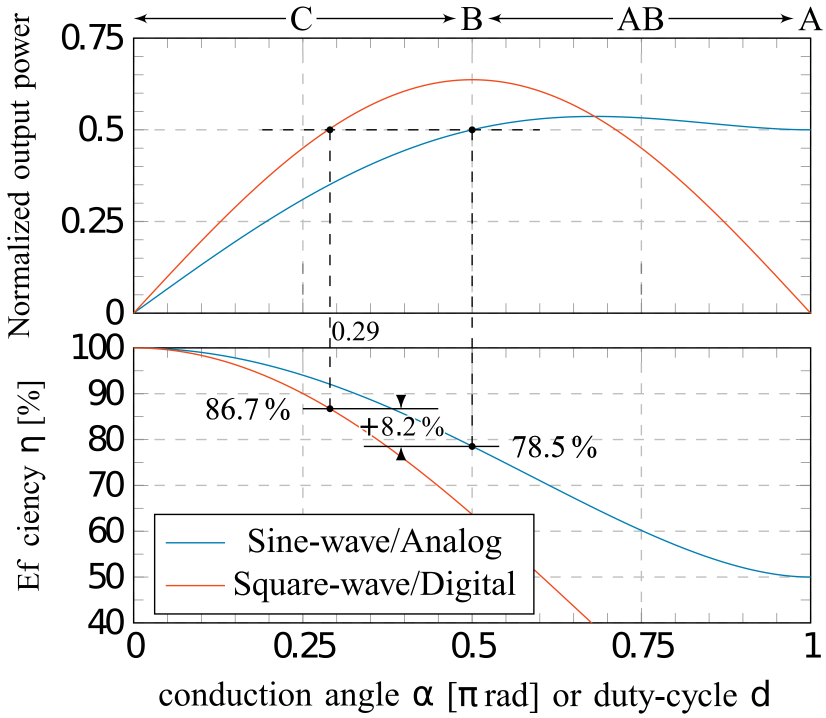

Figure 2.2: Ideal analog and digital AB/C behaviour, output power and drain efficiency versus conduction angle/duty-cycle from [34].

this is in the case of zero output power and is called a class-C PA. The reason for this is that using a low-duty cycle will make the current a pulse, just like in the analog case. This aspect means that the DC voltage becomes lower and, therefore, less voltage and current overlap, increasing the efficiency. However, this will come at the cost of reduced output power because of a shorter current pulse. In the case of a 50% duty cycle, the maximum output power is similar to that of a Class-B PA. This characteristic is because the fundamental frequency output power has not yet decreased, but the DC output power has decreased. Note that this comes at the cost of more non-linearity. Increasing the conduction angle even more will result in a Class-A PA in the case of a sine wave, but in the case of a digital PA, this is no longer the case; this is where the duty cycle resemblance to the conduction angle stops.

On can conclude that for the same output power, the drain efficiency is increased by 8.2% in case of the DTX compared to the analog case. Even though this is a decent improvement, the efficiency of 86.7% is still not better compared to a well designed Class F PA. Moreover, it is probably not worth the effort of creating such a square wave input. However, one may ask why one would use such a current-mode DTX. Instead of resistive-mode Class E/Class F the reasons are as follows:

- At higher frequencies, the transistor may not be able to reach the triode region after being turned off. Therefore, it is automatically a current-mode transistor in the saturation region.
- Current-mode transistors have a linear relationship between the number of fingers turned on and the output power. Compared to switching it to a triode and using Class E, Which needs unequal sizing to correct for this non-linearity.
- Triode operating region Class E may need to use over-dimensioning to provide a sufficiently low on-resistance to reach high efficiencies. Otherwise, the on-resistance losses could result in an even lower drain efficiency compared to current-mode devices. Over-dimensioning results in a lower power density and PAE.

2.1.3. Class D and D^{-1} PA

Class D and D^{-1} PAs use the transistor in its true switching modes, using another transistor to short its even-order harmonics. Or, explained differently, it provides the continuity of the sine wave flowing through the load. In Figure 2.3, one can see the square wave voltage and the half-sine current flowing through the load, where v_{sat} is the result of the non-finite on resistance. The series resonator L_0C_0 is ideally a pass for the fundamental frequency and infinite impedance at every other frequency. The second transistor represents a short at even-harmonics.

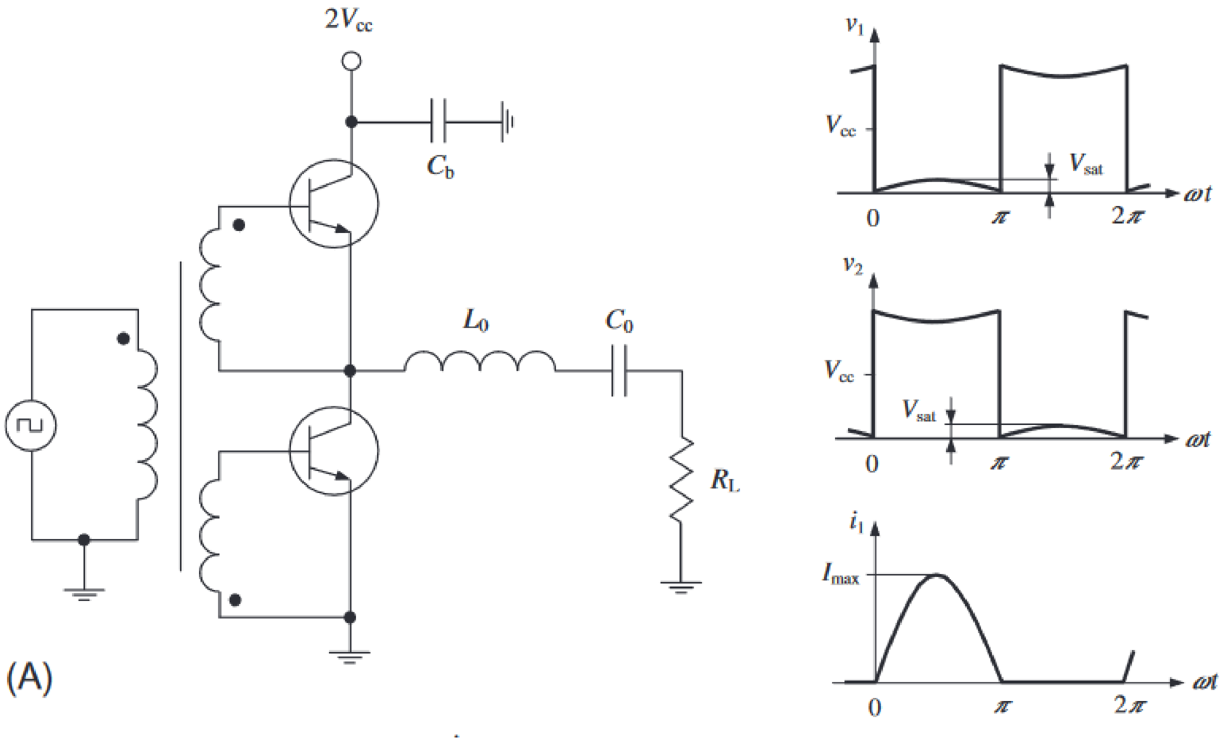

Figure 2.3: A classical Class D architecture using BJTs from [22].

The Class D PA has, therefore, a square voltage at the drain and a half-sine current wave flowing through the drain; therefore, it is called a voltage-switching Class D PA. A Class D^{-1} PA has a square current wave flowing through the drain and a half-sine voltage wave at the drain; therefore, it is also called a current switching Class D PA. One could design a final stage in Class D/D^{-1}; however, severe limitations exist. The main reasons are as follows: The final stage uses GaN HEMT devices; in this technology, there is no complementary device available, which results in the need for a differential load or a balun. However, the balun is hard to implement for higher frequencies, especially when high-order harmonics need to be accounted for. Another issue is the drain-to-source capacitance, which will limit the drain efficiency. But further research could provide more insight into this issue. Another solution is using a differential load, which is not always applicable in radar applications. Another problem with Class D is the large output capacitance present at high-power transistors; this severely limits the performance possible at higher frequencies. However, with a differential RLC tank, some of this output capacitance can be adsorbed, and decent efficiencies are possible [42]. In this paper, a PAE of 62% was reached at 2.6 GHz using Class D^{-1} with a differential RLC tank.

2.1.4. Class F and F^{-1} PA

The Class F was first invented in 1920 when they found that for different waveforms, anode efficiencies could be improved [23]. Class F is defined as a square wave voltage and a half-sine wave current, as shown in Figure 2.4a. The figure shows two lines depending on how many harmonics are controlled; in the ideal case, all harmonics are controlled, and one can create a square wave voltage and a half-sine wave current both out-of-phase. This feature results in a theoretical efficiency of 100%. We can also mathematically describe the waveforms as follows:

$$
\begin{aligned}
i(\theta) &= \frac{1}{\pi} + \frac{1}{2}\sin(\theta) - \frac{2}{\pi}\sum_{k=1}^{\infty}\frac{\cos(2k\theta)}{4k^2-1} \\
v(\theta) &= \frac{1}{2} + \frac{2}{\pi}\sum_{k=1}^{\infty}\frac{\sin((2k-1)\theta+\pi)}{2k-1}
\end{aligned}
\tag{2.5}
$$

From these equations, we can derive that the current needs shorts at even harmonics and the voltage needs an open circuit at odd harmonics. These conditions can be realized using components like resonators or transmission lines. The inverse Class F, also called current-mode Class F, is also shown in Figure 2.4.

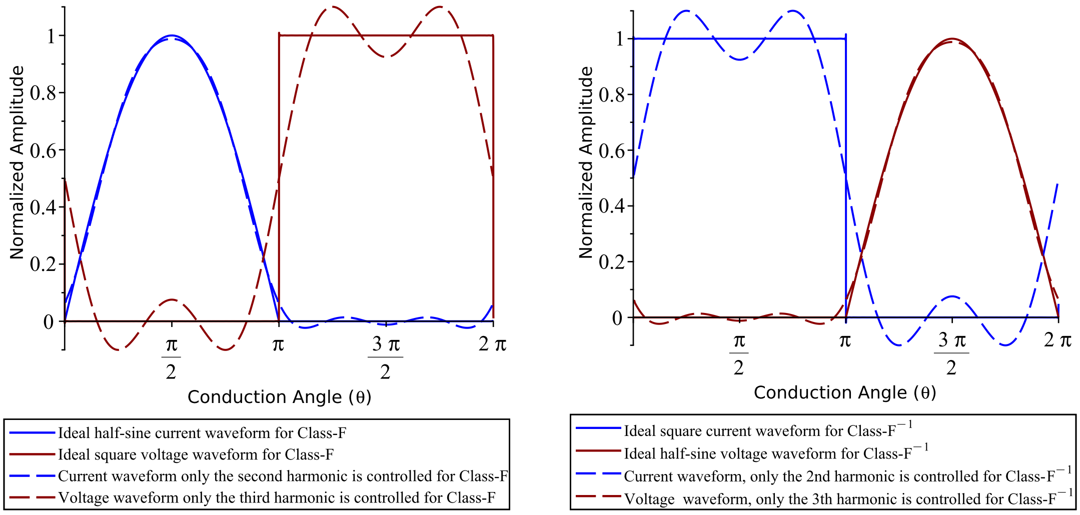

(a) (b)

Figure 2.4: (a) Comparison of ideal Class F waveforms and the case of limited controlled harmonics. (b)Comparison of ideal Class F waveforms and the case of limited controlled harmonics.

The voltage and current waveforms are inverted; therefore, the mathematical equations are also inverted as follows:

$$
\begin{aligned}
i(\theta) &= \frac{1}{2} + \frac{2}{\pi}\sum_{k=1}^{\infty}\frac{\sin((2k-1)\theta)}{2k-1} \\
v(\theta) &= \frac{1}{\pi} + \frac{1}{2}\sin(\theta+\pi) - \frac{2}{\pi}\sum_{k=1}^{\infty}\frac{\cos(2k\theta)}{4k^2-1}
\end{aligned}
\tag{2.6}
$$

To realize such waveforms at the drain of the active device, we need to have shorts at odd-harmonics and an open circuit at even-harmonics. This solution can also be realized using components like resonators or transmission lines.
Due to the compactness of the report, I will not go into detail on how to design such circuits, but for now, it seems that many different configurations are possible to realize such a PA. In practical implementations, it is not possible to reach the 100% efficiency promised by Class F; the reason is that a limited number of harmonics can practically be controlled due to the size of the output capacitance, which will dominate at higher harmonics. In practice, control up to and including the third harmonic is implemented most of the time. This fact limits the theoretical drain efficiency of Class F

to around 88% [26]; however, this is still better compared to the maximum 78.8% drain-efficiency of Class B. Another benefit is the square-wave voltage, which increases the peak amplitude by a factor of $4/\pi$ resulting in improved output power compared to class AB. A Class F needs relatively many components, which will complicate the wideband performance of such a PA and increase the losses in the matching network.

2.1.5. Class E PA

Instead of trying to control all the higher harmonics separately, we can also use the drain-to-source capacitance to find the ideal termination at all the higher harmonics. This configuration is called Class E and has been invented multiple times since 1966 [22][15]. The circuit of a single-ended Class E PA can be found in Figure 2.5. It consists of a transistor with a square wave applied to its gate. The amplifier configuration is a single-ended common-source amplifier with a reactive load. A series RLC filter at the load take care of all frequencies but the fundamental frequencies, just like before.

A parallel capacitor is used to ensure a continuous current wave through the load. The drain is connected to the supply with either an RFC, which functions as a DC-Feed, an inductor, or a $\lambda/4$ transmission line. The choice for an inductor instead of a $\lambda/4$ transmission line or RFC is due to the expected size in the S-band and improved performance. When a finite inductor is used, more sub-modes for Class E are possible, which makes it possible to design a Class E PA at 3.15 GHz.

I will now discuss the theory using the work from M. Acar [2]. Multiple Class E configurations are possible; however, we use this topology in this thesis. More variants can be seen in [22]. The final design will be discussed in a later chapter.

2.1.5.1. The Theory of Class E

To solve the Class E SMPA, first, the definitions are stated, and the definition for efficiency is given. Design equations are used to find the optimal solutions using time analysis.

2.1.5.2. Definitions and basic explanation

The circuit used is given in Figure 2.5. The transistor shown is analyzed as a switched resistor. The capacitor C_ds can be either the output capacitance of the transistor or an added capacitor. Component X can be either a capacitor or an inductor, depending on the solution. The inductor L can be either a DC feed or a finite inductance. The resonator circuits L_0 and C_0 resonate at the fundamental frequency. Load impedance R_x can vary between 1 and 1000Ω depending on the solution and needs to be matched in the end to 50 Ω, but that will not be part of the discussion here.

To simplify the discussion, we assume R_{on} is far smaller than R_{out}. In practice, this is only sometimes the case. For the basic explanation, the DC-Feed inductor is ideal, which means it has an infinite inductance; therefore, it is short for DC and an open connection for AC signals. This aspect also means that the current from the DC power source is constant and, therefore, independent of time. Note, however, that in the next section, the inductor is no longer infinite; however, assuming an infinite inductor simplifies the explanation here. Also, zero-voltage slope switching and non-zero-voltage slope switching are possible. The primary explanation below is the most simple variant of the Class E circuit and discusses zero voltage slope switching; in the time analysis further on, it will also discuss non-zero voltage slope switching and non-zero on-resistance.

Defining symbols:

- The DC current from the DC power supply is called I_{DC} and its voltage V_{DD}.
- The current through the elements C, C_0, L_f and R_x are in the same order called $i_C(t)$, $i_x(t)$, $i_L(t)$ and $i_x(t)$.
- The current through the switch is called i_{switch}.

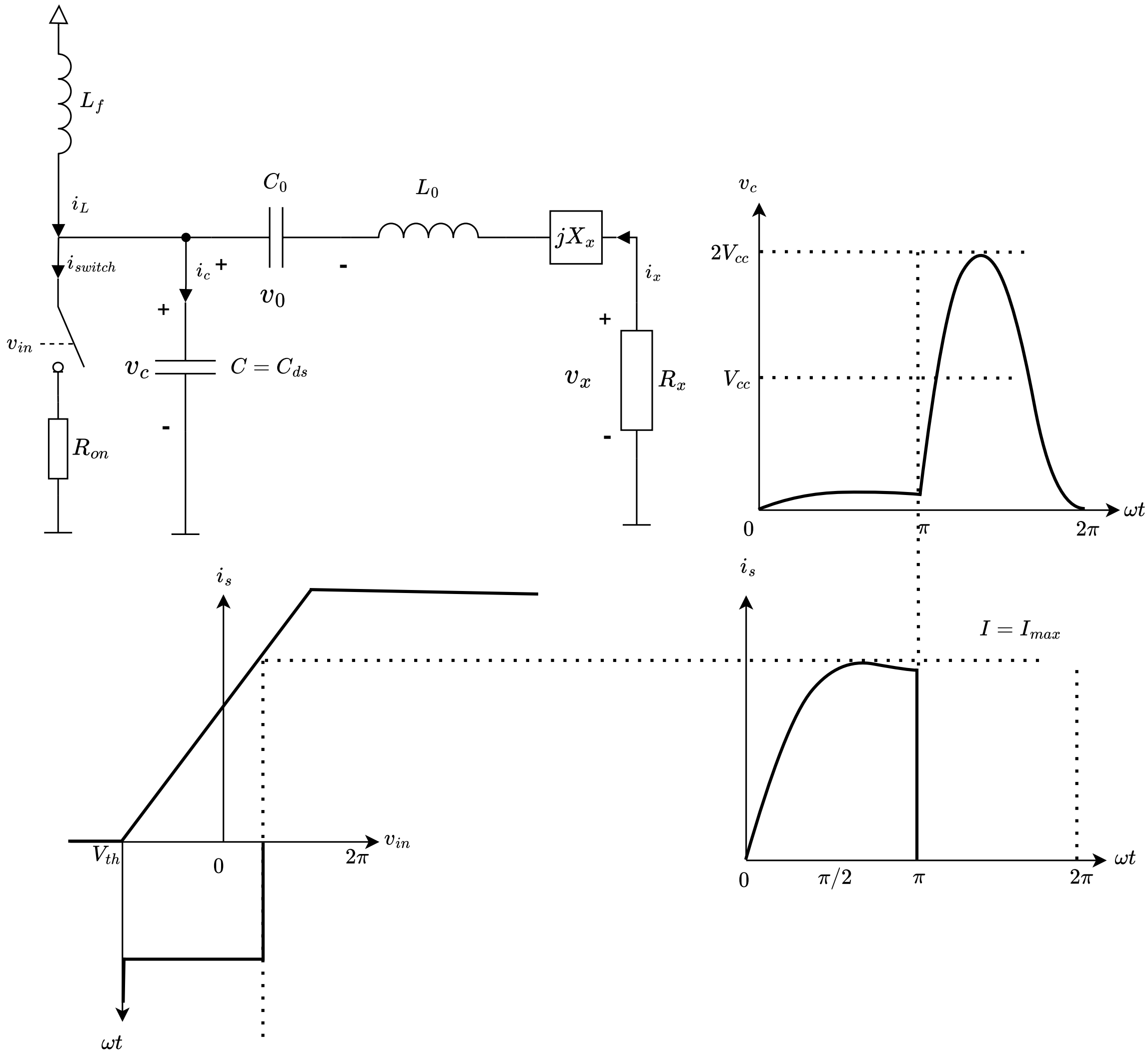

Figure 2.5: The Class E circuit has a transistor modeled as a switched resistor. On the right, the capacitance voltage versus phase is plotted. At the bottom right, the switch current versus phase is plotted. And at the bottom left, the switch current versus input voltage is plotted.

- The voltage over the capacitance C_{ds} and the drain is called $V_C(t)$.
- The voltage over the load R_x is called $v_x(t)$.
- The total period (T_{period}) is $1/f_0$ where f_0 is the operating frequency.

2.1.5.3. Explaining the on-off regions:

To explain the Class E power amplifier, the analysis is split into two parts: the time the switch is on and the time the switch is off; the moment of switching is called t_{switch}.

- For $t < t_{switch}$ (switch is open), if the switch is open all the current I_{DC} is split between the load resistance (R_x) and the parallel capacitance(C), therefore, $I_{DC} = i_{load}(t) + i_C(t)$. The switch is in an open connection, therefore $i_{switch}(t) = 0$ A and the voltage over the switch(V_{DS}) is time-dependent and it is a sine wave it increases in the start because there is a charge build-up in C and decreases due to the inductance L_0. If the voltage is zero and the slope is zero(ZVZVSS) the switch is closed.
- For $t > t_{switch}$ and $t < T_{period}$ (switch is closed), the switch acts as a current sink in the

ideal case($R_{on} = 0$) or almost a short in the non ideal case, which means that $i_{switch}(t) = I_{DC} + i_x(t) + i_C(t)$. $i_{switch}(t)$ first is zero and also behaves as a sine wave where it first rises due to the LC oscillation where after it lowers.

Defining the efficiency:
The combinations makes a sine wave on the load. The drain efficiency of an amplifier is defined as the output power divided by the DC power consumption. The power can only be consumed by R_{out} and R_{on}. We also know that, power can only be consumed by a real impedance, therefore, the power consumption can be defined as:

$$P_{DC} = I_x^2 R_x/2 + P_{switch} \tag{2.7}$$

Where P_{switch} can be defined as:

$$P_{switch} = \frac{1}{R_{on}T_{period}} \int_{t_{switch}}^{T_{period}} v_C^2(t)\,dt \tag{2.8}$$

Note that if R_{on} is zero, V_C would also be zero, which in turn makes P_{switch} zero. The drain efficiency can therefore be expressed in Equation 2.2, which is 100% in the case of an ideal switch and zero voltage switching (ZVS). There are Class E amplifiers that use either non-zero voltage[19] or non-zero voltage slope switching[3]. The non-zero voltage slope switching will be discussed in the next section. The non-zero voltage switching will not be explained here due to the lower drain efficiency of this solution, which could result in lower peak drain voltages[3]. A more general solution is given in a later section.

2.1.5.4. The time analysis

In this subsection the time analysis is done for the circuit. The analysis from Mustafa Acar [3] [2] [4] are used for this subsection. First, the current and voltage waveforms will be defined in terms of designer parameters, after which the final component parameters are calculated in terms of these designer parameters. At the end, the constraints on the design are shown.

Circuit analysis:
This analysis aims to solve the circuit with three designer parameters analytically. The parameters or the *tuning nobs* are shown in Table 2.1, and are as follows: the parameter d where the duty-cycle $= d{\cdot}50\%$. The parameter q, which decides the Class E subclass or modulation angle, will be more about this parameter later—the parameter k, which is related to the slope at the zero voltage switching moment. Initially, only zero-volt and zero-slope switching was done, but better results could be reached when there is a non-zero voltage slope at the moment of switching.

Parameter	Definition	Function
d	$d \cdot 50\%$, duty-cycle	change the output power
q	$1/(2\pi C L_f)$, resonant frequency	change the required load and current profiles
k	$C\omega k$, voltage-slope at switching	change the output power and peak drain current

Table 2.1: Three parameters used to design a basic Class E amplifier.

Note that the current $I_R(t)$ should be sinusoidal. This condition is, however, only the case with a resonator with an infinite Q-factor. In this analysis, an ideal resonator is assumed; in this case, we can state the following:

$$i_x(t) = I_x \sin(\omega t + \varphi) \tag{2.9}$$

Where φ is the conduction angle, ω is the operating frequency, and I_R is the peak amplitude of the load resistance. Now we will analyze the circuit for two different time intervals when the switch is open and closed, and then we will combine this with the boundary conditions to achieve a final solution.

- In the time interval 0 < t < $d \cdot \pi/\omega$,* the switch is closed, and the current in the switch is the combination of the current through the inductor $I_L(t)$ and the current from the resistor $I_R(t)$. The current through the output capacitor $I_C(t)$ is zero because the voltage over the active device and its output capacitance are zero.

$$\begin{aligned} i_{switch}(t) &= i_L(t) + i_x(t) \\ &= \frac{V_{DD}}{L_f}t - i_{L_f}(0) + I_x \sin(\omega t + \varphi) \\ i_{L_f}(0) &= C\omega V_{DD}k - I_x \sin(\varphi) \end{aligned} \tag{2.10}$$

The current through the inductor at time $t = 0$ is $I_x \sin(\varphi)$ in the case of a zero voltage slope, and for a non-zero voltage slope, a constant is added: $C \cdot \omega \cdot V_{DD} \cdot k$, which is related to the formula $i_C(t) = C \cdot dV_C/dt$, therefore related to the amount of charge stored on the capacitor.

Here, we need to define the two parameters, q and p. The parameter q was explained and is related to the resonating frequency of the components L and C in the way that $q = 1/(\omega\sqrt{LC})$. The parameter p is used as a temporary variable for solving the circuit and is defined as $p = \omega L I_x / V_{DD}$. Equation 2.10 will be rewritten in terms of the design parameters k and q and the temporary parameters φ and p.

$$i_{switch}(t) = \omega \cdot q^2 \cdot V_{DD} \cdot \left(\frac{k}{q^2} + p\sin(\omega t + \varphi) - p\sin(\varphi) + \omega \cdot t\right) \tag{2.11}$$

- In the time interval $d \cdot \pi/\omega$ < t < $2 \cdot \pi/\omega$, the switch is opened, and the following differential equation can be set up:

$$LC\frac{d^2 v_C(t)}{dt^2} + v_C(t) - V_{DD} - \omega L i_x \cos(\omega t + \varphi) = 0 \tag{2.12}$$

Where the solution to this differential equation is as follows:

$$v_C(t) = C_1 \cos(q\omega t) + C_2 \sin(q\omega t) + V_{DD} - \frac{q^2}{1 - q^2} p V_{DD} \cos(\omega t + \varphi) \tag{2.13}$$

With the yet-unknown constants called C_1 and C_2. These two constants will be calculated with the use of two boundary conditions.

When analyzing the circuit, we know that the voltage over the capacitance starts at zero and that the current at the switching time passes through from the switch to the parallel capacitance. This operation ensures that a continuous current flows through the load despite the discontinuous behavior of switching. These two conditions can, therefore, be summarized as follows:

$$\begin{aligned} &v_C(d \cdot \pi/\omega) = 0 \\ &\left.\frac{dv_C(t)}{dt}\right|_{t = d\cdot\pi/\omega} = i_{switch}(d \cdot \pi/\omega) \end{aligned} \tag{2.14}$$

With the boundary Equations 2.14 and Equations 2.10 and 2.13, C_1 and C_2 can be solved, resulting in a rather long equation that will not be stated further here. However, this voltage equation is still dependent on the unknowns p, φ. These unknowns can then be solved using the definition of zero voltage (ZVS) and non-zero voltage slope switching (ZVSS). The mathematical definition is therefore as follows:

$$\begin{aligned} &v_C(2\pi/\omega) = 0 \\ &\left.\frac{dv_C(t)}{dt}\right|_{t = 2\pi/\omega} = \omega V_{DD} k \end{aligned} \tag{2.15}$$

*Where d is the duty cycle times a half ($d \cdot 50\%$)

Using the two boundary conditions 2.15, we can set up 2 equations to solve the two unknowns p, φ, making both the voltage and current waveforms a function of d, q, k, V_{DD} and ω. The following

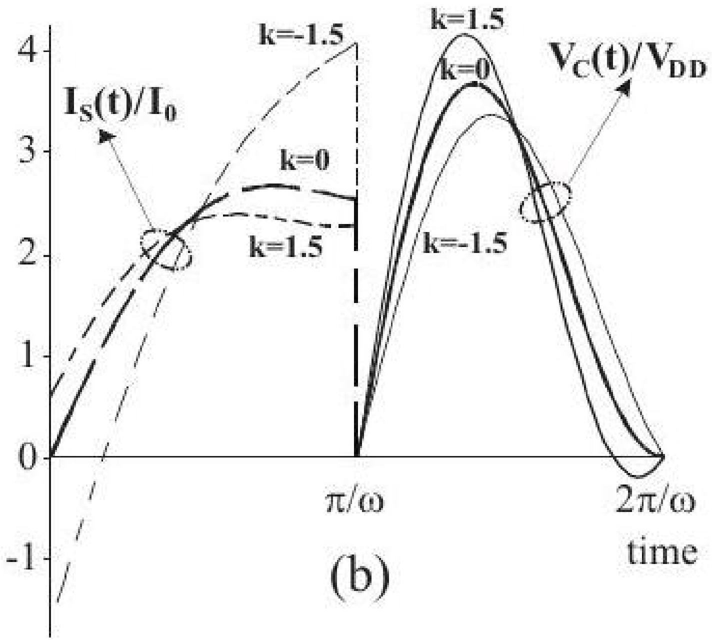

Figure 2.6: Both the current and voltage waveforms of a Class E SMPA for different values of k from [3].

design set will be stated here and not further explained; more explanation can be found in [2]. These equations relate the different component values to the voltage waveforms, and therefore they are called the solution set.

$$
\begin{aligned}
K_L &= \frac{\omega L}{R} \\
K_C &= \omega C R \\
K_P &= \frac{P_{OUT} R}{V_{DD}^2} \\
K_X &= \frac{X}{R}
\end{aligned}
\tag{2.16}
$$

Where design set $K = \{K_L, K_C, K_P, K_X\}$ presents solutions using the following equations:

$$
K_L(q,k) = \frac{p(q,k)}{\frac{\pi}{2p(q,k)} + \frac{2\cos(\varphi(q,k))}{\pi} - \sin(\varphi(q,k)) + \frac{k\pi}{q^2 p}} \tag{2.17}
$$

$$
K_C(q,k) = \frac{1}{q^2 K_L(q,k)} \tag{2.18}
$$

$$
K_P(q,k) = \frac{1}{2}\frac{p(q,k)^2}{K_L(q,k)^2} \tag{2.19}
$$

$$
\begin{aligned}
V_R &= \frac{1}{\pi}\int_0^{2\pi/\omega} (v_C(t)\sin(\omega t + \varphi))\, dt \\
V_X &= \frac{1}{\pi}\int_0^{2\pi/\omega} (v_C(t)\cos(\omega t + \varphi))\, dt \\
K_X(q,k) &= \frac{V_X}{V_R}
\end{aligned}
\tag{2.20}
$$

Next one can chose a required q and k, how to chose them is explained later. Using the four equations, and given V_{DD}, ω, and C (this can be seen as a given for now and is the output capacitance of the transistor), the component values L, X, R, and the output power P_{out} can be calculated.

The function of the resonator L_0 C_0 is to pass the fundamental frequency; therefore, $\omega = 1/(\sqrt{L_0 C_0})$. Choosing the loaded quality factor $Q_L = \omega L_0/R$ results in two equations with two variables, which is solvable.

The only constraints are the maximum drain current and the maximum drain voltage (the breakdown voltage). In this technology, the maximum drain voltage is >100V and, therefore, is not essential. In the case where it is important, one can look at non-zero voltage switching, reducing the supply current, and using Class E/F$_x$. But, the maximum drain current is important. This condition is for the Class E circuit $\max(i_{switch}(t))$ using Equation 2.10 and can be approximated for high enough q values as $i_{switch}(d \cdot \pi/\omega)$. One should check the maximum drain current at the end; when it is too high, the parameter k should be lowered. Values for k lie primarily between 2 and -2.

The assumption to be made up until now is that R_{on} (the saturation resistance) is zero. Although this is true for an ideal switch, it is not true in practice, especially when one tries to modulate the output power by changing R_{on}, as in[6]. Therefore, one variable called m is added, which is defined as $m = \omega C R_{on}$, and this is further analyzed in [2]. At peak power, the R_{on} is sufficiently low (around 6Ω) to be circumvented from the solution and still reach very high efficiencies.

2.1.6. Class E/F$_x$ PA

An additional variation of the Class E is the Class E/F$_x$ amplifier. This amplifier combines the high-efficiency ZVS and ZVSS waveforms with different tunings of the higher harmonics. The idea behind this is that the shape of the current wave can be improved so that the RMS current is lower and therefore the drain efficiency increases [25]. According to [43], an added benefit is the improved efficiency with load variation compared to the quasi-load-Independent Class E (q=1.3). To analyze such a circuit, we need to change our topology in a more generalized case; the more generalized Class E circuit can be found in Figure 2.7. It is a combination of both the Class E and Class F^{-1}, where in the classical Class E configuration, only one series resonator for the fundamental frequency is present, and in the classical Class F^{-1}, ideally an infinite number of harmonics exist, and also the output capacitance C_{ds} is neglected. The ZVS and ZVSS Class E configurations have, for a known C_{ds} (the drain-to-source capacitance of the transistor at high frequencies), only one optimal load and, therefore, one type of waveform. For a Class E with finite DC feed inductance, more configurations are possible. As stated previously, the idea behind the parameter q is to add another frequency to change the shape of the waveform. This condition can also be achieved by adding multiple resonators to the load, which is what Class E/F is about.

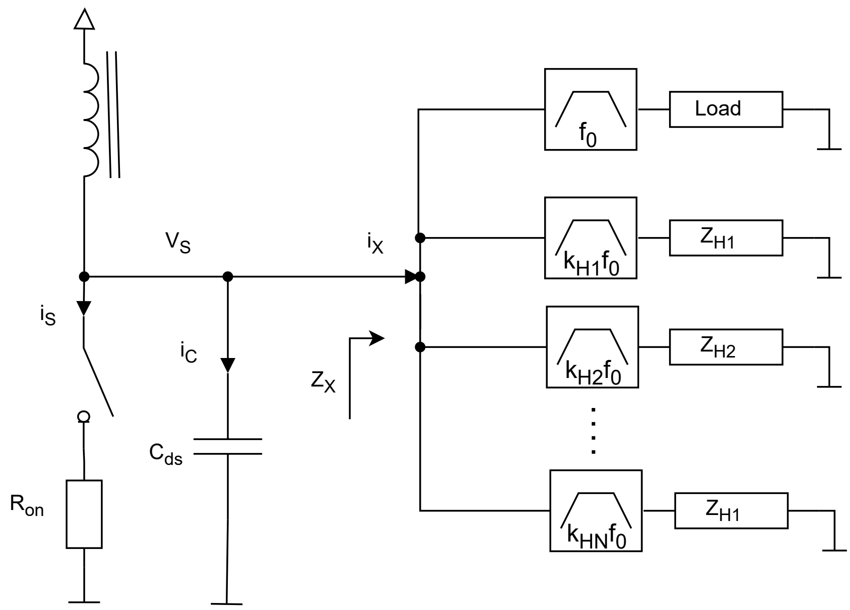

Figure 2.7: The general Class E/F configuration using an ideal switch and DC-Feed by [25]. When the band-pass filters are resonators at frequency $k_{Hx} \cdot f_0$, current i_x is a decomposition of the multiples of f_0. Where i_C is the current through the capacitance and v_S is the voltage over both the switch and the capacitance. In he original analysis R_{on} was assumed to be zero.

To solve such a circuit, we can analyze it in the time domain, as was done previously with Class E analysis, instead of analyzing it in the frequency domain. In this regard, we will not state the derivation here but only present the results; the derivation can be found in [26]. But before the results are presented, the question remains: how would one design such a circuit? To explain that, one should look at Figure 2.8. The first two rows are the harmonic terminations of both Class E and Class F^{-1}, respectively. In Class E, the fundamental frequency is loaded with the parallel capacitance in parallel with a complex load, and all higher harmonics are terminated with the parallel capacitance. Class F^{-1} is terminated at higher harmonics, and an alternating open or closed termination is presented. The combination of both is called Class E/F, where at some harmonics, a Class F^{-1} termination is seen by the drain, and at other harmonics, a Class E termination. Although many solutions are possible, Figure 2.9 shows some possible waveforms for different terminations.

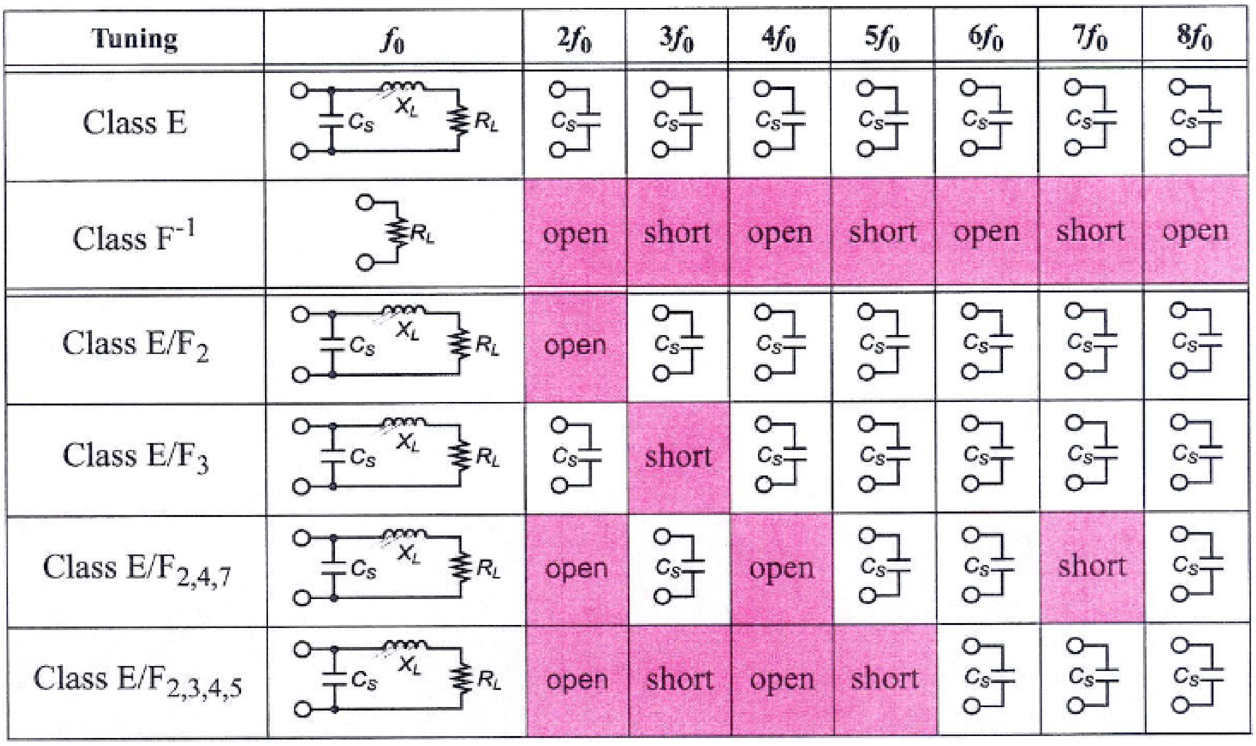

Tuning	f_0	$2f_0$	$3f_0$	$4f_0$	$5f_0$	$6f_0$	$7f_0$	$8f_0$
Class E	C_S, X_L, R_L	C_S	C_S	C_S	C_S	C_S	C_S	C_S
Class F^{-1}	R_L	open	short	open	short	open	short	open
Class E/F_2	C_S, X_L, R_L	open	C_S	C_S	C_S	C_S	C_S	C_S
Class E/F_3	C_S, X_L, R_L	C_S	short	C_S	C_S	C_S	C_S	C_S
Class E/$F_{2,4,7}$	C_S, X_L, R_L	open	C_S	open	C_S	C_S	short	C_S
Class E/$F_{2,3,4,5}$	C_S, X_L, R_L	open	short	open	short	C_S	C_S	C_S

Figure 2.8: This figure shows for each harmonic the termination, where a Class E has all its higher harmonics terminated with a capacitance, and the Class F^{-2} has all of its higher harmonics terminated with either an open or short. It also shows a mix of the two dependent on the harmonic selected. The figure is from [26].

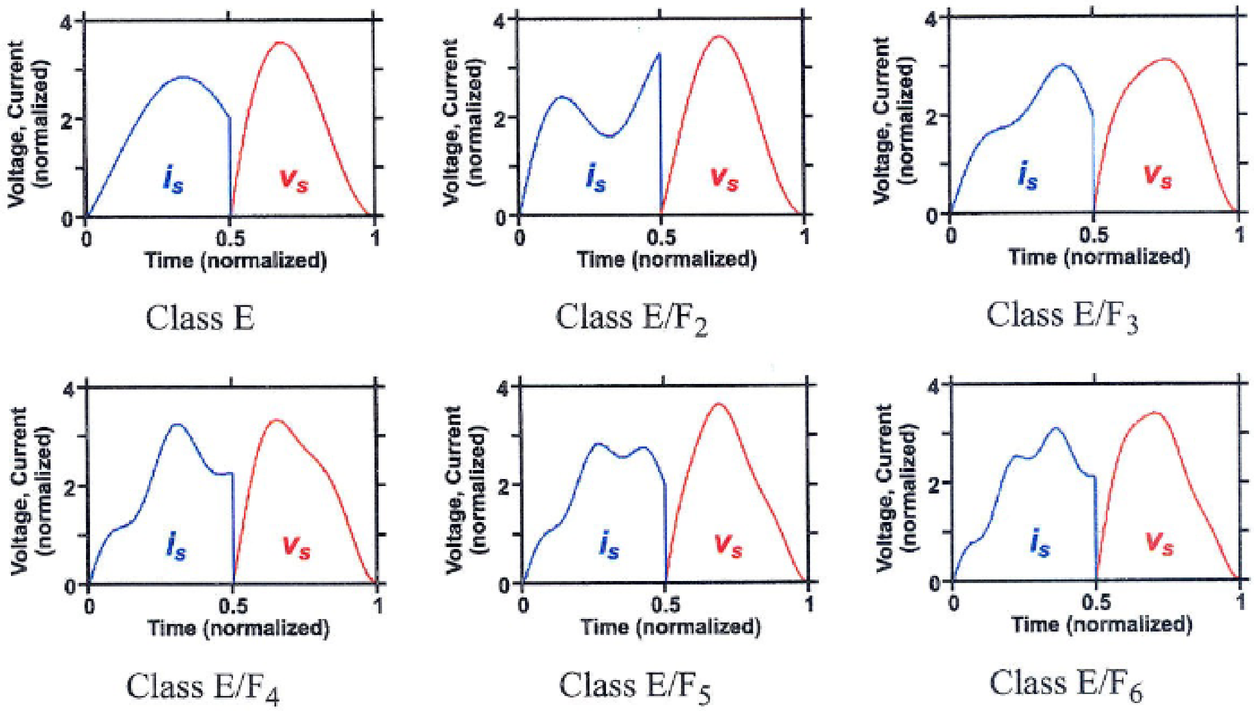

Figure 2.9: The voltage and current waveforms change depending on the number of harmonics selected. This behavior will change both the efficiency and output power. This figure is from [26].

To compare different sub-classes, we can look at Table 2.2, where comparison is made with a non-ideal non-zero resistance Class E with $q = 0$ but with ideal resonators. One can quickly see that the efficiency improvements of Class E/F_2; however, this is at the cost of the total gain of the amplifier, even though the reduced gain, PAE, is increased, mainly because this particular reference Class E amplifier is not gain-limited. Class E/F$_{2,3}$ is also interesting because the gain is reduced very little, but the efficiency is improved significantly. However, when more controlled harmonics are added, the losses of the matching network are increased, limiting the possible efficiency gain when controlling more harmonics. The author also showed that a higher operating frequency can be reached when using a Class E/F$_2$ instead of a classical Class E.

Table 2.2: he different sub-classes change the amplifier's efficiency and gain; the combination of both results in a certain PAE. For reference, a Class E with non-zero on-resistance and with a limited amount of gain is chosen. The last two classes, Class E/F$_{odd}$ can be easily realised in a push-pull configuration and are not realizable in a single-ended configuration. This figure is from [26].

Tuning	Gain	η_D	PAE
class E	20dB	80%	79%
class E/F$_2$	15dB	**93%**	**90%**
class E/F$_3$	21dB	81%	80%
class E/F$_{2,3}$	20dB	**87%**	**86%**
class E/F$_{odd}$ "2E"	18dB	87%	86%
class E/F$_{2,odd}$ "2E"	18dB	**90%**	**89%**

2.2. Efficiency enhancement in power-back-off

Recently, there has been more focus on highly efficient power amplifiers, especially in power back-off, due to the new wireless communication protocols, which have high crest factors. One can either use multiple transistors and a form of load modulation or dynamically change the operating voltage, like in envelope tracking[13]. Envelope tracking is limited by the efficiency and bandwidth of the DC–DC converter; for high bandwidths and high-efficiency PAs, this is, therefore, not optimal. To reach high efficiencies in power back-off, one can choose a power combiner that combines multiple amplifiers into one. This configuration is called a multiple-input amplifier. In this section, different types of power combiners are discussed to increase the efficiencies in power back-off. First, the Doherty multiple-input amplifier, which is the most often used, is discussed. Next, the Chireix out-phasing amplifier and a new guy on the block, the load-modulated (un)balanced amplifier is. In the end, there is a discussion on the pros and cons of every amplifier.

2.2.1. Fundamentals of a power combiner

A power combiner, equivalent to a power divider or power splitter, combines the power from different sources into one or multiple outputs. A power combiner can be used in many applications, such as signal modulation and increasing the output power. The most simple combiner has two inputs and one output. Although they can be constructed using transmission lines, lumped components, or waveguides, the basics are the same. For a coupler, ideally, the following characteristics hold:

- High port isolation between the two input ports is also called high directivity.
- Zero losses when combining two signals, irrespective of phase and amplitude differences. This condition requires a varying coupling.
- There is no reflection of the combiner's inputs and output, which results from a good impedance match at all ports.
- There is no bandwidth limitation. In other words, the combination is independent of frequency.

The following sections discuss various combiner structures, which all compromise some of these characteristics.

2.2.2. Doherty Amplifier

The Doherty amplifier was initially invented by William H. Doherty in 1936 to increase power-back-off efficiency. The Doherty power amplifier uses two separate amplifiers connected using a λ/4 transmission line, which acts as an impedance transformer for one of the amplifiers. Combining the two amplifiers results in optimum efficiency at their maximum power and power back-off; the correct combination also results in decent linearity. One of the main downsides is that the λ/4 transmission line is bandwidth-limiting for the overall system. Figure 2.10 shows the classical circuit for two identical amplifiers with both a maximum current of $I_{max}/2$. The optimal resistance for a signal PA with the maximum current I_{max} is called R_{opt}. For a class-B PA, R_{opt} is defined as follows:

$$R_{opt} = \frac{V_{DC}}{I_{max}/2} \tag{2.21}$$

The impedances seen by both the main and the auxiliary device are as follows:

$$\begin{aligned} Z_{1T} &= \frac{R_{opt}}{2} \cdot \left(1 + \frac{I_2}{I_{1T}}\right) \\ Z_2 &= \frac{R_{opt}}{2} \cdot \left(1 + \frac{I_{1T}}{I_2}\right) \end{aligned} \tag{2.22}$$

For the maximum output power, $I_{1T} = I_2 = I_{max}$, we can see that $Z_{1T} = Z_2 = R_{opt}$. For the choice of the optimum characteristic impedance of the $\lambda/4$ transmission line, we need to look at the

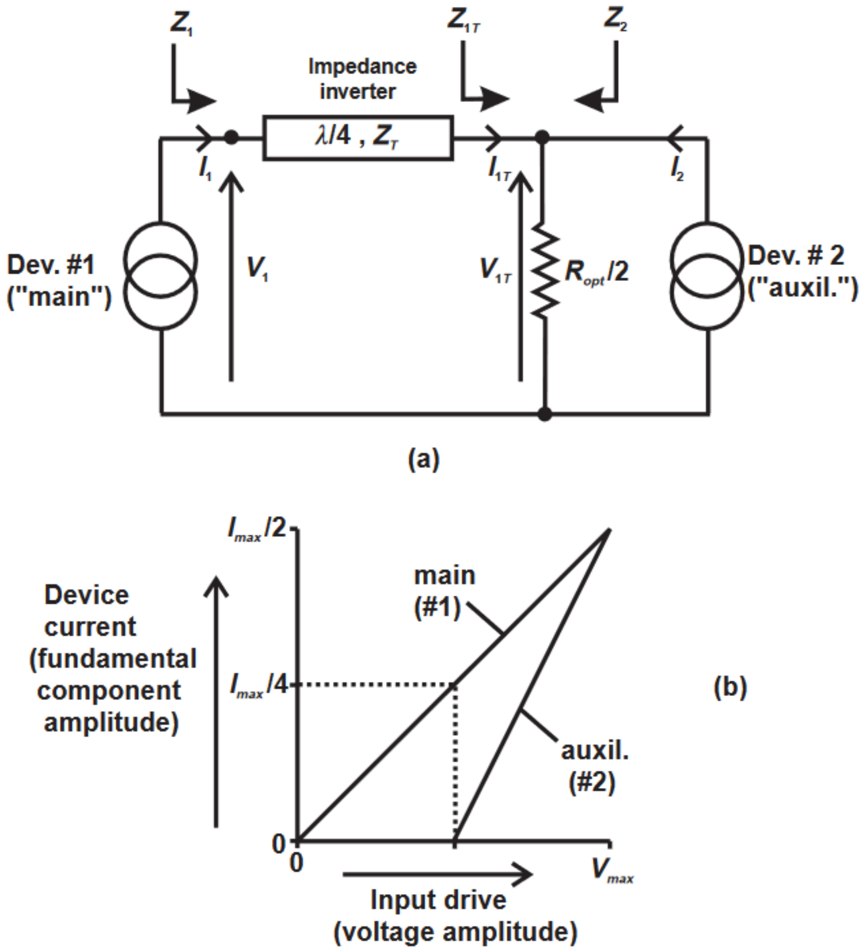

Figure 2.10: Doherty amplifier analysis where (a) is the circuit and (b) are the output currents for the main and auxiliary PA versus input voltage from [15].

efficiency of the primary device. Z_1 needs to keep an optimal impedance when the input voltage increases further. Instead of looking at the optimal impedance, one can look at the optimal voltage over the main device and the auxiliary device. The optimal drain-to-source voltage is V_{DC} and stays constant for $Z_{1T} = R_{opt}$ [15]. In other words, the drain efficiency of the main device stays theoretically constant at 78.5% for Class B. However, the auxiliary device has varying dynamic drain voltage over its power-back-off range, but at the maximum output power, the drain efficiency is again optimal. The resulting waveform can be found in a later section at 2.17.

Besides the increased efficiency at power-back-off, it is still linear [15]. When no longer using an ideal highly linear device and neglecting things like the sub-threshold current, the IM3 will no longer be as high as expected.

Many papers using the Doherty concept have been published. For comparison reasons, we will focus now on DTX-like configurations such as [1] that designed a four-way Doherty at 5 GHz with drain efficiencies of 47.4% at peak power, and down to 40.6% at -12dB power-back-off. The system efficiency at PBO is 18.1%.

2.2.3. Chireix Outphasing Amplifier

The original Chireix outphasing amplifier was invented in the 1930s by Chireix; it was also conceived to increase the efficiency of power back-off. Instead of keeping the phase constant and changing the input voltage, it changes the phase and keeps the input voltage constant. There are many types of outphasing amplifiers, but we will now begin with explaining the basic configuration similar to the one proposed by Chireix from [15] and leave the explanation of alternatives to this structure out of scope.

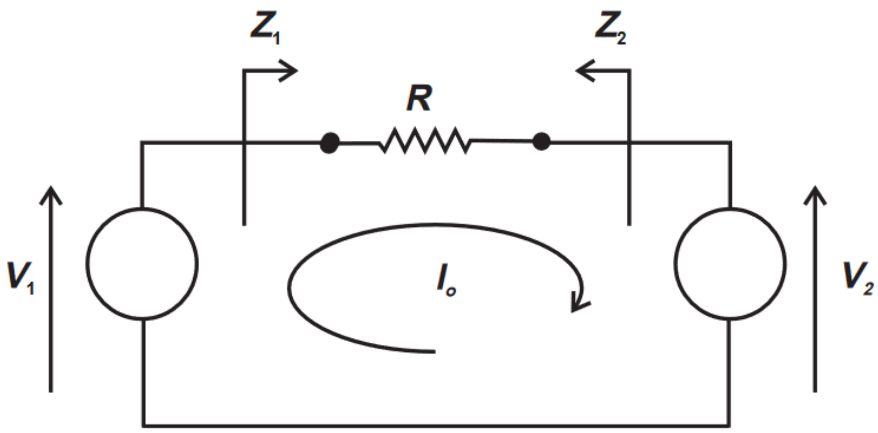

Figure 2.11: A simple outphasing circuit[15]

The primary circuit is shown in Figure 2.11, where the transistors act like voltage sources with constant amplitude but varying phases. Transistors can behave like voltage generators when they are switching from the rail-to-rail voltage, i.e., clipped. The voltage sources are defined as follows:

$$\begin{aligned} V_1 &= V \cdot (\cos(\phi) + j\sin(\phi)) \\ V_2 &= V \cdot (\cos(\phi) - j\sin(\phi)) \end{aligned} \tag{2.23}$$

The current through the load is according to the circuit defined as follows:

$$I_{R_L} = \frac{V1 - V2}{R_L} \tag{2.24}$$

Which results in the impedance seen by voltage-source the voltage sources:

$$\begin{aligned} Z_1 &= \frac{R_L}{2}(1 - j \cdot \cot\phi) \\ Z_2 &= \frac{R_L}{2}(1 + j \cdot \cot\phi) \end{aligned} \tag{2.25}$$

These impedances, therefore, resemble a resistance and reactance in series. These can also be converted to resistance and reactance in parallel as follows:

$$\begin{aligned} Z_1 &= -\frac{R}{4 \cdot \sin 2\phi} \cdot j // \frac{R}{2 \cdot \sin^2\phi} \\ Z_2 &= \frac{R}{4 \cdot \sin 2\phi} \cdot j // \frac{R}{2 \cdot \sin^2\phi} \end{aligned} \tag{2.26}$$

These can, after that, be compensated by putting another complimentary reactance part in parallel, as shown in Figure 2.12, resulting in only the real impedance seen at both of the sources, and therefore, of a certain ϕ, the optimal impedance can be chosen. This can be done at a higher PBO than Doherty [10]. But this reaction compensation will limit the bandwidth. The voltage over the resistor is given as follows:

$$V_{R_L} = V_1 - V_2 = 2j \cdot V \sin\phi \tag{2.27}$$

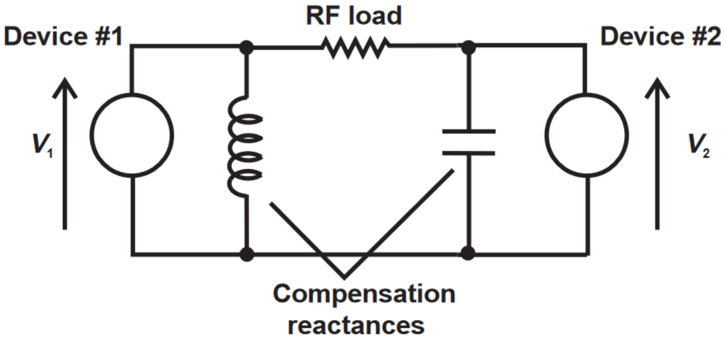

Figure 2.12: A simple compensated outphasing circuit from [15].

The amplitude is doubled compared to a single voltage source with the amplitude modulation as a function of ϕ, together with a phase rotation of 90 degrees with respect to the original source. Even though ideally, the virtual ground is in the middle of the resistor, due to non-idealities, the virtual ground is often shifted to the left or right, which results in lower efficiency when using a Balun, especially at GHz frequencies. A mismatch between the two transistors limits the OPBO power and efficiency [20].

[20] designed a Class E outphasing PA operating at 1.8 GHz; at peak power, the drain efficiency is 65.3%; at -12 dB PBO, 37.2%; and a PAE at PBO is 22.1%. The author used $\lambda/4$ transmission lines as a power-combining network and used two asymmetric devices together with changing the duty cycle for increased efficiency in PBO.

2.2.4. Load-Modulated Balanced Amplifier

The LMBA concept was first invented by Paul Dent[17]. The amplifier uses a hybrid splitter to split the main amplifier into two signals 90 degrees out of phase with each other. These two out-of-phase signals are then combined with a hybrid coupler. Generally, a hybrid coupler's isolated port is terminated with a resistor; however, in this case, it is replaced with another amplifier, which provides impedance modulation for the two main amplifiers. This mechanism is then used to improve PBO efficiencies up to 6-7 dB. Because many variations are possible, I will start by explaining the most basic LMBA. Variations of these configurations are discussed, such as the pseudo-Doherty Load-Modulated Balanced Amplifier (PD-LMBA), the Asymmetrical pseudo-Doherty Loud-Modulated Balanced Amplifier (PD-ALMBA), and the Hybrid Asymmetrical Load-Modulated Balanced Amplifier (H-ALMBA), all to increase efficiency in PBO. For clarity, we start with what one calls the different amplifiers, referring to Figure 2.13.

PA symbol	Original LMBA [17]	Pseudo-Doherty LMBA [10] and this work
PA_{B1}	First Primary PA	First Peaking PA
PA_{B2}	Second Primary PA	Secondary Peaking PA
PA_C	Auxiliary PA	Main PA

Table 2.3: Different names used by authors.

2.2.4.1. The Original LMBA

The basic configuration of an LMBA is shown in Figure 2.13, where one can see two PAs that are called PA_{B1} and PA_{B2}, which have current amplitude I_B and a phase difference of 90 degrees. The two PAs are combined using a hybrid coupler, added in phase at the load, and added 180 degrees out of phase at the isolated port, which is, in this case, not terminated by an isolation resistor but by another PA called PA_C. The 180 degrees out of phase and equal amplitude cancel each other at the isolation port; however, the in-phase combination results in an addition of amplitude. The third PA is called PA_C, with a current I_C, and controls the impedance seen by PA_{B1} and PA_{B2}. The wave originating from PA_C is split into PA_{B1} and PA_{B2}, where after it is reflected, it ends up canceling at the output of PA_C and in phase combined at the load. Therefore, all the amplifiers are added in phase, and in the ideal case, no power is lost. However, when reflecting on the outputs of PA_{B1} and PA_{B2}, the impedance at that node changes, resulting in load modulation for PA_{B1} and PA_{B2}. As such, after explaining the configuration basics, we can set up the impedances seen at the following nodes: Due to symmetry, Z_B is defined as follows:

$$Z_{B1} = Z_{B2} = Z_B \tag{2.28}$$

Z_0 is the characteristic impedance of the hybrid coupler, and due to the cancellation of waves at the output of PA_C, the impedance seen by PA_C is constant and equal to the characteristic impedance of the hybrid coupler as follows:

$$Z_C = Z_0 \tag{2.29}$$

Next, derived [41] that the powers are combined lossless as follows:

$$P_{R_L} = 2 \cdot P_B + P_C \tag{2.30}$$

When phases are no longer added in phase, the impedance can be transformed into the real domain and its reactance component, as seen in Equation 2.34. We need to do some math to determine the amount of impedance that can be transformed. To start using the Z-matrix of a hybrid coupler, the following equation can be set up:

$$\begin{bmatrix} V_1 \\ V_2 \\ V_3 \\ V_4 \end{bmatrix} = \begin{bmatrix} 0 & 0 & -j & -j\sqrt{2} \\ 0 & 0 & -j\sqrt{2} & -j \\ -j & -j\sqrt{2} & 0 & 0 \\ -j\sqrt{2} & -j & 0 & 0 \end{bmatrix} \cdot \begin{bmatrix} I_1 \\ I_2 \\ I_3 \\ I_4 \end{bmatrix} \tag{2.31}$$

Next, it assumes that each power amplifier can be reduced to a voltage-dependent current source that reduces the need for additional matching, and the voltage at each node is simply the load impedance multiplied by the load current. A further assumption is that the load impedance is equal to the characteristic impedance, which results in no mismatch losses. In the Z-matrix, the currents are out of the matrix, not entering it; therefore, the following is true:

$$\begin{aligned} I_1 &= I_o \\ I_2 &= -j \cdot I_B \\ I_3 &= -j \cdot I_C \cdot e^{j\phi} \\ I_4 &= -I_B \end{aligned} \tag{2.32}$$

The voltages at each node depend on the impedances when the PAs are appropriately matched. This aspect means that we can set up the voltages in terms of the input impedances:

$$\begin{aligned} V_1 &= -I_o \cdot Z_0 \\ V_2 &= -I_B \cdot Z_{B1} \\ V_3 &= -j \cdot I_C \cdot Z_0 \\ V_4 &= -j \cdot I_B \cdot Z_{B2} \end{aligned} \tag{2.33}$$

We can combine Equations 2.31, 2.32 and 2.33 and solve it for the input impedances Z_{B1} and Z_{B2}, which are equal and is called Z_B. And is defined as follows:

$$Z_{B1} = Z_{B2} = Z_B = Z_0 \cdot \left(1 + \sqrt{2}\frac{I_C e^{j\phi}}{I_B}\right) \tag{2.34}$$

If I_C is non-zero, it modulates the input impedance seen by the PAs P_{B1} and P_{B2}. The problem, however, is that this depends on the current ratio. To transform this into a ratio of powers, we need to look at how the power is defined:

$$\begin{aligned} P_B &= \frac{|I_B|^2}{\Re(Z_B)} \\ P_C &= \frac{|I_C|^2}{\Re(Z_0)} \end{aligned} \tag{2.35}$$

Combining Equations 2.34 and 2.35, we can determine that the ratio of P_B/P_C is defined as follows:

$$\frac{P_C}{P_B} = 0.5 \cdot \left|\frac{Z_B}{Z_0} - 1\right|^2 \cdot \frac{\Re(Z_0)}{\Re(Z_B)} = \alpha \tag{2.36}$$

After that, this power ratio α can be used to determine the input reflection seen by the PAs PA_{B1} and PA_{B2}. This process is done by transforming Equation 2.36 and using the classical reflecion coefficient formula 2.37.

$$\Gamma_B = \frac{Z_B - Z_0}{Z_B + Z_0} \tag{2.37}$$

The resulting reflection coefficients are after that defined as follows:

$$|\Gamma_{B1}|^2 = |\Gamma_{B2}|^2 = \frac{\alpha}{\alpha + 2} \tag{2.38}$$

One can use this formula to determine the maximum impedance transformation possible when varying the phase ϕ and/or the amplitude I_C.

The classical LMBA concept [41] uses the balanced PA_{B1} and PA_{B2} as the primary PAs and the PA_C as the auxiliary PA. This feature means that at power-back-off, the primary PA reaches its maximum efficiency, and at max power, both the primary and the auxiliary PA reach their maximum efficiency. First, note that we can set ϕ to 0, decreasing the impedance Z_B when I_C rises. Which results in the following equation:

$$Z_B|_{\phi=0} = Z_0 \cdot \left(1 - \sqrt{2}\frac{I_C}{I_B}\right) \tag{2.39}$$

Therefore, when I_C rises, the input impedance seen by P_B will decrease. As a result the output power P_B will also increase. To make this idea more precise, we can plot the currents I_C and I_B versus P_{R_L}, which represents the total output power; this plot is shown in Figure 2.14. Up to a chosen Output Power Back-Off (OBO), I_C is zero and only I_B is increasing. After the OBO point, I_C starts increasing, and in the process also decreases impedance Z_B, increasing I_B. Although this process results in non-linearity in the P_{in} versus P_{out} dependency(AM-AM distortion), it improves the efficiency in the power-back-off range. The resulting efficiency versus output power curve can be found in 2.18. The maximum OBO point that can be reached is around 6–7 dB; in the following subsections, different methods are discussed to reach a lower OBO.

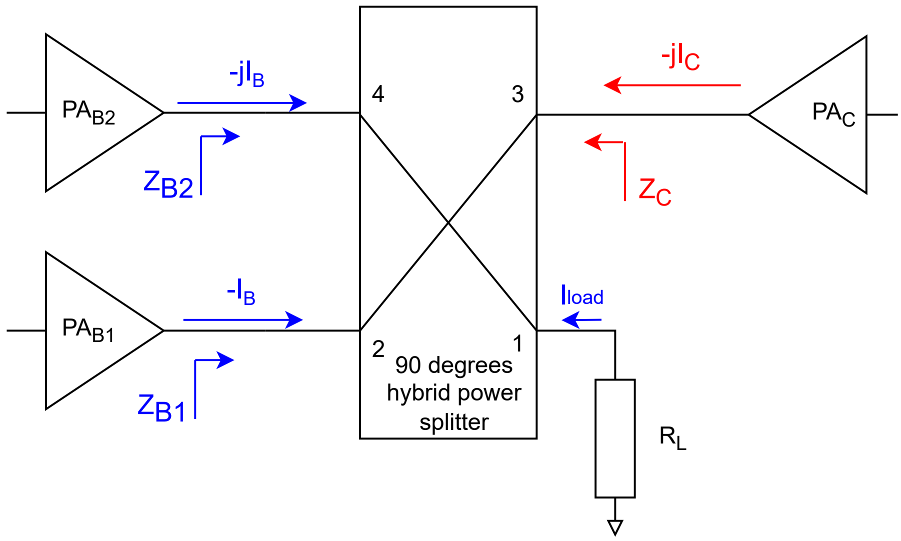

Figure 2.13: The most basic LMBA configuration with two 90 degrees out of phase with equal amplitude I_B called the primary PAs and one controlling PA called the Auxiliary PA. The PAs are combined on a load called R_l.

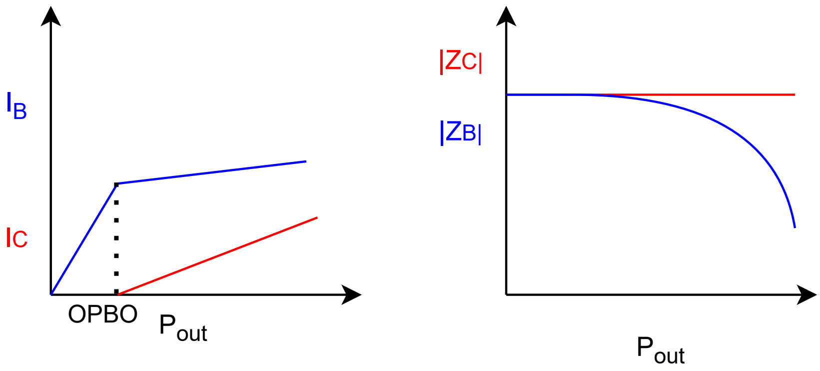

Figure 2.14: The Classical LMBA uses load modulation for PA_B by increasing the current I_C and decreasing the impedance Z_B seen. At maximum power, both I_B and I_C are maximum and at its highest efficiency.

To summarize everything stated in this section, we divide the operation into three regions, also shown in Figure2.14:

Here, the primary PA (PA_C) increases in power, which increases current IC. This condition, in turn, lowers the impedance seen by the auxiliary PA (PA_B), which increases its output power PB.

- **Primary PA is only on**: First, the primary PA (PA_B) starts and achieves optimum efficiency at OBO while the auxiliary PA (PA_C) stays off.
- **Auxiliary PA starts**: Here, the auxiliary PA (PA_C) increases in power, which increases current I_C. This condition, in turn, lowers the impedance seen by the primary PA (PA_B) which increases its output power P_B.
- **Auxiliary PA saturates**: At the end, the auxiliary PA (PA_C) saturates, so PA_B is also no longer increased.

2.2.4.2. The Pseudo-Doherty Load-Modulated Balanced Amplifier

Due to the need for lower OBO and improved linearity, [10] found a way to improve both and called it the Pseudo-Doherty Load-Modulated Balanced Amplifier (PD-LMBA). This architecture switches the main and auxiliary PAs, which results in an increased OBO range. First, note that Z_C is constant and equal to Z_0 without additional matching. Therefore, the idea is to keep a constant power at PA_C, which results in a 78.5% efficiency for Class-B at OBO. If I_B stays constant, we get impedance modulation only dependent on the input current I_B by using 2.34. This load modulation looks like the Doherty load modulation stated in 2.22. However, it does not need the $\lambda/4$ line for impedance inversion, which limits the bandwidth. A downside, however, is that the wave coming from PA_C is reflected once at PA_B before it reaches the load; this path causes extra-efficiency losses at OBO[10]. Lastly, the impedance seen by PA_B in OBO is suboptimal, decreasing the OBO range's efficiency.

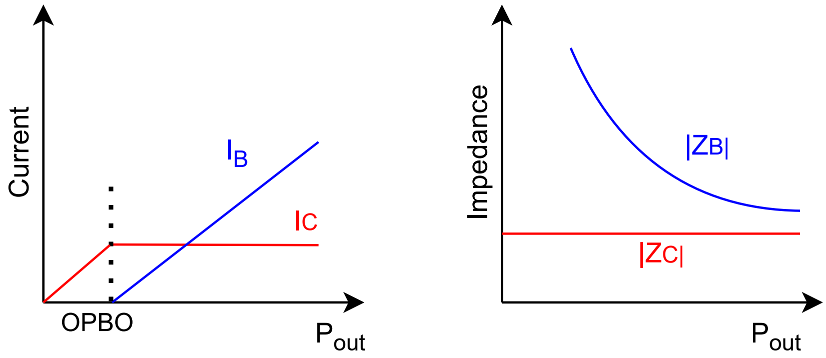

Figure 2.15: The PD-LMBA uses load modulation for PA_B by increasing the current I_B and decreasing the impedance Z_B seen while keeping I_C constant simultaneously. Both PA_B and PA_C are at maximum output power at their highest efficiency.

To summarize the operation, we separate the result in three regions, as shown in Figure 2.15:

- **The main PA is off**: P_B is off, and only P_C is rising where the impedance Z_C is constant, and Z_B is infinite because I_B is zero in equation 2.39. This results in the following load impedances seen:

$$\begin{aligned} Z_C &= Z_0 \\ Z_{B1} &= \infty \\ Z_{B2} &= \infty \end{aligned} \tag{2.40}$$

- **The main PA is rising**: P_B is rising; therefore, I_B is rising, and Z_B is falling according to Equation 2.39. Also, P_C stays constant at $P_{C,max}$ also called P_C often in this section. This results in the following load impedances seen:

$$\begin{aligned} Z_C &= Z_0 \\ Z_{B1} &= Z_0\left(1+\sqrt{2}\frac{I_C}{I_B}\right) \\ Z_{B2} &= Z_0\left(1+\sqrt{2}\frac{I_C}{I_B}\right) \end{aligned} \tag{2.41}$$

- **the main PA is saturated**: P_B is at its maximum, and Z_B is optimal ($Z_B = Z_B(P_{max})$). Also P_C still stays constant at $P_{C,max}$.

To design such a PD-LMBA, we use the given that the total power is the addition of the three separate PAs 2.30. At OBO, we know that only the auxiliary PA (P_C) is still active, and the main PAs are turned off($PA_{B1,2}$); using this information, we can state the following:

$$
\begin{aligned}
OBO_{lin} &= \frac{P_C}{P_C + P_{B1} + P_{B2}} = \frac{P_C}{P_{max}} \\
OBO_{lin} &= 10^{OBO_{dB}/10}
\end{aligned}
\tag{2.42}
$$

When one, for example, chooses an OBO of -10 dB with a P_{max} of 50 W P_C should be 5 W. We know that PB1 and PB2 should be 22.5 W in that case. For a P_B of 22.5 W, a specific resistance of Z_B is necessary at peak power. This condition depends on the utilized PA class. For example, for Class-B, the following holds:

$$
\Re(Z_B) = \frac{V_{DD}^2}{2 \cdot P_B} \tag{2.43}
$$

For Class E, it is dependent on the solution space K[2], where R is for higher operating frequencies defined as follows:

$$
\begin{aligned}
\Re(Z_B) &= \frac{K_C(m,q,k)}{\omega C_{ds}} \\
\Im(Z_B) &= K_X(m,q,k)R
\end{aligned}
\tag{2.44}
$$

Where C_{ds} is the output capacitance of the transistor, for now, it is assumed to be constant and independent of the voltage waveform at the drain. This assumption is partially correct, but this simplification is now used. Next, we assume a constant impedance seen by PA_C, which is Z_C. Using an impedance transformer, we can transform the constant impedance at port 3 Z_0 to Z_C by either a transformer, lumped elements, or a $\lambda/4$ transmission line. The $\lambda/4$ limits the bandwidth, making it a sub-optimal choice; the transformer is bulky and adds losses, which is also not optimal, and the lumped components add extra losses. Another solution is using an asymmetric LMBA, which is challenging to design, although it is a promising solution[8]. The last solution can be found in Equation 2.46, where one can change the supply voltage[9]. All in all, depending on the requirements, a solution can chosen. For transforming, we assume now a transformer with n:1 couplings where n is at the side of PA_C. We can state the following:

$$
Z_C = Z_0 \cdot n^2 \tag{2.45}
$$

After calculating Z_C and Z_B using the requirements, we must choose the characteristic impedance Z_0. This application uses a symmetric hybrid and a transformer for impedance transformation. Using equation 2.34 and a ϕ of zero, one can use equation 2.39. Note that this equation only involves real numbers, which limits the possibility of Class E, which often also consists of a reactance part. But for now, we limit the analysis to Class-AB. To determine Z_0, we use the classical power definition and use that to define both the currents I_C and I_B as follows:

$$
\begin{aligned}
|I_B(P_B = P_{maxB})| &= \sqrt{\frac{P_B \cdot 2}{\Re(Z_B)}} = \sqrt{\frac{(P_{max} - P_C) \cdot 2}{2\Re(Z_B)}} \\
|I_C| &= \sqrt{\frac{P_C \cdot 2}{Z_0}}
\end{aligned}
\tag{2.46}
$$

At maximum power, both Z_B and Z_C is optimal ($Z_B = Z_B(P_{max})$); therefore, we can combine Equations 2.39 and 2.46 to come up to the following equation:

$$Z_0 = \frac{-2P_C\Re(Z_B) + P_C Z_B - P_{max} Z_B + 2\sqrt{\Re(Z_B)^2 P_C^2 - \Re(Z_B) P_C^2 Z_B + \Re(Z_B) P_C P_{max} Z_B}}{-P_{max} + P_C} \tag{2.47}$$

And when Z_B is only real the following holds:

$$Z_0 = Z_B \cdot \frac{P_C + P_{max} - 2\sqrt{P_C P_{max}}}{P_{max} - P_C} \tag{2.48}$$

Note that this is only true when PA_C is properly matched. But in my opinion this simplifies the design of a LMBA a lot compared to analyzing it using currents as in [40]. After Z_0 is determined, one can chose the impedance transformation ratio n^2 by using equation 2.45.

In this section, various subtleties are removed, like AM-PM distortion, where a change of P_B changes the output phase, which can be compensated by a phase change in PA_C using either digital pre-distortion (DPD) or a constant phase offset. Another problem is that when PAB is completely turned off, PA_B ideally should perfectly reflect the wave coming from PA_C, but this does not happen in practice. A big downside is that if implemented in an analog fashion, PA_C needs to be overdriven, which comes at the cost of non-linearity. Also, in between the two optimum points, P_{max} and P_{OBO}, there is a region where there is a non-optimal impedance seen by PA_B, which in turn results in an efficiency decrease that is similar to the behavior in Doherty; however, due to the stronger load-pulling of two balanced PAs, a higher OBO can be reached. Lastly, an ideal hybrid is assumed; a non-ideal hybrid also results in losses, especially becoming more significant at OBO. Also, when using a DTX, not the input amplitude but the number of fingers driven are changed, and it is often no longer driven by a sine-wave but a square wave, resulting in a slightly different behavior. An analog PD-LMBA was designed with a peak drain efficiency of 72% and at 10 dB OBO 58%[10] operating with a bandwidth of 1.5–2.7 GHz.

2.2.4.3. Hybrid Asymmetrical Load-Modulated Balanced Amplifiers

The Hybrid Asymmetrical Load-Modulated Balanced Amplifier(H-ALMBA)[9] is a combination of the Hybrid Load-Modulated Balanced Amplifier(H-LMBA)[30] and the Pseudo-Doherty Asymmetrical Load-Modulated Balanced Amplifiers[11]. The combination increases OBO and maximum power efficiency, exploiting a three-way Doherty efficiency enhancement.

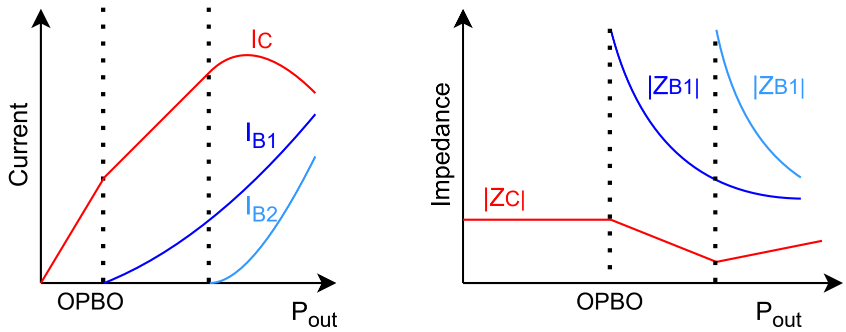

Figure 2.16: The HAPD-LMBA uses load modulation for PA_{B1} by increasing the current I_{B1} and decreasing the impedance Z_{B1}. The same happens for PA_{B2} when turned on. PA_C is also being modulated due to the asymmetry between I_{B1} and I_{B2}. Both PA_{B1}, PA_{B2} and PA_C are at their highest efficiency at peak power.

To analyse why we divide its operation in four regions as follows:

- **Low-Power Region**: The low-power region is the same as PD-LMBA; $PA_{B1,2}$ are turned off and PA_C increases in power, where Z_C stays constant and equal to Z_0. The impedances are, therefore, as follows:

$$\begin{aligned} Z_C &= Z_0 \\ Z_{B1} &= \infty \\ Z_{B2} &= \infty \end{aligned} \tag{2.49}$$

- **Doherty Region**: Only PA_{B1} is turned on, while PA_{B2} stays off. This results in behavior similar to a two-way Doherty; the impedance Z_{B1} starts at infinity and lowers to a value depending on the ratio of the two currents I_C/I_{B1}. Z_C is no longer constant but depends on I_{B1}, as a result, Z_C slightly decreases, which in turn increases the power P_C.

$$\begin{aligned} Z_C &= Z_0\left(1 - \sqrt{2}\frac{I_{B1}}{I_C}\right) \\ Z_{B1} &= Z_0\sqrt{2}\frac{I_C}{I_{B1}} \\ Z_{B2} &= \infty \end{aligned} \tag{2.50}$$

- **ALMBA Region**: When PA_{B1} reaches a certain output power, PA_{B2} is turned on. This condition results in the same behavior as discussed before ALMBA. The impedance Z_C moves back to the original value Z_0 in the case when $P_{B1} = P_{B2}$, which results in a decrease of P_C but an increase in total output power.

$$\begin{aligned} Z_C &= Z_0\left(1 - \sqrt{2}\frac{I_{B1} - I_{B2}}{I_C}\right) \\ Z_{B1} &= Z_0\frac{I_{B2} + \sqrt{2}I_C}{I_{B1}} \\ Z_{B2} &= Z_0\frac{I_{B2} - I_{B1} + \sqrt{2}I_C}{I_{B2}} \end{aligned} \tag{2.51}$$

The H-ALMBA [9] improves upon the efficiency of in the -6 dB OBO range. The H-ALMBA has a peak drain-efficiency of 82%, at 6 dB OBO, a drain-efficiency of 69%, and at 10 dB OBO 61%, operating in the ultra wide bandwidth of 0.55–2.2 GHz. Note, even though the reported drain efficiency at OPBO is high the PAE should be significantly lower at OPBO in the case that the amplifier is gain limited.

2.2.4.4. Outphasing Load-Modulated Balanced Amplifier

The only Class E LMBA currently reported in the literature is [18]. It uses a combination of an outphasing topology realized using a quadrature hybrid coupler as a non-isolating combiner and the LMBA concept to reach higher efficiencies in PBO. The authors used the classical LMBA concept; therefore, the control PA is the main PA for maximum power, and the auxiliary PAs are used in PBO using outphasing. This mixed approach of using a combination of outphasing and current injection [38] is basically an outhasing PA using a hybrid coupler and using the classical LMBA structure to increase the PBO range. According to the author, this reaches higher efficiencies in PBO. The design obtains 80%, 70%, and 60% at power levels of 9.5, 13.5, and 15 dB PBO, respectively. A downside of this design is the drain efficiency at peak power, which is as low as 60%.

2.2.5. Comparison of Doherty, Outphasing, LMBA and PD-LMBA

Up to this section, almost no comparison is made between the different efficiency enhancement techniques. [33] made such a comparison to various typologies with respect to broadband performance and efficiency in PBO. The comparison was made using a GaN HEMT with a gate length of 140 nm and a unit gate width of 50 um with four fingers at 15–21 GHz. The analysis is done with a device at its current source reference plane for comparison. The Doherty architecture uses $\lambda/4$ transmission lines to combine two amplifiers, as discussed before. This feature limits the operation bandwidth; however, the losses in the power combination network are limited, as shown in 2.17. In Figure 2.17a, one can see the performance when no losses in the combination network are pressing, and in Figure 2.17b one can see when the losses are pressent. The degradation of performance is far more significant for LMBA in comparison to Doherty. In Figure 2.17a, the outphasing architecture uses a comparable power combiner network and, therefore, offers a similar behavior as shown in 2.18, with its main downside of bad linearity in the PM-AM and, thus, needing DPD. The LMBA and PD-LMBA have lower overall efficiency because of the losses in the power combination network. The amount of extra loss strongly depends on the type of quadrature hybrid. The losses are also partly due to non-ideal reflections at the hybrid coupler ports. This aspect is especially prevalent at PD-LMBA at OBO.

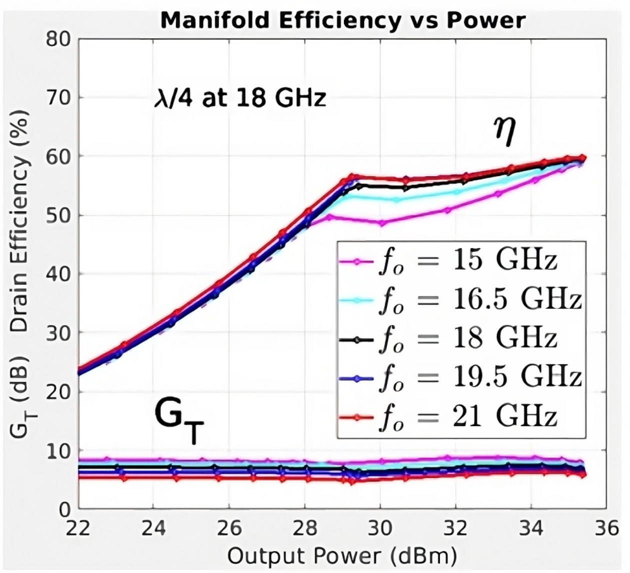

Figure 2.17: The drain efficiency of a Doherty PA using GaN HEMT with transmission lines designed at 18 GH from [33].

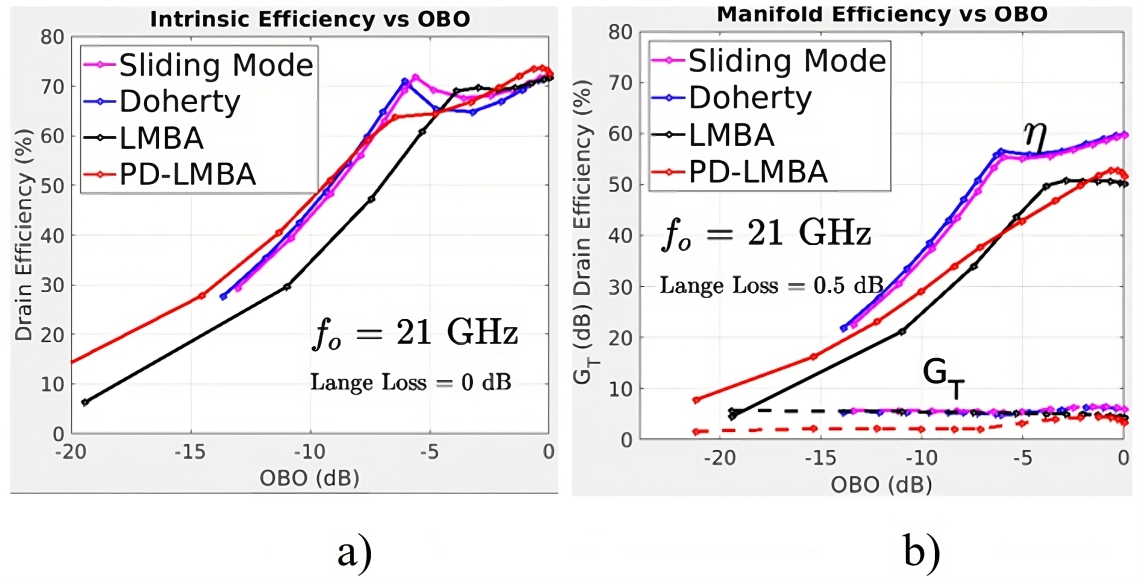

Figure 2.18: (a) The comparison of drain-efficiency and gain for at 21 GHz different efficiency enhancement techniques where the sliding-mode means outphasing. (b) When losses in the combination network is added the LMBA concept decreases in efficiency. From [33]

One should keep in mind that this study made use of Class-B type amplifiers. When one makes use of Class F type amplifiers, the performance in OPBO is better than in LMBA's[12] due to the higher efficiencies of PA_C.

In the case where wideband performance is of the utmost importance, one should still use LMBA. Mainly because a hybrid coupler has theoretically no bandwidth limitation, contrary to a Doherty and an outphasing configuration.

3
Modelling of Class E

Although Class E is popular in literature, its practical applications are less common. There are a few reasons for this: the difficulty of implementing amplitude modulation with good linearity, the high peak drain voltage, the complexity of designing a matching network, and the drain-to-source capacitance limiting the maximum frequency, limiting the power density. This section will focus on the maximum Class E frequency for different configurations. Thereafter, there is a discussion on the nonlinearities of both the drain-to-source capacitance and the on-resistance. Ultimately, a comparison is made between a nonlinear and linear transistor in a Class E configuration.

3.1. The maximum frequency of Class E

Class E has many different types of implementations. But the most common implementation is using a shunt capacitance and series resonator as in Figure 3.1. In the most basic variant, the inductance for biasing the drain is a DC-Feed. When one assumes an ideal resonator, Class E has four design components: VDD, C, R_x and X_x. And there are two requirements for an ideal Class E: Zero Voltage Switching (ZVS) and Zero Voltage Slope Switching (ZVSS):

$$\begin{aligned} & v_C(2\pi/\omega) = 0 \\ & \left.\frac{dv_C(t)}{dt}\right|_{t=2\pi/\omega} = 0 \end{aligned} \tag{3.1}$$

The operating frequency f_0 is often specified at the start, and the technology sets the supply voltage V_{DD}. This results in the four specifications (f_0, V_{DD}, VS and VSS) and four unknowns ($POUT$, C, R_x and X_x); thus, the circuit can be solved. However, the drain-to-source capacitance limits the solution at GHz frequencies, which puts a minimum value of C. When C is equal to C_{ds}, f_0 equals to $f_{E,max}$. In the general case, combining 2.16, the following can be said:

$$f = \frac{K_C}{K_P}\frac{P_{OUT}}{2\pi C V_{DD}^2} \tag{3.2}$$

When C_{ds} is the limiting factor:

$$f_{E,max} = \frac{K_C}{K_P}\frac{P_{OUT}}{2\pi C_{ds} V_{DD}^2} \tag{3.3}$$

In the case of the Class E variant with shunt capacitance, series resonator, and DC feed:

$$f_{E,max} = 0.0507\frac{P_{OUT}}{2\pi C_{ds} V_{DD}^2} \tag{3.4}$$

In the case of GaN, the maximum drain-to-source current limits the output power. When the drain-to-source current exceeds the maximum drain-to-source current of the transistor, the transistor is

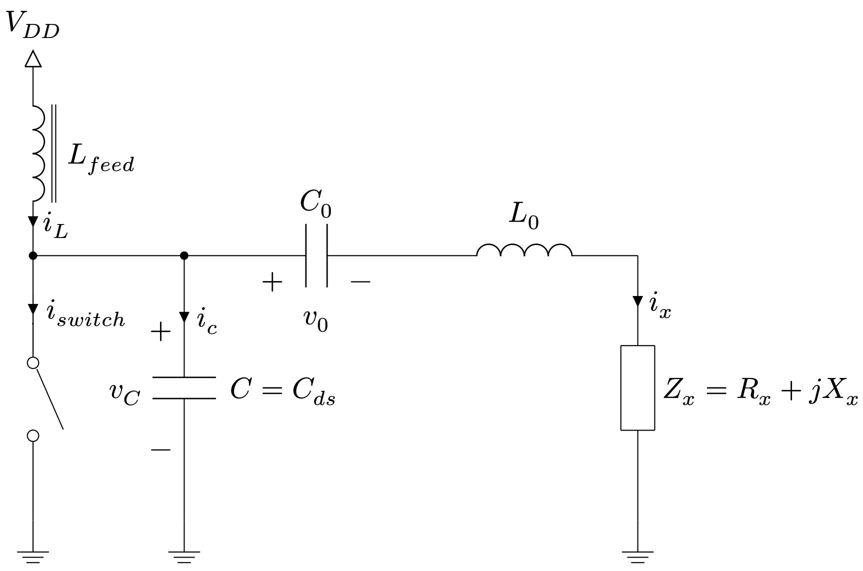

Figure 3.1: Class E with series resonator, shunt capacitor, and DC feed.

no longer operating in the triode region but in the saturation region. This greatly increases the on-resistance, which decreases the drain efficiency. In the case of a Class E with a series resonator and DC feed, the maximum drain-to-source current is where the derivative to time of the drain-to-source current equals zero 2.5. The time point at which this happens can be calculated as follows:

$$\begin{aligned} i_{switch}(t) &= i_x(t) + i_L(t) = I_R \cdot \sin(\omega t + \phi) + I_0 \\ \left.\frac{di_{switch}(t)}{dt}\right|_{t_{max}} &= I_R \cdot \omega \cdot \cos(\omega t_{max} + \phi) = 0 \\ t_{max} &= \frac{\frac{\pi}{2} - \phi}{\omega} \end{aligned} \tag{3.5}$$

Where ϕ is the conduction angle, and ω is the angular operating frequency. At time t_{max}, the maximum drain-to-source current is as follows:

$$I_{ds,max} = I_R + I_0 \tag{3.6}$$

Where I_0 is the DC current flowing through the DC feed, and $I_{ds,max}$ is the maximum drain-to-source current. Next, to determine the conduction angle (ϕ), we need to set up the voltage and current relationship of the drain-to-source capacitance:

$$\begin{aligned} C \cdot \frac{dv_c(t)}{dt} &= i_c(t) \\ \int_0^{v_c} C dv_c &= \int_{\pi/\omega}^{t} i_c(t) dt \\ C \cdot v_C &= \frac{I_R}{\omega}(\sin(\phi) \cdot (\pi - \omega \cdot t) - \cos(\omega t + \phi) - \cos(\phi)) \\ v_C &= \frac{I_R}{\omega C}(\sin(\phi) \cdot (\pi - \omega \cdot t) - \cos(\omega t + \phi) - \cos(\phi)) \end{aligned} \tag{3.7}$$

The transistor is on from π/ω to $2\pi/\omega$, as shown in Figure 2.6. To find ϕ, we can use the zero-voltage switching requirement:

$$\begin{aligned} v_c(t)|_{t=\frac{2\pi}{\omega}} &= 0 \\ \phi &= \arctan\left(-\frac{2}{\pi}\right) \end{aligned} \tag{3.8}$$

And for zero initial current:

$$\begin{aligned} \left.\frac{dv_c(t)}{dt}\right|_{t=\frac{2\pi}{\omega}} &= 0 \\ i_c(0) = 0 &= I_R \cdot \sin(\phi) + I_0 \\ I_0 &= -I_R \cdot \sin(\phi) \end{aligned} \tag{3.9}$$

Combining 3.9 and 3.5:

$$I_{ds,max} = -\frac{I_0}{\sin(\phi)} + I_0 \tag{3.10}$$

The output power in the case of a DC feed is as follows:

$$P_{out} = V_{DD} \cdot I_0 = V_{DD} \frac{I_{ds,max}}{1 - (\sin(\phi))^{-1}} \tag{3.11}$$

This results in the equation:

$$f_{E,max} = 0.0174 \frac{I_{ds,max}}{2\pi C_{ds} V_{DD}} \tag{3.12}$$

The relationship between the output power and maximum drain-to-source current will evolve more for different Class E configurations. Therefore, most research mainly focuses on equation 3.3 and expects a similar relationship. The analysis can be done for multiple configurations, such as a Class E with a series resonator and a finite DC feed or a Class E with a parallel resonator. These are all analyzed in [22], and the results are summarized in the table below:

Class E Configuration	$\frac{f_{E,max} C V_{DD}^2}{P_{OUT}}$	$\frac{P_{out} R}{V_{DD}^2}$
Class E with series filter and DC feed(q=0)	0.051	0.577
Class E with series filter Quasi Load Independent (q=1.3)	0.073	1.274
Class E with series filter Parallel Circuit(q=1.412)	0.079	1.363
Class E with series filter max frequency (q=1.9)	0.156	0.136
Class E with quarter-wave line and series filter	0.093	0.465
Class E with shunt capacitance and shunt filter	0.097	0.428

Table 3.1: The normalized maximum Class E frequency and the output power for a specified load impedance for different configurations of Class E.

From Table 3.1, one can see that the absolute highest maximum frequency of Class E is the series filter variant with a q equal to 1.9. However, the output power is very low in comparison to other configurations. The Parallel circuit Class E with series filter is an often-used configuration. It has a relatively high output power and a high $f_{E,max}$. The Class E with shunt capacitance and shunt filter has a higher $f_{E,max}$ but a lower output power, which results in a lower power density and PAE.

So far, in our analysis, we have assumed zero-voltage slope switching (ZVSS) and zero-voltage switching (ZVS). However, in the case of non-ZVSS and non-ZVS, this $f_{E,max}$ can be increased. For example, the previous analysis in Section 2.1.5.1 used the parameter k to describe the slope at switching time. Following the same analysis, one can find the values for K_C and K_P as a function of k. However, the improvement on $f_{E,max}$ will again be at the cost of output power.

3.2. The nonlinear drain-to-source capacitance

It is common knowledge that the drain-to-source capacitance of a realistic FET is nonlinear, and in the case that the transistor is operating at $f_{E,max}$, the shunt capacitor C is an equation to the drain-to-source capacitance C_{ds}; therefore, this nonlinearity becomes highly relevant. The drain-to-source capacitance depends on the drain-to-source voltage, drain-to-gate voltage, and operating frequency; therefore, it should be simulated accordingly. For example, using the model from the PDK: UMS GH15, we can plot the Y parameter as follows:

$$\Im\{Y(1,1)\} = \omega C(v,f) \tag{3.13}$$

One can find the capacitance as follows:

$$C(v,f) = \frac{\Im\{Y(1,1)\}}{\omega} \tag{3.14}$$

Using small-signal analysis is not the most accurate way of approximating the behaviour, but it is quick and very accurate, as shown later in Figure 3.7. The drain-to-source voltage is swept from 0 up to 100 V at the operating frequency of 3.15 GHz; the results are shown in Figure 3.2. Multiple mathematical models can be used to model the drain-to-source capacitance. For MOSFET, most often equation 3.15a [22] or 3.15b [16] is used; for GaN, something more like Equation 3.15c [21] is used.

$$C(v) = C_{j0}\left(1+\frac{v}{V_{bi}}\right)^{-\gamma} \tag{3.15a}$$

$$C(v) = C_{j0}\left(1+\frac{v}{V_{bi}}\right)^{-\gamma} + C_l \tag{3.15b}$$

$$C(v) = C_{ds,i} + C_{gd0}\cdot(1+\tanh(P_{1dgd}V_{gs}))\cdot(1-\tanh(P_{1dgd}V_{ds}+P_{1cc}V_{gs}V_{ds})) \tag{3.15c}$$

(3.15d)

Where C_{j0}, C_l, γ, $C_{ds,i}$, C_{gd0}, P_{1dgd}, and P_{1cc} are fitting parameters, and V_{bi} is an estimated bias voltage. To make the equations solvable, the choice is made for the less accurate 3.15a. For example, this is also commonly done in [22]. Using a least-squares approximation, the estimated parameters C_{j0}, V_{bi}, and γ are in this case: 1.6e-13, 69, and 0.5, using Figure 3.2. When γ equals a 0.5 it equates into the inverse root.

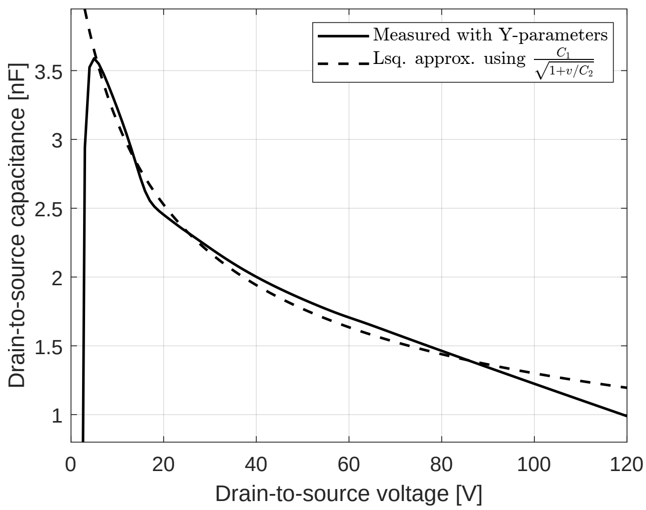

Figure 3.2: The nonlinear drain-to-source capacitance (together with the gate-to-source capacitance) is simulated using the UMS GH15 NF=5 nonlinear model. The solid line is the measured capacitance using Y-parameters, and the dashed line is a least squares approximation.

Parameters	Linear capacitance values	Nonlinear capacitance values
C_{j0}	-	0.255 nF
C	0.21 nF	-
V_{bi}	-	69 V
P_{out}	8.14 W	8.14 W

Table 3.2: The linear and nonlinear capacitance parameters used for Figure 3.3.

To determine the change in waveforms analytically, we need to use two equations: energy conservation and the voltage-to-current relationship of the drain-to-source capacitance. For simplicity, we assume a DC feed; this lowers the order of the differential equations to solve. The setup is shown in Figure 3.1. The current through the drain-to-source capacitance can be found by combining 3.5 and 3.9:

$$i_C(t) = I_0\left(1 - \frac{\sin(\omega t + \phi)}{\sin(\phi)}\right) \tag{3.16}$$

Where I_0 is the DC current supplied and $\phi = -\arctan\left(\frac{2}{\pi}\right)$. Next, one can again set the voltage-to-current relationship of the capacitor, working it out in the case of the nonlinear capacitance (3.15):

$$\begin{aligned}
C \cdot \frac{dv_c(t)}{dt} &= i_c(t) \\
\int_0^{v_c} C dv_c &= \int_{\pi/\omega}^{t} i_c(t)dt \\
-2C_0V_{bi} + \frac{2C_0V_{bi}}{\sqrt{\frac{v}{V_{bi}}+1}} + 2C_0\frac{v}{\sqrt{\frac{v}{V_{bi}}+1}} &= \frac{I_0}{\omega}\left(\frac{\sqrt{\pi^2+4}\cos(\omega t)}{(2\sqrt{1+4/\pi^2})} - \frac{\sqrt{(\pi^2+4}\sin(\omega t)}{(\pi\sqrt{1+4/\pi^2})} + t\omega - \frac{3\pi}{2}\right)
\end{aligned} \tag{3.17}$$

Next, because of energy conservation, we know that the DC power at the input is equal to the AC power at the output. Note that this is only the case for an ideal lossless Class E. This results in the following equation:

$$I_0 = \frac{P_{out}}{V_{DD}} \tag{3.18}$$

Combining 3.17 and 3.18 and solving it for v results in a rather lengthy equation that is solvable analytically. The resulting voltage waveform and the linear drain-to-source capacitance are shown in Figure 3.3. The parameters used are stated in Table 3.2. When using the nonlinear capacitance, the peak voltage can be up to 1.3 times higher compared to the linear capacitance. In [22], they stated that the output load impedance varies by maximally 5%, and the output voltage is unaffected. Although the approximation is decent, it is far from perfect. Even though the drain-to-source capacitance is clearly non-constant, an average drain-to-source capacitance of around 2.1 pF is chosen. The final comparison between the nonlinear and linear cases is stated later in this section, but variation can be significant.

3.3. The nonlinear on-resistance

Using a lossless loading network, the on-resistance is the only power loss component. Therefore, an accurate approximation of its value is of great importance. The on-resistance is defined as drain-to-source voltage divided by the drain-to-source current (v_{ds}/i_{ds}), where the gate is biased to 1 V, which is close to the GaN Schottky breakdown voltage of around 1.5 V, which results in Figure 3.5b. The drain-to-source voltage versus current curve, as shown in Figure 3.4,can be approximated as linear in the triode region, but at the transition between the triode region and saturation region, it is clearly not linear, and unfortunately, in this region, the resistor will operate at maximum power. The

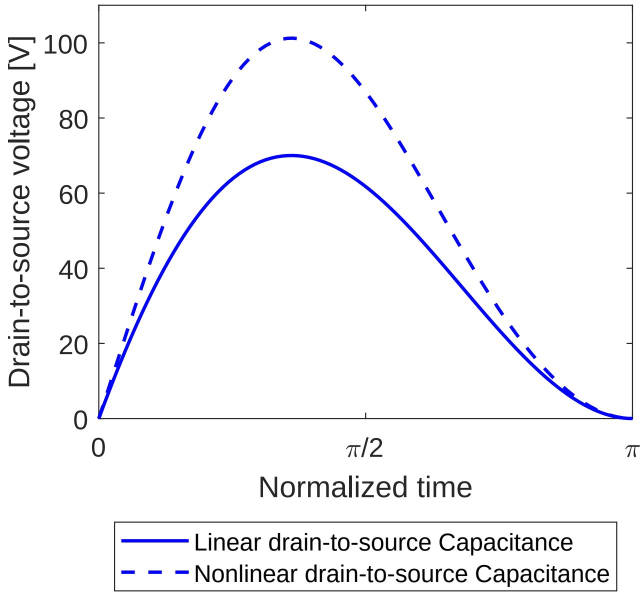

Figure 3.3: The drain voltage comparison of linear and nonlinear drain-to-source capacitance. To reduce the peak voltage the drain-to-source voltage needs to be reduced, or a Class E/F3 should be used.

designer, therefore, needs to choose a linear on-resistance at maximum output power; this is not necessarily the on-resistance when v_{ds} equals zero voltage.

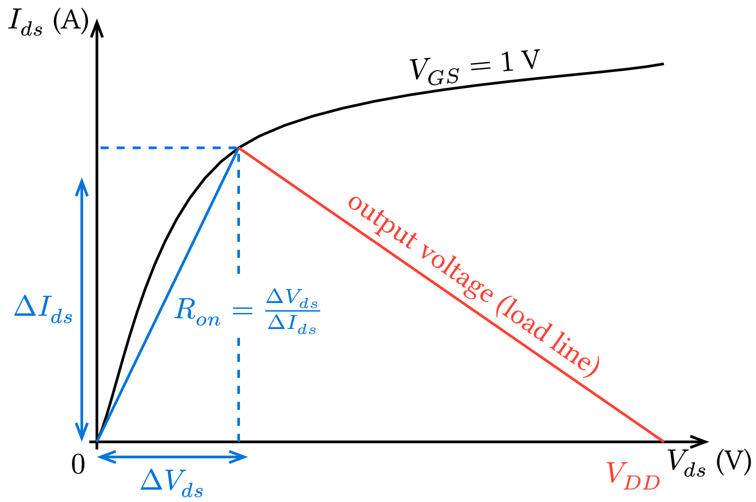

Figure 3.4: The on-resistance is shown to be dependent on the load-line. Where it is linear when it is operating the triode region but nonlinear when it is operating close to the saturation region.

It is also important to note that the v_{ds}/i_{ds} curve depends somewhat on frequency depending on the model used [32]. Therefore, a more accurate approximation can be made by designing a switching amplifier. In this case, the drain is biased with a DC feed, the load is connected with a DC decoupling capacitor, and the load resistor is varied depending on the required v_{ds} during on time. This results in the time domain Figure 3.5a, where both the i_{ds} and v_{ds} are plotted. The on-resistance can be approximated at a one-time point or monitoring the voltage-to-current relationship through time approximation at $\tilde{1}$20 ps. Both methods' results are similar, but the DC simulation is faster and has good results.

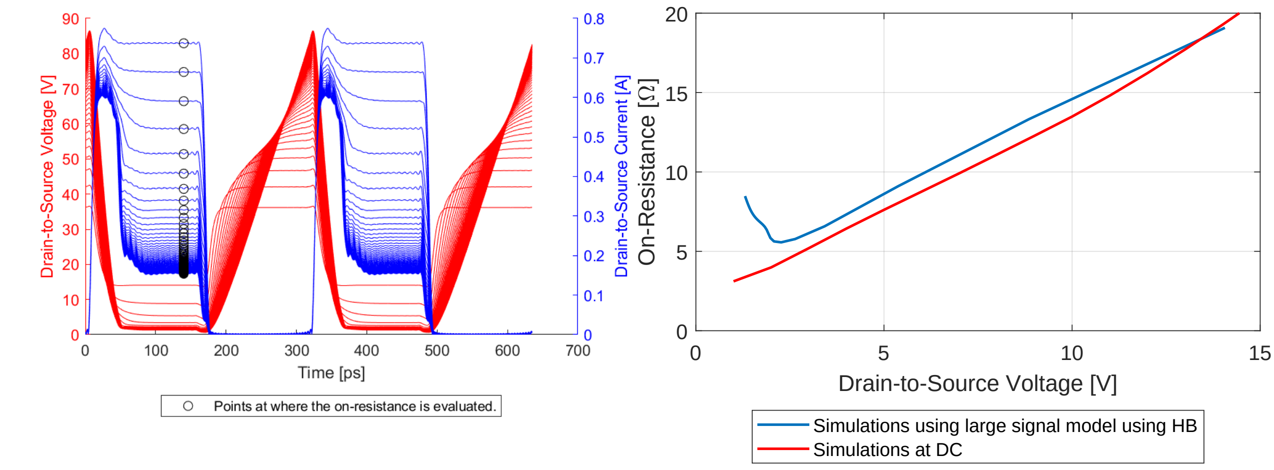

(a) The voltage and current waveforms for a switching PA are simulated using the UMS GH15 nonlinear model.

(b) The on-resistance comparison of the DC or HB methods versus drain-to-source voltage.

Figure 3.5: 3.5a shows the drain-to-source voltage and current, where the black circles show the evaluation points of the on-resistance. These black circles are thereafter plotted in 3.5a, where one can see that the DC simulations are accurate up to low voltages, after which both methods seem to be less accurate. However, this is not an important region because this is only for very low output powers. The general approximation used is a constant of 8 Ω.

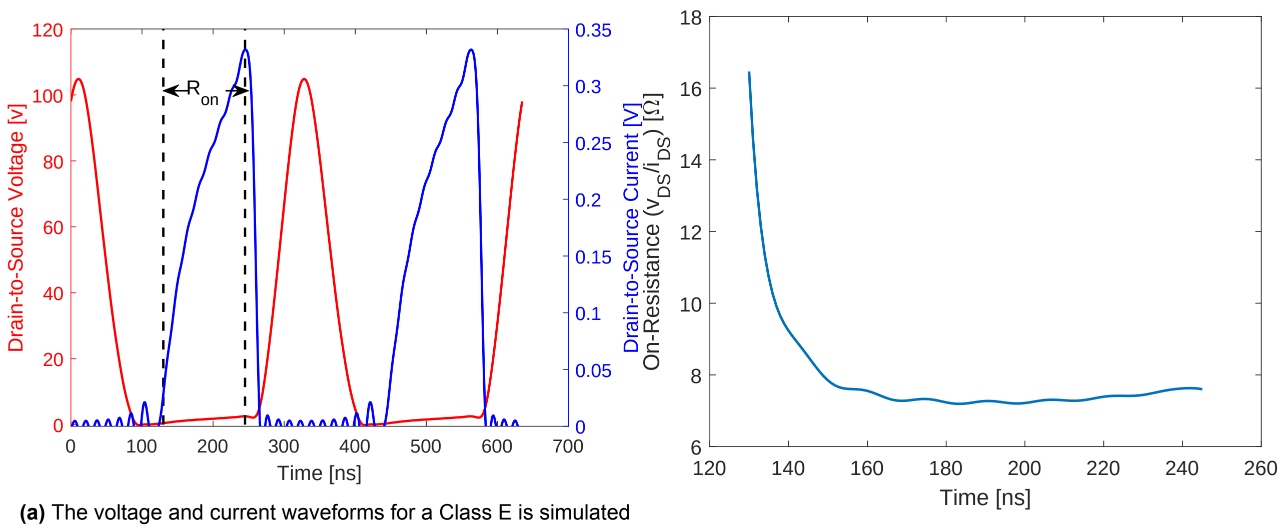

(a) The voltage and current waveforms for a Class E is simulated using the UMS GH15 NF=5 nonlinear model.

(b) The on-resistance versus time when the transistor is turned on.

Figure 3.6: 3.6a shows the drain-to-source voltage and current waveforms for a Class E with a q of 1.412. The dashed lines show the region where the transistor is turned on. Figure 3.6b exhibits the on-resistance in this region. In the end, the on-resistance is approximated at 8Ω.

To determine the effective on-resistance during Class E operation becomes a little bit more difficult. This is because the dynamic drain-to-source voltage changes depending on the configuration. Using a UMS GH15 with five fingers, we can design a Class E with a q of 1.412. One can plot the following figures in this configuration: 3.6b. The drain-to-source voltage and current with ZVS and ZVSS. Note that tuning is not easy, and depending on the operating frequency, ZVS and/or ZVSS are not even possible (Equation 3.3). In Figure 3.6b, the on-resistance is plotted during the on time of the transistor. It is easy to recognize that even though the on-resistance is nonlinear, a decent, constant approximation is possible. In this case, the on-resistance is approximated by 8 Ω, due to the flatness of the voltage waveform.

3.4. Comparing the nonlinear and linear model

A linear model is used for stable and fast modeling. In this section, the accuracy of the linear model is shown by comparing a linear and nonlinear model for Class E simulation. The analysis of the previous sections are used to estimate the parameters of the linear model. First, we assume that a Class E model with finite inductance should be used; the application uses load modulation; therefore, the choice falls upon Quasi Load Independent (QLI) Class E (q=1.3). An advantage of QLI Class E is that when the real load changes, the drain efficiency stays, ideally, almost unchanged. This is because the transistor stays ZVS; only the slope changes; therefore, it becomes non-ZVSS. First, the setup of Figure 2.5 is used where the switching device is either a switch with non-zero on-resistance or the nonlinear UMS GH15 model with five fingers. The width of the transistor is maximal at 175 um, and the supply voltage is 25 V. The drain-to-source capacitance at 25 V is 0.21 pF (Figure 3.2), and the on-resistance is 8 Ω.

A method later discussed is used to find the required load in the case of finite on-resistance for ZVS and ZVSS. All the required values are stated in Table 3.3. This results in Figure 3.7, which shows the two waveforms under each other. The linear model (top one) has an ideal ZVS and ZVSS, and the nonlinear model (bottom one) has neither. Further tuning can be applied, but this will complicate the process, and the benefits are limited. To determine whether the Quasi Load Independent (QLI) behaviour is present, we can look at Figure 3.8. The real load impedance is swept from 150 to 300, with the optimal load is 152 Ω as shown in the table, and the drain efficiency is plotted. Although the drain efficiency is almost constant in the ideal case, this non-ideal model is not used when the real load impedance changes. The linear model varies between 90% and 86% drain efficiency, but the nonlinear model varies between 90% and 82%. This is expected because the nonlinear model is no longer ZVS. Even though the drain efficiency degradation is worse for the nonlinear model than the linear model, the QLI behaviour is still clearly present.

Parameter	Value	Unit
f_0	3.15	GHz
V_{DD}	25	V
R_{on}	8	Ω
C_{ds}	0.21	pF
L_f	7.1	nF
R_x	152	Ω
X_x	46	Ω
L_0	77	nF
C_0	33	fF

Table 3.3: QLI Class E parameters for both the nonlinear model and the linear.

3.5. Amplitude modulation

A single-ended Class E configuration does not support amplitude modulation (AM); therefore, additional circuitry is needed to implement AM. Supply modulation could provide AM modulation, but this would limit the maximum drain efficiency. An alternative method is changing the transistor's on-resistance; in this method, the transistor consumes the power instead of the source. This will keep the maximum drain efficiency high but decrease the drain efficiency in Power-Backoff (PBO). In the case of a simple switchmode pulsed power amplifier A, the effect of the on-resistance on the output power can be described as:

$$P_{out} = \frac{8}{\pi^2} \frac{R_L}{(R_L + R_{on})^2} \frac{V_{DD}^2}{\left(1 + \frac{R_{on}}{R_L+R_{on}}\right)^2} \approx \frac{8}{\pi^2} \frac{R_L}{(R_L + R_{on})^2} V_{DD}^2 \tag{3.19}$$

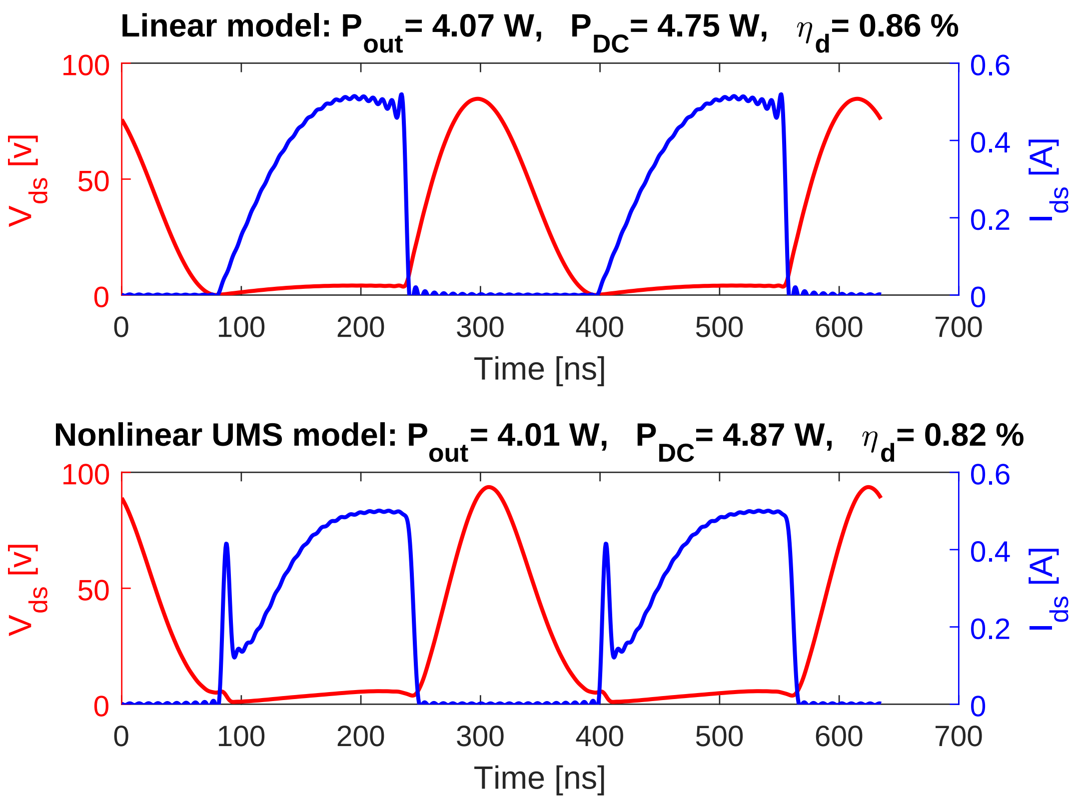

Figure 3.7: Using Table 3.3, simulating QLI Class E using both the linear and nonlinear models. The linear model has an ideal ZVS and ZVSS, and the nonlinear model has neither. However, the expected output power and DC power are approximately the same.

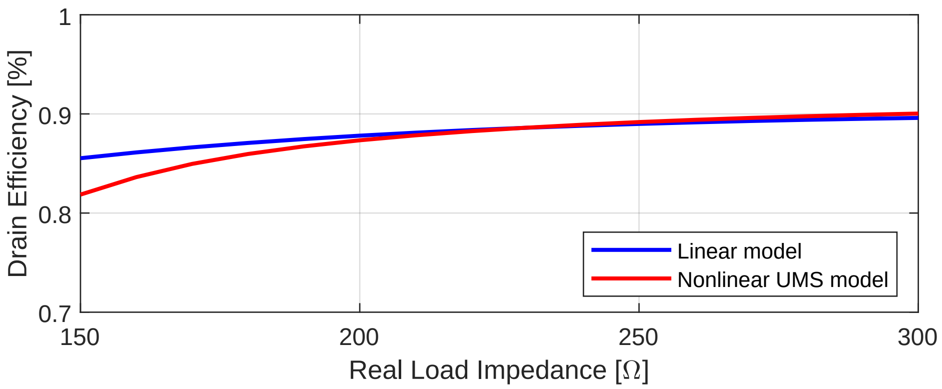

Figure 3.8: Drain efficiency is plotted versus load using Table 3.3. Where the nonlinear and linear drain efficiencies are remarkably similar.

Which is clearly not a linear relationship. In Figure 3.9, the drain efficiency versus output voltage amplitude is plotted. It shows that Class E, a switch mode device, is clearly nonlinear, and Class B is not. Two ways to dynamically change the on-resistance are changing the gate bias voltage and changing the number of transistors that are turned on[7]. The gate bias voltage can be changed so that the drain-to-source voltage-to-current relationship changes and, therefore, the on-resistance. The effect of the gate-to-source voltage on the R_{on} can be found in Figure 3.4. It is clear that the slope at a drain-to-source voltage of 0 V changes depending on the gate-to-source voltage. The advantage of this method is the ease of implementing such a circuit because it only requires one driver and a variable-biasing circuit. An alternative is to change the number of active transistors; in this case, multiple drivers can drive each transistor separately. The advantage is that when fewer transistors are turned on, the output power is lower, but the driving power is also lower (because fewer transistors need to be driven), improving the PAE in PBO. This last method is therefore applied. In

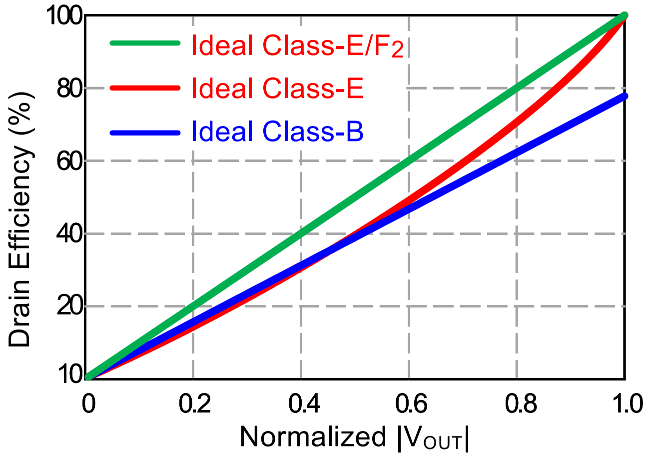

Figure 3.9: The drain-efficiency versus normalized $|V_{out}|$ for different PA Classes, from [24]. For Class E/F_2, we can see that the drain efficiency is a linear function of the output voltage, therefore the output power, just like in Class-B.

this case, the linear and the nonlinear models can again be compared, shown in Figure 3.10. In the right figure, the output power versus input Code Word (CW) is plotted, and the nonlinear model's linearity is clearly worse. This is mainly due to the nonlinearity of the on-resistance; this can be seen in the left figure. A different output power is seen for the same number of transistors that are turned on. This means the on-resistance is good, approximated at maximum output power, but bad in PBO. The on-resistance in PBO seems to be greater in the nonlinear model.

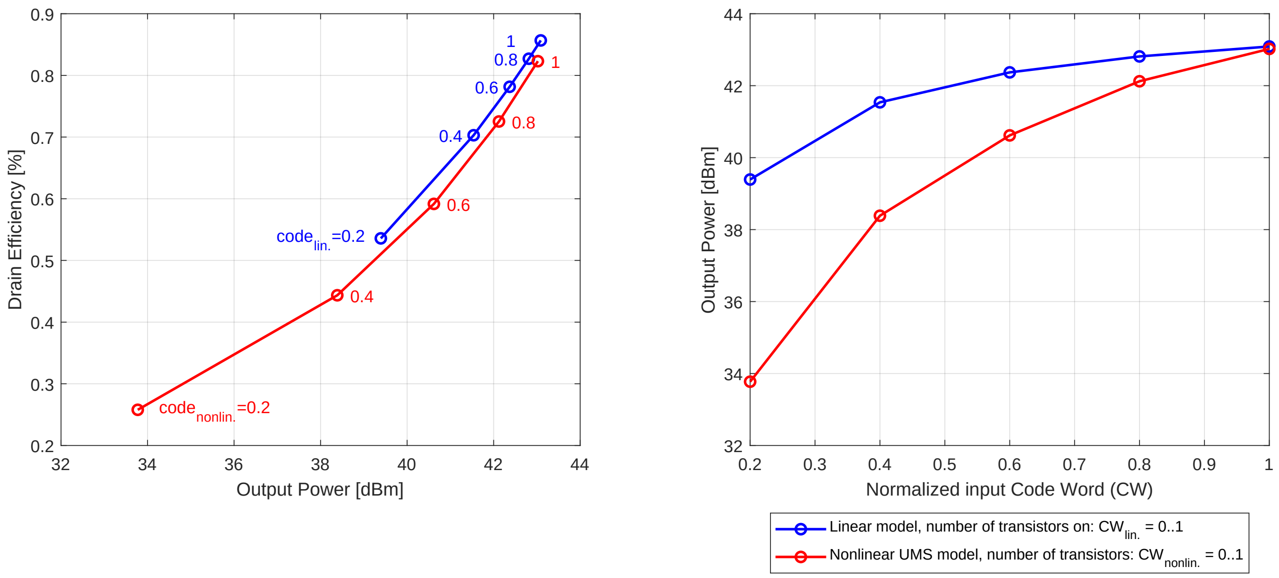

Figure 3.10: On the left, the drain efficiency is plotted versus the output power. The normalized code word is defined between 0 and 1, where 0 means no transistors are turned on, and one means all the transistors are turned on. At the right is the output power versus normalized input Code Word plotted, where it is clear that the power linearity is worse for the nonlinear model compared to the linear model.

4

The state-space approach

Class E is solved most of the time in the time domain because the large discontinuity caused by switching requires theoretically infinite harmonics. Calculating these harmonics requires a lot of computing power, which is impractical. In contrast to Class E, for Class F/F-1, the higher-order harmonics are often ignored, resulting in the often-used frequency-domain solution. All-in-all, for Class E, the time-domain solution is required, but in the time domain, we still have multiple ways to find a solution: solving directly the classical differential equations, solving using a Laplace transform, or using the general solution for a state-space. Earlier analysis in this report solves the differential equations using the direct method. These differential equations were two second-order differential equations, in the case that a finite inductor is used and assuming an ideal series resonator filter [2]. But without using ideal components, a classical Class E exists out of four integrators and, therefore, two fourth-order differential equations (Equation 4.6). In this case, using Laplace transforms to simplify the analysis is useful. However, in the case of a three-way Class E power amplifier, a circuit can exist out of 12 integrators, and a more systematic way to solve such a circuit is necessary. In this case, the state-spaces approach becomes useful because of their fast general solutions using eigenvalues.

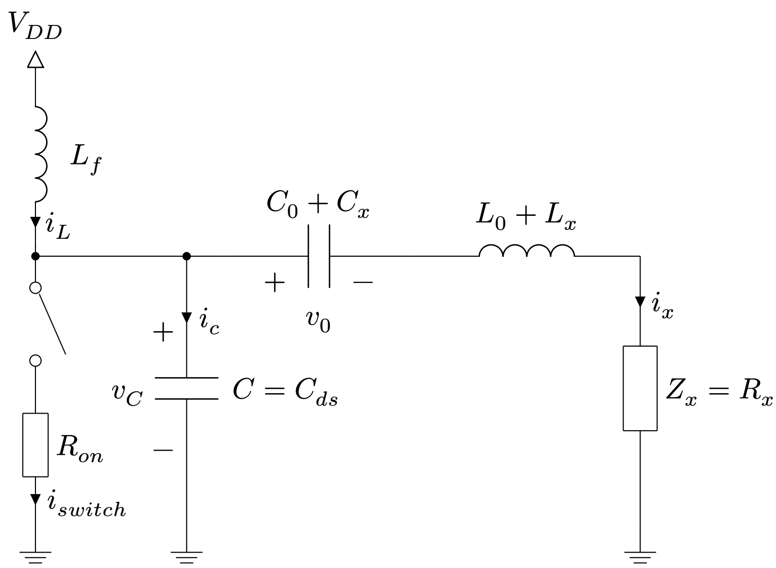

Figure 4.1: The Class E with a shunt capacitance, a finite dc feed, and a series resonator.

4.1. Setting up the state-space equations

In [39], the state-space approach is applied for Class E. The analysis consists of first setting up the four first-order state-space equations. These are combined into a state-space matrix, where the general solution can be found by assuming continuity of voltage and currents. The analysis is done for Figure 4.1, where L_x and C_x are used for adding a reactive part to the load (instead of adding an ideal component as in Figure 2.5). There are two capacitors and two inductors; this results in four integrators and, therefore, four equations. The state variables are defined in matrix $\mathbf{q}(t)$ as follows:

$$\mathbf{q}(t) = \begin{bmatrix} i_L(t) \\ i_x(t) \\ v_c(t) \\ v_0(t) \end{bmatrix} \tag{4.1}$$

A capacitor differentiates the voltage, and an inductor differentiates the current. Therefore, in the case that the switch is on and as a function of the state variables, we can set up the four equations:

$$L_F \frac{di_l(t)}{dt} = V_{DD} - v_c(t) \tag{4.2a}$$

$$(L_x + L_0)\frac{di_x(t)}{dt} = v_c(t) - v_0(t) - R_x i_x(t) \tag{4.2b}$$

$$C_{ds}\frac{dv_C(t)}{dt} = i_L(t) - i_x(t) - \frac{v_C(t)}{R_{on}} \tag{4.2c}$$

$$(C_x + C_0)\frac{dv_0}{dt} = i_x(t) \tag{4.2d}$$

$$\tag{4.2e}$$

When the switch is off, R_{on} becomes very large (>10 kOhm). This changes the third equation 4.2c as follows:

$$C_{ds}\frac{dv_C(t)}{dt} = i_L(t) - i_x(t) \tag{4.3}$$

These equations can now be put in the state-space matrix format:

$$\frac{d\mathbf{q}(t)}{dt} = \mathbf{A} \cdot \mathbf{q}(t) + \mathbf{B} \tag{4.4}$$

Where there are two $\mathbf{A}$ matrices and two $\mathbf{B}$ matrices called: $\mathbf{A_1}$, $\mathbf{A_2}$, $\mathbf{B_1}$, $\mathbf{B_2}$. Defined as follows:

$$\frac{d}{dt}\begin{bmatrix} i_L(t) \\ i_x(t) \\ v_c(t) \\ v_0(t) \end{bmatrix} = \begin{bmatrix} 0 & 0 & -1/L_f & 0 \\ 0 & -R_x/(L_f+L_0) & 1/(L_f+L_0) & -1/(L_f+L_0) \\ 1/C_{ds} & -1/C_{ds} & -1/(R_{on}C_{ds}) & 0 \\ 0 & 1/C_x + 1/C_0 & 0 & 0 \end{bmatrix} \begin{bmatrix} i_L(t) \\ i_x(t) \\ v_c(t) \\ v_0(t) \end{bmatrix} + \begin{bmatrix} V_{DD}/L_f \\ 0 \\ 0 \\ 0 \end{bmatrix}$$

$$\dot{\mathbf{q}}_\mathbf{1}(t) = \mathbf{A_1} \cdot \mathbf{q_1}(t) + \mathbf{B_1} \tag{4.5}$$

In case that the transistor is turned on.

$$\frac{d}{dt}\begin{bmatrix} i_L(t) \\ i_x(t) \\ v_c(t) \\ v_0(t) \end{bmatrix} = \begin{bmatrix} 0 & 0 & -1/L_f & 0 \\ 0 & -R_x/(L_f+L_0) & 1/(L_f+L_0) & -1/(L_f+L_0) \\ 1/C_{ds} & -1/C_{ds} & 0 & 0 \\ 0 & 1/C_x + 1/C_0 & 0 & 0 \end{bmatrix} \begin{bmatrix} i_L(t) \\ i_x(t) \\ v_c(t) \\ v_0(t) \end{bmatrix} + \begin{bmatrix} V_{DD}/L_f \\ 0 \\ 0 \\ 0 \end{bmatrix} \tag{4.6}$$

$$\dot{\mathbf{q}}_\mathbf{2}(t) = \mathbf{A_2} \cdot \mathbf{q_2}(t) + \mathbf{B_2}$$

In case that the transistor is turned off.

4.2. Solving the State-Space Equations

The general solution of any state-space equation is as follows:

$$\mathbf{q}(t) = e^{\mathbf{A}t}\mathbf{q_0} + \int_0^t e^{\mathbf{A}(t-\tau)}\mathbf{B}\,d\tau \tag{4.7}$$

Where $\mathbf{q_0}$ is the initial condition of the state. Note that $e^{\mathbf{A}t}$ is the exponential matrix; although it is analogous to the ordinary exponential function, its computation is slightly more difficult. It can be derived in multiple ways. When using eigenvalues and eigenspaces, the solution in the diagonalizable case is as follows:

$$e^{\mathbf{A}t} = \mathbf{T}^{-1} \cdot \begin{bmatrix} e^{\lambda_1 t} & \dots & 0 \\ \vdots & \ddots & \vdots \\ 0 & \dots & e^{\lambda_N t} \end{bmatrix} \cdot \mathbf{T} \tag{4.8}$$

Where the following holds:

1. N is the length of the matrix $\mathbf{A}$ (N x N)
2. λ is an eigenvalue of matrix $\mathbf{A}$ (The solution to $\det(\mathbf{A} - \lambda\mathbf{I})$)
3. $\mathbf{T}$ is the eigenspace matrix $\mathbf{A}$ (The combined vectors resulting from the eigenvalues)

In the case that all components are linear and time-invariant and **A** is time-independent, Equation 4.7 can be rewritten using:

$$\int_0^t e^{\mathbf{A}(-\tau)}\,\mathbf{B}\,d\tau = \mathbf{A}^{-1}\left(\mathbf{I} - e^{-\mathbf{A}t}\right)\,\mathbf{B} \tag{4.9}$$

Which results in:

$$\mathbf{q}(t) = e^{\mathbf{A}t}\,\mathbf{q_0} + e^{\mathbf{A}t}\left((\mathbf{A}^{-1}\left(\mathbf{I} - e^{-\mathbf{A}t}\right)\right)\,\mathbf{B} \tag{4.10}$$

We can apply the solution 4.10 to the two state-space equations 4.5 and 4.6. This results in the general solution for the two equations:

$$\mathbf{q_1}(t) = e^{\mathbf{A_1}t}\,\mathbf{q_{01}} + e^{\mathbf{A_1}t}\left(\mathbf{A_1}^{-1}\left(\mathbf{I} - e^{-\mathbf{A_1}t}\right)\right)\,\mathbf{B_1} \tag{4.11a}$$

$$\mathbf{q_2}(t) = e^{\mathbf{A_2}t}\,\mathbf{q_{02}} + e^{\mathbf{A_2}t}\left(\mathbf{A_2}^{-1}\left(\mathbf{I} - e^{-\mathbf{A_2}t}\right)\right)\,\mathbf{B_2} \tag{4.11b}$$

And because $e^{\mathbf{A}t}\mathbf{A}^{-1}$ is commutative this can be simplified into:

$$\begin{cases} \mathbf{q_1}(t) & = e^{\mathbf{A_1}t_1}\,\mathbf{q_{01}} + \mathbf{A_1}^{-1}\left(e^{\mathbf{A_1}t_1} - \mathbf{I}\right)\,\mathbf{B_1} \\ \mathbf{q_2}(t) & = e^{\mathbf{A_2}t_2}\,\mathbf{q_{02}} + \mathbf{A_2}^{-1}\left(e^{\mathbf{A_2}t_2} - \mathbf{I}\right)\,\mathbf{B_2} \end{cases} \tag{4.12}$$

Knowing $e^{\mathbf{A}t}$, $\mathbf{A}$, and $\mathbf{B}$, the only question is still to determine the initial solution $\mathbf{q_0}$. Just like the earlier differential equation solution, the boundary conditions should hold. In other words, we have two equations where the beginning of the beginning of one equation is the start of the other:

$$\begin{cases} \mathbf{q_{02}} = \mathbf{q_1}(t_1) & = e^{\mathbf{A_1}t_1}\,\mathbf{q_{01}} + \mathbf{A_1}^{-1}\left(e^{\mathbf{A_1}t_1} - \mathbf{I}\right)\,\mathbf{B_1} \\ \mathbf{q_{01}} = \mathbf{q_2}(t_2) & = e^{\mathbf{A_2}t_2}\,\mathbf{q_{02}} + \mathbf{A_2}^{-1}\left(e^{\mathbf{A_2}t_2} - \mathbf{I}\right)\,\mathbf{B_2} \end{cases} \tag{4.13}$$

Where t_1 is the switching time from on to off ($t_1 = d \cdot \pi/\omega$). And t_2 is the switching time from off to on ($t_2 = (2-d) \cdot \pi/\omega$). Where d is a measure of the duty cycle between 0 and 2, as defined before. These two equations contain two unknowns; the solution can be found using basic algebra; however, a more general solution can be found in Section 4.6.

4.3. Finding ZVS and ZVSS

Previously, an ideal resonator with infinite Q was assumed; this simplifies the analysis in that the optimum load could simply be determined by looking at the ideal load at the fundamental voltage (Equation 2.20). However, in the case of finite Q, higher harmonics become present at the load. To again find the correct load, a numerical minimization technique is applied. A standard least-squares algorithm is fast and does the job; however, more advanced solvers with range selection are preferred. The parameters to solve for are R_x and either C_x or L_x, depending on the application (both are also possible using more advanced algorithms). The voltage v at switching is defined as $\mathbf{q_{02}}[3]$ and the voltage-slope as $\dot{\mathbf{q}}_{\mathbf{02}}[3]$, referring to equation 4.1.

4.4. Calculating the power and efficiency using the state-space equations

4.4.1. DC Power

In [39], the DC power using these state-space equations is given as follows:

$$P_{DC} = V_{DD} \cdot \frac{1}{T} \cdot \left(\int_0^{t_1} i_f(t)\,dt + \int_{t_1}^{t_2} i_f(t)\,dt \right) \tag{4.14}$$

Where T is the total period and the combination of t_1 and t_2. This can be rewritten using the state-space variables as:

$$P_{DC} = \frac{1}{T}\mathbf{C_{DC}} \left(\int_0^{t_1} \mathbf{q_1}\,dt + \int_0^{t_2} \mathbf{q_2}\,dt \right) \mathbf{C_{DC}}^{\mathbf{T}} \tag{4.15}$$

where:

$$\mathbf{C_{DC}} = \begin{bmatrix} \sqrt{V_{DD}} & 0 & 0 & 0 \end{bmatrix} \tag{4.16}$$

The length of the $\mathbf{C_{DC}}$ matrix depends on the state-space size. We need to apply some tricks to find the integral of $\mathbf{q_1}$. We can integrate equation 4.4, knowing that matrices $\mathbf{A}$ and $\mathbf{B}$ are time-independent. After that, simplify the equations:

$$\begin{aligned} \int_0^{t_n} \frac{d\mathbf{q}(t)}{dt}\,dt &= \mathbf{A} \int_0^{t_n} \mathbf{q}(t)\,dt + \mathbf{B} \int_0^{t_n} \mathbf{q}(t)\,dt \\ \mathbf{q}(t_n) - \mathbf{q}(0) &= \mathbf{A} \int_0^{t_n} \mathbf{q}(t)\,dt + \mathbf{B}t_n \\ \int_0^{t_n} \mathbf{q}(t)\,dt &= \mathbf{A}^{-1} \left(\mathbf{q}(t_n) - \mathbf{q}(0) - \mathbf{B}t_n \right) \end{aligned} \tag{4.17}$$

Next, t_n can be replaced by either t_1 or t_2. The generalized solution, not discussed in the paper, for a total of N different state-spaces sequenced is therefore:

$$P_{DC} = \frac{1}{T}\mathbf{C_{DC}} \left(\mathbf{I_{DC}} \right) \mathbf{C_{DC}}^{\mathbf{T}} \tag{4.18}$$

Where $\mathbf{I_{DC}}$ is the total DC current found as:

$$\mathbf{I_{DC}} = \sum_{n=1}^{N} \mathbf{A_n}^{-1} \left(\mathbf{q}(t_n) - \mathbf{q}(0) - \mathbf{B_n}t_n \right) \tag{4.19}$$

N is the total amount of state spaces, and t_n is the different switching times.

4.4.2. Total output power

The total output power is generally defined as:

$$P_{total\,out} = R_x \cdot \frac{1}{T} \cdot \int_0^T i_x^2(t)\,dt \tag{4.20}$$

The problem, however, is that the total waveform described by two equations defined in different intervals. Therefore, the integral needs to be separated between two intervals:

$$P_{total\,out} = R_x \cdot \frac{1}{T} \cdot \left(\int_0^{t_1} i_x^2(t)\,dt + \int_{t_1}^{t_2} i_x^2(t)\,dt \right) \tag{4.21}$$

Nevertheless, because both equations are solved starting from zero, the solution can be found in a few intermediate steps. Next, define the intermediate variables:

$$\mathbf{W_1} = \int_0^{t_1} \mathbf{q_1 q_1}^{\mathbf{T}}\,dt \tag{4.22a}$$

$$\mathbf{W_2} = \int_0^{t_2} \mathbf{q_2 q_2}^{\mathbf{T}}\,dt \tag{4.22b}$$

Both $\mathbf{W_1}$ and $\mathbf{W_2}$ can be further solved, as shown in [39].

$$P_{total\,out} = \frac{R_x}{T} \cdot (\mathbf{W_1}[\mathbf{2},\mathbf{2}] + \mathbf{W_2}[\mathbf{2},\mathbf{2}]) \tag{4.23}$$

4.4.3. Fundamental output power

Note that the interest lies in the fundamental output power. This was not discussed in the cited paper [39]; this analysis is, therefore, an extension of the original paper. To find the fundamental output power, the fundamental Fourier series component of the current is found with:

$$P_{out,f0} = \frac{R_x \cdot i_{x,f0} \cdot i_{x,f0}^*}{2} \tag{4.24}$$

Where:

$$i_{x,f0} = \frac{2}{T} \cdot \int_0^T e^{-2\pi j \cdot \frac{t}{T}} \cdot i_x(t)\,dt \tag{4.25}$$

The solution until now makes use of two different state-space equations, and in a next section up to 2^3 state-space equations. All these equations hold for a certain time. The signal is defined in separate time intervals, which can be separated as follows:

$$i_{x,f0} = \frac{2}{T} \cdot \left(\int_0^{t_1} e^{-2\pi j \cdot \frac{t}{T}} \cdot i_x(t)\,dt + \int_{t_1}^{t_2} e^{-2\pi j \cdot \frac{t}{T}} \cdot i_x(t)\,dt + \dots \right) \tag{4.26}$$

First, we know that the state-space variable is defined as $\mathbf{q} = \begin{bmatrix} i_l & i_x & v_C & v_0 \end{bmatrix}$, where i_x is the current that flows through the hybrid coupler. Defining $\hat{\mathbf{q}}(1)$ as the fundamental component of the state-space variables. Now equation 4.26 can be expressed using state-space variables as:

$$\hat{\mathbf{q}}(1) = \cdot\frac{2}{T} \cdot \left(\int_0^{t_1} e^{-2\pi j \cdot \frac{t}{T}} \cdot \mathbf{q}(t)\,dt + \int_{t_1}^{t_2} e^{-2\pi j \cdot \frac{t}{T}} \cdot \mathbf{q}(t - t_1)\,dt + \dots \right) \tag{4.27}$$

Where the whole state is integrated over time, this results in the fundamental currents and voltages in one matrix. This is in the general case, in practice we only care about the fundamental output current and fundamental drain-to-source voltage. The total period is the combination of the separate time steps, the total number of time steps is called N:

$$T = t_0 + 1_1 + \dots + t_N = \sum_{n=0}^{N} t_n \tag{4.28}$$

Next, we need to do some time shifting of the integral:

$$\int_0^{dt_n} e^{-2\pi j\cdot\frac{t+t_{n-1}}{T}} \cdot \mathbf{q}(t)\,dt \tag{4.29}$$

Were dt_n is equal to $t_n - t_{n-1}$. Like before, to compute the integral, some derivation is required; this can be found in Appendix B. The result is as follows:

$$\begin{aligned}\hat{\mathbf{q}}(1) &= \frac{2}{T}\sum_{n=1}^{N}\left(\mathbf{A}_n - \frac{2\pi j}{T}\cdot\mathbf{I}\right)^{-1} \\ &\cdot\left(e^{-2\pi j\frac{t_n}{T}}\cdot\mathbf{q}_n(t_n - t_{n-1}) - e^{-2\pi j\frac{t_{n-1}}{T}}\cdot\mathbf{q}_n(0) - j\frac{T\mathbf{B}_n}{2\pi}\left(e^{-2\pi j\frac{t_n}{T}} - e^{-2\pi j\frac{t_{n-1}}{T}}\right)\right)\end{aligned} \tag{4.30}$$

The output power can thereafter be defined as:

$$P_{out,f0} = \frac{R_x \cdot i_{x,f0}\cdot i^*_{x,f0}}{2} \tag{4.31}$$

Where $i_{x,f0}$ is equal to the second element of $\hat{\mathbf{q}}(1)$.

4.4.4. Fundamental drain-to-source voltage and current

The final analysis is about the drain-to-source voltage and current. The problem is that the drain-to-source current is not in the state matrix, but the drain-to-source voltage is. Therefore, we start by defining the drain-to-source voltage, which is equal to v_c This can be described as follows:

$$v_{c,f0} = \frac{2}{T}\cdot\left(\int_0^{t_1} e^{-2\pi j\cdot\frac{t}{T}}\cdot v_c(t)\,dt + \int_{t_1}^{t_2} e^{-2\pi j\cdot\frac{t}{T}}\cdot v_c(t)\,dt + \ldots\right) \tag{4.32}$$

The solution to this integral is the third element of $\hat{\mathbf{q}}(1)$. Next, we can determine the drain-to-source current as follows:

$$i_{ds,f0} = \frac{2}{T}\cdot\left(\frac{1}{\mathbf{R_{eq}}(1)}\int_0^{t_1} e^{-2\pi j\cdot\frac{t}{T}}\cdot v_c(t)\,dt + \frac{1}{\mathbf{R_{eq}}(2)}\int_{t_1}^{t_2} e^{-2\pi j\cdot\frac{t}{T}}\cdot v_c(t)\,dt + \ldots\right) \tag{4.33}$$

Where R_{eq} is the matrix that combines R_{on} and R_{off} at each time moment, where the index represents the time step (see 4.42). And by applying the same analysis as for equation 4.30, we can derive the following analysis:

$$\begin{aligned}i_{ds,f0} &= \begin{bmatrix}0 & 0 & 1 & 0\end{bmatrix}\cdot\frac{2}{T}\sum_{n=1}^{N}\frac{1}{\mathbf{R_{eq}}(n)}\left(\mathbf{A}_n - \frac{2\pi j}{T}\cdot\mathbf{I}\right)^{-1} \\ &\cdot\left(e^{-2\pi j\frac{t_n}{T}}\cdot\mathbf{q}_n(t_n - t_{n-1}) - e^{-2\pi j\frac{t_{n-1}}{T}}\cdot\mathbf{q}_n(0) - j\frac{T\mathbf{B}_n}{2\pi}\left(e^{-2\pi j\frac{t_n}{T}} - e^{-2\pi j\frac{t_{n-1}}{T}}\right)\right)\end{aligned} \tag{4.34}$$

4.5. Hybrid Coupler state-space

The Z-matrix of a LMBA is given in 2.31, and for clarity, it is shown here again:

$$\begin{bmatrix}V_1\\V_2\\V_3\\V_4\end{bmatrix} = Z_0\cdot\begin{bmatrix}0 & 0 & -j & -j\sqrt{2}\\ 0 & 0 & -j\sqrt{2} & -j\\ -j & -j\sqrt{2} & 0 & 0\\ -j\sqrt{2} & -j & 0 & 0\end{bmatrix}\cdot\begin{bmatrix}I_1\\I_2\\I_3\\I_4\end{bmatrix} \tag{4.35}$$

Extra integrators will appear if the Fourier transform is taken from the matrix. This is because:

$$\mathfrak{F}\left\{\frac{dx(t)}{dt}\right\} = 2\pi f j X(f) \tag{4.36}$$

A common LMBA configuration is as follows: three ports have different phases, and one port is loaded with a resistor, as shown in Figure 4.2. These phase shifts can be implemented using another hybrid coupler or digitally. The phase shift is added to both the voltage and current, resulting in a matrix change. This is only accurate for the fundamental frequency; the second harmonic phase is compensated by a factor of two and, therefore, is not accurately described as explained in Appendix D. Note that only the typical phase shifts are applied; this is done to remove the complex part of the matrix simply. This simplifies the mathematics later on.

$$\begin{bmatrix} v_{load} \\ e^{1j\cdot\phi_1}\cdot v_1 \\ e^{1j\cdot\phi_3}\cdot v_3 \\ e^{1j\cdot\phi_2}\cdot v_2 \end{bmatrix} = Z_0 \begin{bmatrix} 0 & 0 & -j & -j\sqrt{2} \\ 0 & 0 & -j\sqrt{2} & -j \\ -j & -j\sqrt{2} & 0 & 0 \\ -j\sqrt{2} & -j & 0 & 0 \end{bmatrix} \cdot \begin{bmatrix} i_{load} \\ e^{1j\cdot\phi_1}\cdot i_1 \\ e^{1j\cdot\phi_2}\cdot i_3 \\ e^{1j\cdot\phi_2}\cdot i_2 \end{bmatrix} \tag{4.37}$$

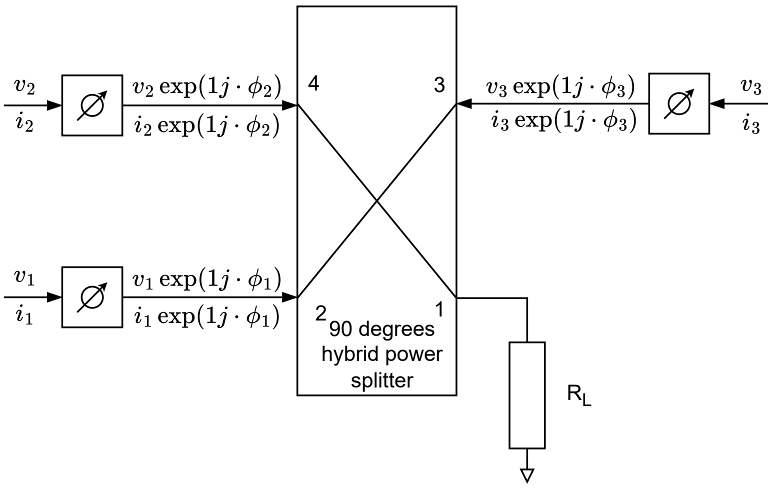

Figure 4.2: Applying rotation to the signal.

Next, the matrix can be transformed, for the fundamental frequency D, using $\phi = \left[180°, 270°\ 270°\right]$, the classical LMBA out-phasing angles, which results in the new equation:

$$\begin{bmatrix} v_{load} \\ -v_1 \\ -j\cdot v_3 \\ -j\cdot v_2 \end{bmatrix} = Z_0 \begin{bmatrix} 0 & 0 & -j & -j\sqrt{2} \\ 0 & 0 & -j\sqrt{2} & -j \\ -j & -j\sqrt{2} & 0 & 0 \\ -j\sqrt{2} & -j & 0 & 0 \end{bmatrix} \cdot \begin{bmatrix} i_{load} \\ -i_1 \\ -j\cdot i_3 \\ -j\cdot i_2 \end{bmatrix} \tag{4.38}$$

This can be simplified as follows:

$$\begin{bmatrix} v_{load} \\ v_1 \\ v_3 \\ v_2 \end{bmatrix} = Z_0 \begin{bmatrix} 0 & 0 & -1 & -\sqrt{2} \\ 0 & 0 & -\sqrt{2} & 1 \\ 1 & -\sqrt{2} & 0 & 0 \\ \sqrt{2} & -1 & 0 & 0 \end{bmatrix} \cdot \begin{bmatrix} i_{load} \\ i_1 \\ i_3 \\ i_2 \end{bmatrix} \tag{4.39}$$

Next, we can substitute $v_{load} = i_{load}\cdot Z_0$, which reduces the rank of the matrix from 4 to 3:

$$\begin{bmatrix} v_1 \\ v_2 \\ v_3 \end{bmatrix} = \begin{bmatrix} 0 & Z_0 & Z_0\sqrt{2} \\ -Z_0 & 2\frac{Z_0^2}{R_{load}} & \sqrt{2}\frac{Z_0^2}{R_{load}} \\ -\sqrt{2}Z_0 & \sqrt{2}\frac{Z_0^2}{R_{load}} & \frac{Z_0^2}{R_{load}} \end{bmatrix} \cdot \begin{bmatrix} i_1 \\ i_2 \\ i_3 \end{bmatrix} \tag{4.40}$$

The last step is to transform the frequency domain matrix into the time domain matrix, but because there are no complex parts anymore in the equation, the following holds:

$$\begin{bmatrix} v_1(t) \\ v_2(t) \\ v_3(t) \end{bmatrix} = \begin{bmatrix} 0 & Z_0 & \sqrt{2}Z_0 \\ -Z_0 & 2\frac{Z_0^2}{R_{load}} & \sqrt{2}\frac{Z_0^2}{R_{load}} \\ -\sqrt{2}Z_0 & \sqrt{2}\frac{Z_0^2}{R_{load}} & \frac{Z_0^2}{R_{load}} \end{bmatrix} \cdot \begin{bmatrix} i_1(t) \\ i_2(t) \\ i_3(t) \end{bmatrix} \tag{4.41}$$

Where R_{load} is the real load, it can be a complex load, but in that case, complex parts will again appear, making the solution more complicated. This result can connect three PAs together and find the voltage and current waveforms. However, general phase rotation has not yet been implemented. Moreover, this is important when, for example, the phase is optimized. In the next section, we will discuss this problem.

4.6. Phaseshifting and combining three PAs

To solve a switching PA using the state-space method, the general solution in Equation 4.13 can be applied, but this is just in the case of two switching moments. When three PAs are connected, a maximum of 2^3 different state-space equations can be added together. During each switching moment, the state-space initial solutions should be consistent with the end of the previous state-space. This can be mathematically stated as follows:

$$\begin{aligned} \mathbf{q_{02}} &= e^{\mathbf{A_1}t_1} \cdot q_{01} + \mathbf{A_1}^{-1}\left(e^{\mathbf{A_1}t_1} - \mathbf{I}\right) \cdot \mathbf{B_1} \\ \mathbf{q_{03}} &= e^{\mathbf{A_2}t_2} \cdot q_{02} + \mathbf{A_2}^{-1}\left(e^{\mathbf{A_2}t_2} - \mathbf{I}\right) \cdot \mathbf{B_2} \\ &\dots \end{aligned}$$

The main problem when applying this method is that the number of unique state-space equations depends on the number of out-of-phase amplifiers. To determine the sequential order of the different state-space questions, the following is done:

1. Find the number of unique rising and falling edges within the range of $0 - 2\pi$.
2. Sort them in sequential time order.
3. Find the time difference between all unique edges.
4. Use the mod function to normalize the time difference.
5. Use logic to determine whether the time is shorter than the duty cycle, determining whether the transistor is on or off.
6. Step to the next edge and repeat.

This algorithm can describe the R_{on} matrix at each time step. For example, referring to Figure 4.3, the on matrix looks something like this:

$$R_{on} \cdot \begin{bmatrix} 0 & 1 & 1 & 0 & 0 \\ 0 & 1 & 1 & 0 & 0 \\ 0 & 0 & 1 & 1 & 0 \end{bmatrix} \tag{4.42}$$

Where the columns represent the time steps and the rows which PA it is (three in this case). In this case, five state-space variables need to be solved sequentially. To find the solution to these five state spaces, we need to present them sequentially. To start, we need to rewrite the equations as follows:

$$\mathbf{q_{02}} = e^{\mathbf{A_1 t_1}} \cdot \mathbf{q_{01}} + \mathbf{A_1}^{-1} \cdot \left(e^{\mathbf{A_1 t_1}} \cdot \mathbf{q_{01}} - \mathbf{I}\right) \cdot \mathbf{B_1} \tag{4.43}$$

In which we define $A_{te}(t_x)$ as the exponential matrix at time step t_X. Substituting this, we can rewrite it in a more readable form:

$$\mathbf{q_0}(2) = \mathbf{A_{te}}(1) \cdot \mathbf{q_0}(1) + \mathbf{B_{te}}(1) \tag{4.44}$$

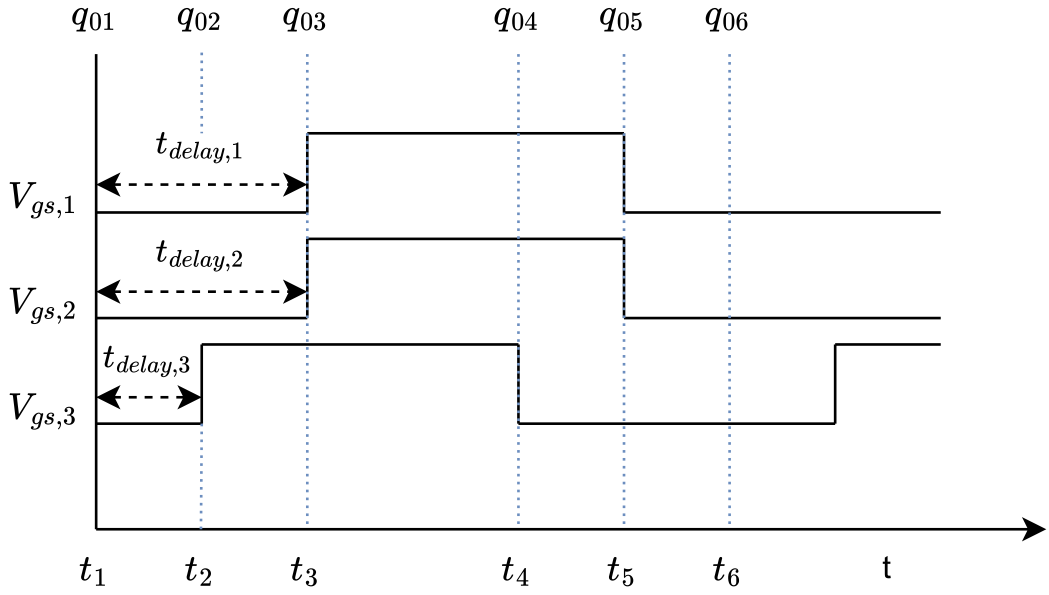

Figure 4.3: For different time steps, for all three amplifiers separately, we have either R_{on} or R_{off} . Depending on the delay there can be two different state-spaces or more. In this figure there are five different state spaces, which all have a different initial state.

Using this notation, we can state the total problem as follows:

$$\begin{aligned} \mathbf{q_0}(n) &= \mathbf{A_{te}}(n-1) \cdot \mathbf{q_0}(n-1) + \mathbf{B_{te}}(n-1) \\ \mathbf{q_0}(1) &= \mathbf{A_{te}}(n) \cdot \mathbf{q_0}(n) + \mathbf{B_{te}}(n) \end{aligned} \tag{4.45}$$

In this equation, n is the state-space number from 1 up to N, where N is the maximum number of state-spaces. The solution for $N > 1$ can be found as follows:

$$\mathbf{q_0}(N) = \frac{\prod_{k=1}^{N-1} \mathbf{A_{te}}(N-k) \cdot \mathbf{B_{te}}(N) + \sum_{k=1}^{N-2} \left(\left(\prod_{l=1}^{N-1-k} \mathbf{A_{te}}(N-l) \right) \cdot \mathbf{B_{te}}(k) \right) + \mathbf{B_{te}}(N-1)}{1 - \prod_{k=1}^{N-1} \mathbf{A_{te}}(N-k) \cdot \mathbf{A_{te}}(N)} \tag{4.46}$$

For example, when filling in $N = 2$:

$$\mathbf{q_0}(2) = \frac{\mathbf{A_{te}}(1) \cdot \mathbf{B_{te}}(2) + \mathbf{B_{te}}(1)}{1 - \mathbf{A_{te}}(1)\mathbf{A_{te}}(2)} \tag{4.47}$$

The other solutions can be found by substitution, using:

$$\mathbf{q_0}(n-1) = \mathbf{A_{te}} \cdot \mathbf{q_0}(n) + \mathbf{B_{te}}(n) \tag{4.48}$$

4.7. The complete solution

The final solution combines three Class E state-space equations into one. and combines it with the hybrid coupler. One can again look at Figure 4.1, but in this case, v_x is no longer connected to a load R_x but to the hybrid coupler. The voltage-to-current relationship of the hybrid coupler is defined in 4.41. This relates the three state-space PAs together; the voltage over the inductor relates the current to the voltage.

$$(L_x + L_0)\frac{di_x(t)}{dt} = v_c(t) - v_0(t) - v_x \tag{4.49}$$

Where in the previous case $v_x = R_x \cdot i_x$, now, using Equation 4.41, v_{x1} is defined as follows:

$$v_{x1} = Z_0 \cdot i_{x2} + \sqrt{2} Z_0 \cdot i_{x1} \tag{4.50}$$

Combining all three Class E Pas results, therefore in N 12x12 matrices where, for example, the total matrix terminated by a load of Z_0 is as follows:

$$\mathbf{A} = \begin{bmatrix} 0 & 0 & -1/L_f & 0 & 0 & 0 & 0 & 0 & 0 & 0 & 0 & 0 \\ 0 & 0 & 1/(L_f+L_0) & -1/(L_f+L_0) & 0 & -Z_0/(L_f+L_0) & 0 & 0 & 0 & -\sqrt{2}Z_0/(L_f+L_0) & 0 & 0 \\ 1/C_{ds} & -1/C_{ds} & -1/(R_{on}C_{ds}) & 0 & 0 & 0 & 0 & 0 & 0 & 0 & 0 & 0 \\ 0 & 1/C_x+1/C_0 & 0 & 0 & 0 & 0 & 0 & 0 & 0 & 0 & 0 & 0 \\ 0 & 0 & 0 & 0 & 0 & 0 & -1/L_f & 0 & 0 & 0 & 0 & 0 \\ 0 & Z_0/(L_f+L_0) & 0 & 0 & 0 & -2Z_0/(L_f+L_0) & 1/(L_f+L_0) & -1/(L_f+L_0) & 0 & -\sqrt{2}Z_0/(L_f+L_0) & 0 & 0 \\ 0 & 0 & 0 & 0 & 1/C_{ds} & -1/C_{ds} & -1/(R_{on}C_{ds}) & 0 & 0 & 0 & 0 & 0 \\ 0 & 0 & 0 & 0 & 0 & 1/C_x+1/C_0 & 0 & 0 & 0 & 0 & 0 & 0 \\ 0 & 0 & 0 & 0 & 0 & 0 & 0 & 0 & 0 & 0 & -1/L_f & 0 \\ 0 & \sqrt{2}Z_0/(L_f+L_0) & 0 & 0 & 0 & -\sqrt{2}Z_0/(L_f+L_0) & 0 & 0 & 0 & -Z_0/(L_f+L_0) & 1/(L_f+L_0) & -1/(L_f+L_0) \\ 0 & 0 & 0 & 0 & 0 & 0 & 0 & 0 & 1/C_{ds} & -1/C_{ds} & -1/(R_{on}C_{ds}) & 0 \\ 0 & 0 & 0 & 0 & 0 & 0 & 0 & 0 & 0 & 1/C_x+1/C_0 & 0 & 0 \end{bmatrix} \tag{4.51}$$

The B matrix is as follows:

$$\mathbf{B} = \begin{bmatrix} V_{DD}/L_f \\ 0 \\ 0 \\ 0 \\ V_{DD}/L_f \\ 0 \\ 0 \\ 0 \\ V_{DD}/L_f \\ 0 \\ 0 \\ 0 \end{bmatrix} \tag{4.52}$$

The $\mathbf{A}$ matrix in Equation 4.51 is a 12x12 matrix where all PAs are on; in the case that one of the PAs is not on, the on-resistance is equal to zero. The next step is to determine the solution to the matrix; this can be done by using equations 4.46 and 4.48, which yields the initial matrix $\mathbf{q_0}$. These equations need the matrices $\mathbf{A_{te}}$ and $\mathbf{B_{te}}$, which require equation 4.8. Next, to find the waveforms, equation 4.10 can be used. One can look at Subsection 4.4 to derive the output power and drain efficiency. In Figure 4.4, the drain-to-source current and voltage are plotted, as well as the output current. One can see in the figure that the drain-to-source waves are slighting out-of-phase. One can see that the turn on moment of the third amplifier is slightly later compared to the first two power amplifiers. But, the output currents have all their minimum all crosses $\pi/2$ perfectly. In other words, the fundamental drain-to-source current are in-phase. The resulting currents can therefore be added in-phase at the load. This design is shown in Figure 4.4a. But the switching moments are not simultaneously when looking at Figure 4.4b. A design methodology is required to find the proper delay at the input so that the currents are added in phase; this method is discussed in the next section. Note that the method is turned into a MATLAB script seen in Appendix H.

4.8. Class E LMBA

This model can be extended to an LMBA configuration, as shown later. But for now, slightly more analysis should be done on designing such an LMBA. This is to understand the necessity. In Figure 4.5, the combination of a possible matching network and the hybrid coupler is shown. The circuit uses a reactance to compensate for the required reactance at the fundamental, and it uses a transformer to provide the correct resistance at the fundamental. When the two peaking amplifiers have the same output power, their matching network is the same. If the two peaking amplifiers have different maximum output powers, their matching networks are not necessarily the same.

The LMBA equations can be summarized as follows:

$$\begin{aligned} Z_C &= Z_0 \left(1 - \sqrt{2}\frac{I_{B1} - I_{B2}}{I_C}\right) \\ Z_{B1} &= Z_0 \frac{I_{B2} + \sqrt{2} I_C}{I_{B1}} \\ Z_{B2} &= Z_0 \frac{I_{B2} - I_{B1} + \sqrt{2} I_C}{I_{B2}} \end{aligned} \tag{4.53}$$

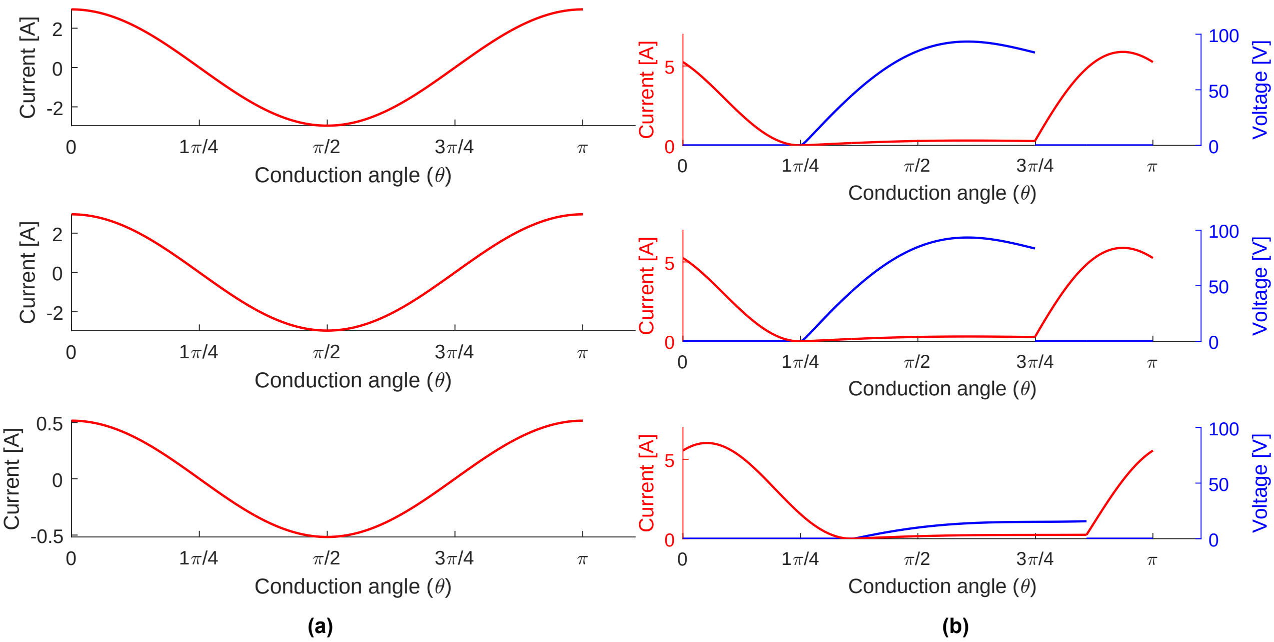

Figure 4.4: On the left, the input current is plotted at the input of the hybrid coupler. The current flows through the resonator for each PA. The first two are equal PA_{B1} and PA_{B2} and the third one is smaller PA_C. The drain-to-source voltage and current for all three PAs are shown on the right. All have ZVS and ZVSS, while the first two have a q of 1.3 and the last one a q of 1.55. Different q values result in different output phases that must be compensated accordingly by changing the input delay.

For a Pseudo-Doherty LMBA, referring to Figure 2.15, the following holds:

- The two peaking amplifiers (P_{B1} and P_{B1}) optimal matching networks are found when all three amplifiers are turned on. In other words: i_1, i_2 and i_3 are non-zero.
- The main amplifier (P_C) is matched at the point when the two peaking amplifiers are turned off. In other words: i_1, i_2 are zero and i_3 is non-zero.

Multiple options are possible to find the transformation ratios and the required reactance for each PA. But my method is as follows:

- Solve each PA separately for ZVS and ZVSS by using [39]. The solution is the optimal load impedance Z_x and the output current i_x.
- Determine the current angle for all Class E amplifiers and compensate it by setting a compensating delay at the input of each PA.
- Compensate the required reactive load by choosing jX_x for each PA accordingly.
- The next step is choosing the characteristic impedance. This depends on the application, but a carefully chosen characteristic impedance results in lower impedance transformation ratios, or even no impedance transformation is sometimes needed. A good starting value can be found using Equation 2.48.
- When all previous steps are implemented correctly, the LMBA equations 4.53 are purely real, and the remaining required load is purely real. This results in 3 equations and 3 unknowns. By knowing the currents and the required load derived earlier, a nonlinear solver can be used to solve the equations 4.54; these equations are derived in C. Anything from a simple semi-Newtonian algorithm to a more complex particle swarm algorithm gives good results.

$$
\begin{aligned}
Z_{1new} &= R_{B1} = Z_0\left(\frac{I_{B2}}{I_{B1}n_1n_2} + \frac{\sqrt{2}I_C}{I_{B1}n_1n_3}\right)\\
Z_{2new} &= R_{B2} = Z_0\left(\frac{2}{n_2^2} + \frac{\sqrt{2}I_C}{I_{B2}n_2n_3} - \frac{I_{B1}}{I_{B2}n_1n_2}\right)\\
Z_{3new} &= R_C = Z_0\left(\frac{1}{n_3^2} + \frac{\sqrt{2}I_{B2}}{I_{B2}n_2n_3} - \frac{\sqrt{2}I_{B1}}{I_{B2}n_1n_3}\right)
\end{aligned}
\tag{4.54}
$$

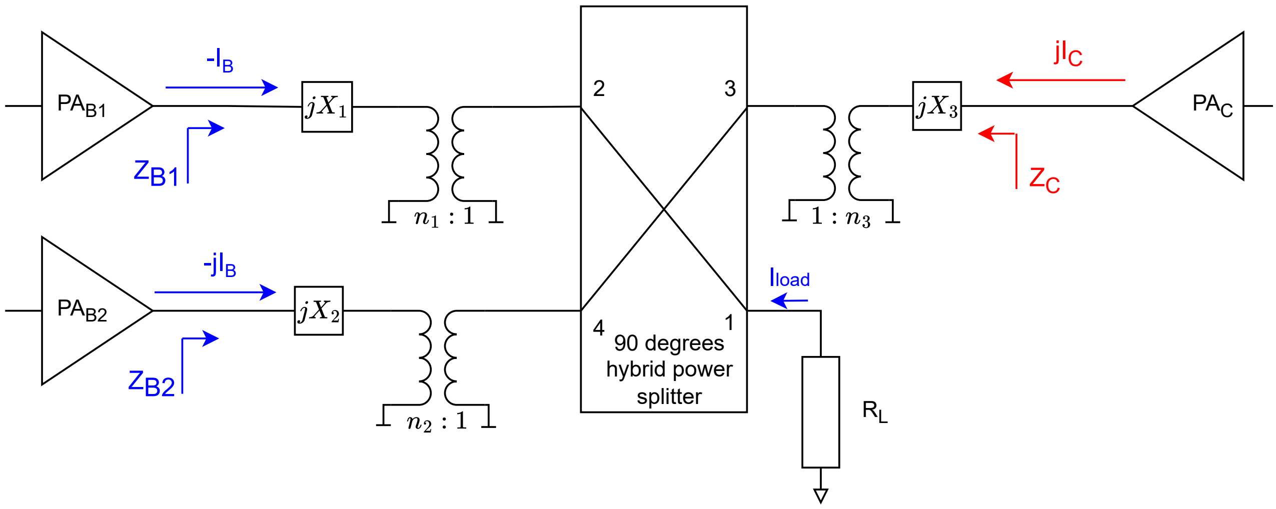

Figure 4.5: Class E LMBA with matching networks. The matching networks exist out of a complex part in series with a transformer; this is done for the simplicity of finding a solution.

When all the design parameters are known, the solution can be found. This can be done using a nonlinear simulation like ADS Keysight or by applying the previous solution in Section 4.7.

4.8.1. Comparison between ADS Keysight and MATLAB

Although, a thorough discussion is needed to interpret the data and properly design a Class E LMBA. For now, we will only look at the differences between the different models. The design chapter will discuss the final design and how to interpret the voltage and current waves. In this subsection, there are two methods to simulate a Class E LMBA: the linear model using the equations previously discussed or the linear model using ADS Keysight. In the case of a high series Q-factor, the results should be the same. This assumption should hold because the second harmonic is sufficiently low at a high Q-factor for the series resonator, this assumption is further discussed in Appendix D. The advantage of using linear models is that they are fast, relatively accurate, and insightful. The elapsed time for a high-resolution LMBA simulation in ADS Keysight is around a second, and using MATLAB takes under a second.

A limit of the LMBA is the maximum impedance transformation due to the phase and amplitude modulation; as described by Equation 2.38. This results in no ideal load being presented, resulting in non-ZVS. Non-ZVS results in losses that can be far greater than just increasing the on-resistance by changing the number of turned-on transistors. Another effect is the changing of the slope (non-ZVSS), which lowers the output power but, in turn, could increase the drain efficiency. All in all, many possible configurations are possible, but a quick and accurate model should be implemented to simulate them all.

By applying the methods previously discussed, some accurate parameters for the transistor can be derived. This transistor has an on resistance of $8\ \Omega$ and a drain-to-source capacitance of $2.1\ pF$, where the width of the transistor is $700\ um$. Next, a QLI Class E is chosen for the best load modulation performance, at the cost of some wideband performance compared to the Parallel Circuit Class E. Lastly, a Q-factor of 10 for the resonator is chosen. The reason is that at very low Q-factors, the second harmonic becomes so high that Equation 4.37 no longer holds. The next important discussion is the sizes of the three PAs, and the answer to this question is not straightforward; the answer will be given in the next Chapter, but for now, we will design the most basic Class E LMBA possible. For an OBO of -10 dB, we can assume that the power of PA_C is one-tenth of the total output power, using Equation 2.42. This makes the number of transistors for PA_C around one-tenth of the total number of transistors. Everything is summarized in Table 4.1.

Figure 4.6 shows the good correspondence of the MATLAB model with the ADS Keysight simulation. It is not perfect, the accuracy depends on the setup and simulation settings.

Parameters	PA_{peak1} (PA_1)	PA_{peak2} (PA_2)	PA_{main} (PA_3)	Unit
Number of transistors	5	5	1	-
q	1.3	1.3	1.3	-
Q_0	10	10	10	-
R_{on} single transistor	8	8	8	Ω
C_{ds} single transistor	0.21	0.21	0.21	pF
voltage switching (VS)	0	0	0	V
voltage slope switching (VSS)	0	0	0	Vs/s

Table 4.1: The parameters where Figure 4.6 is made width.

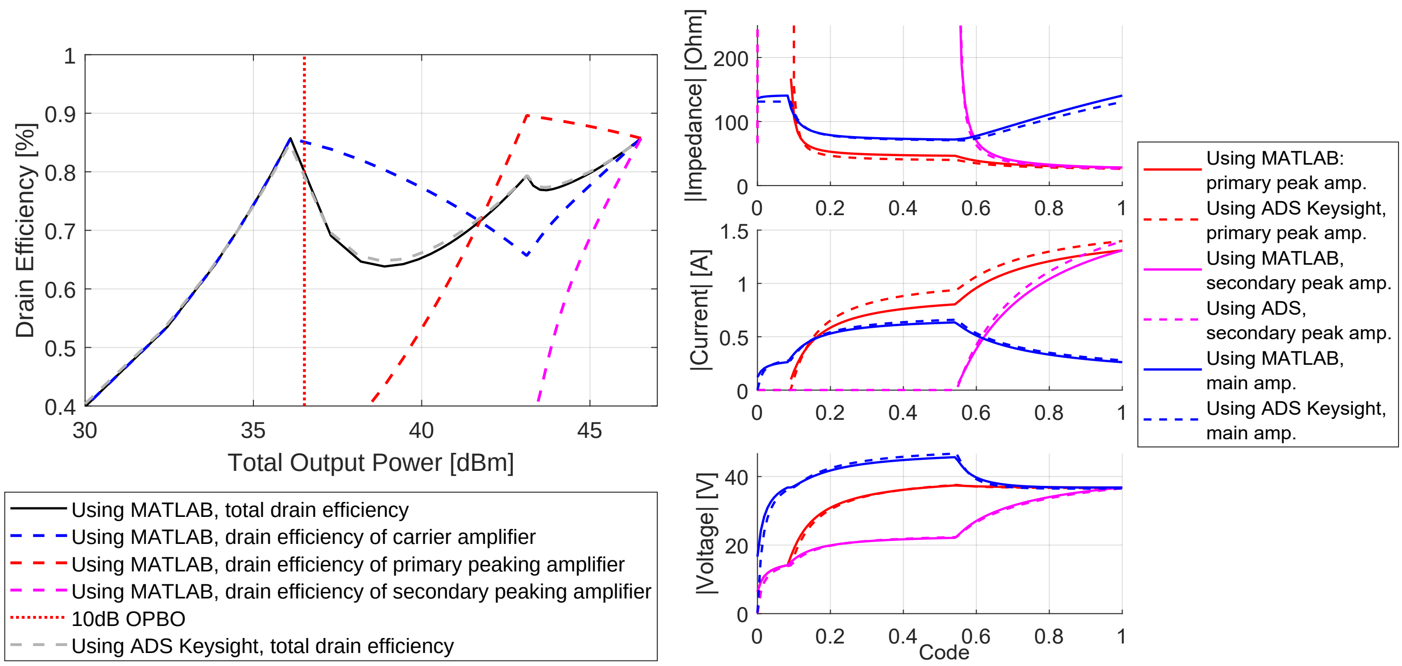

(a) (b)

Figure 4.6: A quick example of a design for a Class E LMBA with >10 dB OPBO. The design uses the design parameter values from 4.1. The ADS model is exactly the same as the MATLAB model in parameters, and therefore, one would expect that they give equivalent results. The results for the drain efficiency are the same, with some numerical errors. For the drain-to-source current, we see some differences; even though everything is automated, there still could be rounding errors or implementation differences. Figure 4.6b can be explained by seeing that first the first main amplifier is turned on, which saturates its drain voltage. Next, the first peaking amplifier is turned on, this saturates its drain voltage. And in turn, the impedance for the main amplifier decreases, which in turn increases the output power of the main amplifier. And lastly, the secondary peaking amplifier turns on, which counteracts the effect for the main amplifier. The main amplifiers input impedance is again back at its original impedance, and all drain currents are added together. It can best be understand using Equation 4.53.

4.8.2. Comparison between linear LMBA and nonlinear LMBA

The linear LMBA uses a linear transistor with constants R_{on} and C_{ds}; however, in reality, this is not the case. The effect of the nonlinearities is highly dependent on the design of the LMBA. This subsection presents two LMBA designs: the previous design and an improved one. These are not the best designs possible, but just an example to show the model's limits. The first design is the same as before, shown in Figure 4.7, but the results are not good. Although the results are correct at both the 10 dB OPBO point and maximum power, where the Equations 4.54 are calculated at, the results between the two points are bad. The main reason is the bad approximation of the on-resistance, which depends on the drain-to-source voltage. The unequal currents from the two peaking amplifiers in PBO cause load modulation for the main amplifier. This load modulation results in a temporary current increase; in this case, the transistor goes out of the triode region into the saturation region. This not only increases the on-resistance significantly but also means that the phases are no longer correctly predicted. If the phases are added wrongly, a negative impedance can be presented to the PAs, as seen in the figure.

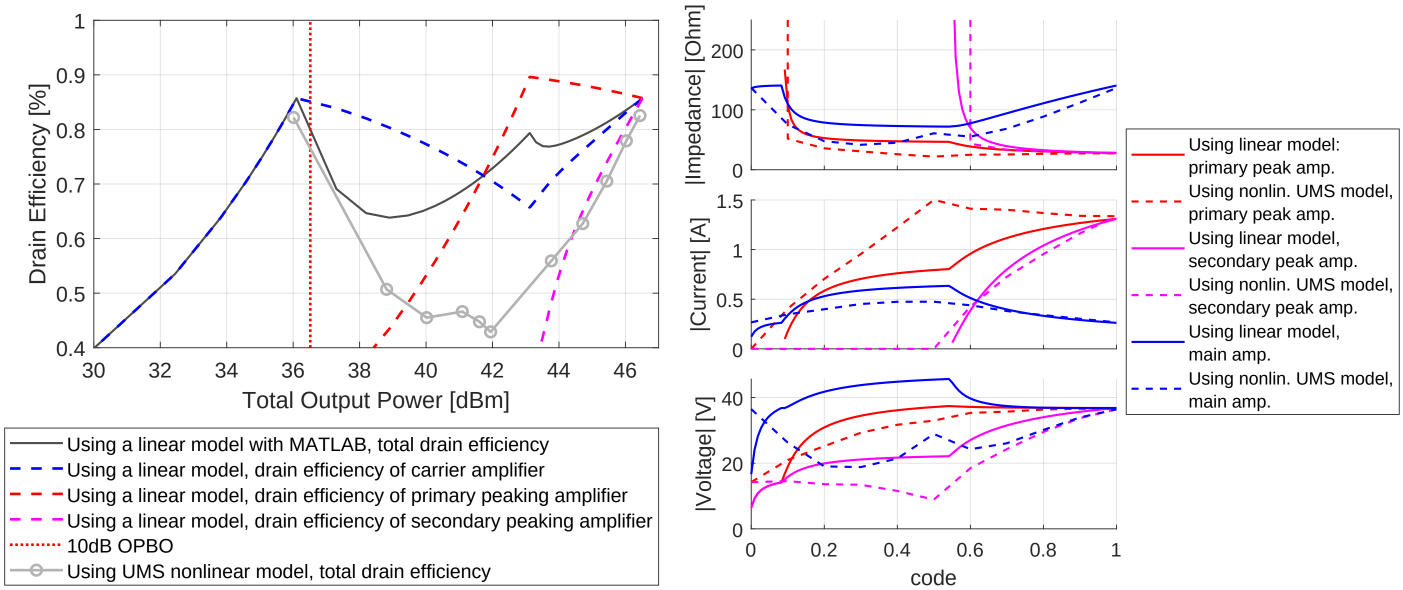

(a) (b)

Figure 4.7: This design uses the same design parameter values from 4.1. Differences are, this time, more pronounced. The reason is that the main amplifier is matched at maximum power at OPBO; however, at -6 dB, the current increases even more because of load modulation caused by the peaking amplifiers, which causes a decrease in drain-to-source voltage and moves the transistor out of the triode region into the saturation region. Therefore, the approximated value of R_{on} is no longer accurate.

The solution is to ensure the transistor never goes into the saturation region. In this case, the PA keeps its high drain efficiency, and the approximated value of R_{on} is good enough. This is done by matching the main amplifier at a lower output power, not at the main PAs' maximum output power. To do this, Class E is matched for non-ZVSS, in this case -38 Vs/s, shown in Tabel 4.2. As a result, the main amplifier stays in the triode region constantly. The resulting Figure 4.8 shows good correspondence with the linear model.

Parameters	PA_{peak1}	PA_{peak2}	PA_{main}	Unit
Number of transistors	6	6	3	-
q	1.3	1.3	1.3	-
Q_0	10	10	10	-
R_{on} single transistor	8	8	8	Ω
C_{ds} single transistor	0.21	0.21	0.21	pF
voltage switching (VS)	0	0	0	V
voltage slope switching (VSS)	0	0	-38	Vs/s

Table 4.2: The parameters where Figure 4.8 is made width.

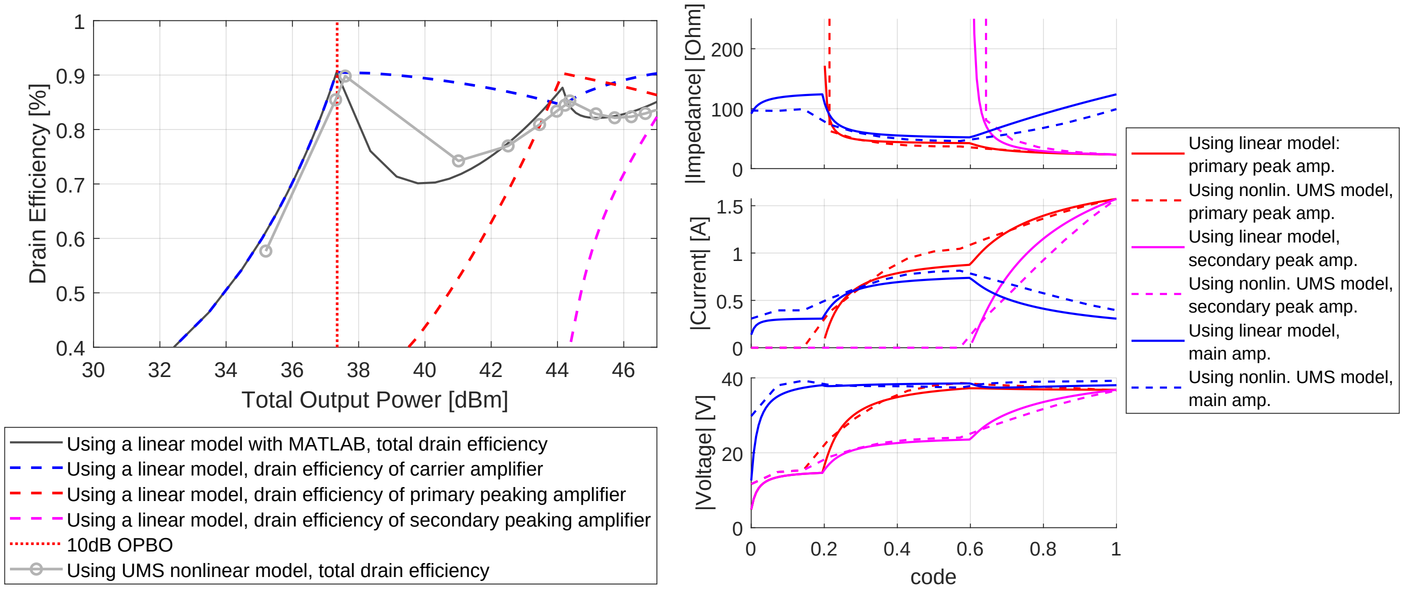

(a) (b)

Figure 4.8: In this case, the results are more accurate when compared to Figure 4.7. The main amplifier is no longer matched for maximum output power at the total maximum output power but at a lower output power. This is done by changing the slope of the Class E configuration, as seen in Table 4.2. In this case, the main amplifier increases output power around a code of 0.5 and decreases output power at a code of 1. In this way, the transistor stays in the triode region and the found value of R_{on} stays accurate.

5

A wideband design

A simple radar signal like a chirp requires a wide range of frequencies, which in turn requires a wideband amplifier. Hybrid couplers are inherently wideband and, therefore, should not limit the wideband performance of the total amplifier. However, Class E is generally not wideband due to its use of a resonating circuit. A continuous mode, Class E, is also hard to implement compared to continuous mode Class J or continuous mode Class F/F^{-1}. In this chapter, the wideband Class E with a series filter is discussed.

5.1. Single-ended Class E with series resonator

The most common Class E variant is the series resonator version in Figure 4.1. The Q-factor of the series resonator determines the wideband performance of such an amplifier. The ideal Q-factor for a given operational bandwidth can also be calculated, as done by [27]. The goal is to have flat imaginary Y-parameters over a certain bandwidth. This can be done by realizing that the series resonator has a negative imaginary Y-parameter slope versus frequency, a parallel resonator has a positive imaginary Y-parameter slope versus frequency, and when combined, the result in a slope of zero at a certain frequency, as shown in 5.1. This point can be mathematically derived by putting

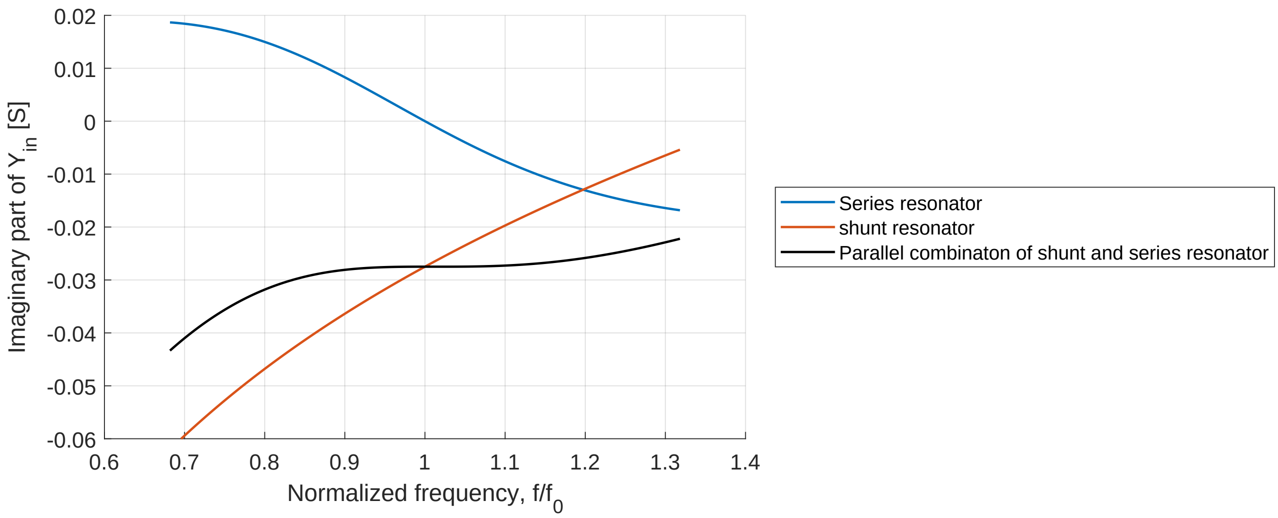

Figure 5.1: Y-parameters for a parallel circuit Class-E.

the derivative of the Y-component to zero:

$$\left.\frac{d\Im\{Y_{in}(\omega)\}}{d\omega}\right|_{\omega=\omega_0} = 0 \tag{5.1}$$

This is solved in [27] as follows:

$$C_{ds} + \frac{1}{\omega_0 L_f} - \frac{2L_0}{R_x^2} = 0 \tag{5.2}$$

But in the case L_x is added, we get the more complicated equation:

$$C_{ds} + \frac{1}{\omega_0^2 \cdot L_f} - \frac{2L_0 + L_x}{L_x^2 \cdot \omega_0^2 + R_x^2} + \frac{2\omega_0^2 L_x^2 \cdot (2L_0 + L_x)}{(L_x^2 \cdot \omega_0^2 + R_x^2)^2} = 0 \tag{5.3}$$

And C_0 is the series resonator capacitance, defined as:

$$C_0 = \frac{1}{\omega_0^2 \cdot L_0} \tag{5.4}$$

Where C_{ds} is the drain-to-source capacitance of the transistor, which is given for a chosen gate width. Next, L_f is the DC-feed inductor that can be chosen; this depends on the parameter q. Besides L_f, L_x also depends on the parameter q. All summarized as follows:

$$\begin{aligned} L_f &= \frac{1}{\omega_0^2 q^2 C_{ds}} \\ R_x &= \frac{\omega_0 L_f}{K_L(q)} = \frac{1}{\omega_0 C_{ds} q^2 K_L(q)} \\ L_x &= \frac{K_X(q) R_x}{\omega_0} \end{aligned} \tag{5.5}$$

The solution to Equation 5.2 is when combining with Equation 5.5 as follows:

$$L_0 = \frac{K_L K_X q^2 - K_L K_X^3 q^2 - K_X^4 q^2 - K_X^4 - 2K_X^2 q^2 - 2K_X^2 - q^2 - 1}{2Cds \cdot \omega_0^2 q^4 K_L^2 (K_X^2 - 1)} \tag{5.6}$$

And lastly, Q_0 for the series resonator is defined as:

$$Q_0 = \frac{\omega_0 (L_0 + L_x)}{R_x} \tag{5.7}$$

The choice of q depends on the requirements. Wide bandwidth Class E configurations most of the time use the parallel-circuit Class E. An alternative configuration is the QLI Class E. Both are summarized as follows:

Configuration	q	K_L	K_X	Q_0
Parallel-circuit Class E	1.412	0.73	0.00	1.03
Quasi-Load Invariant Class E	1.30	1.01	0.26	1.09

Table 5.1: The given parameters for different Class E configurations are obtained using equations from Section 2.1.5.

One can easily see what is unique to the parallel-circuit Class E variant: no reactance compensation is needed because $K_X = 0$. Next, we can plot the Y_{in} parameters for both the parallel-circuit class E and the QLI Class E variants, shown in Figure 5.2.

This figure shows that the parallel-circuit Class E has a more flat response versus frequency compared to Quasi-Load independent (QLI). However, the QLI Y-parameters are also reasonably flat, ranging from 0.7 to 1.1. In the end, we design a load modulated amplifier, and if the load stays only in the real domain, the efficiency of a QLI Class E amplifier stays high, which simplifies the design significantly. For this reason the QLI Class E amplifier is chosen instead of the parallel-circuit Class E amplifier. Therefore, the parallel-circuit Class E configuration is outside the scope from now on. We need to determine the frequency range to determine efficiency and output power versus frequency. The design requirements range from 2.9 to 3.4 GHz; therefore, a center frequency of 3.15 GHz is

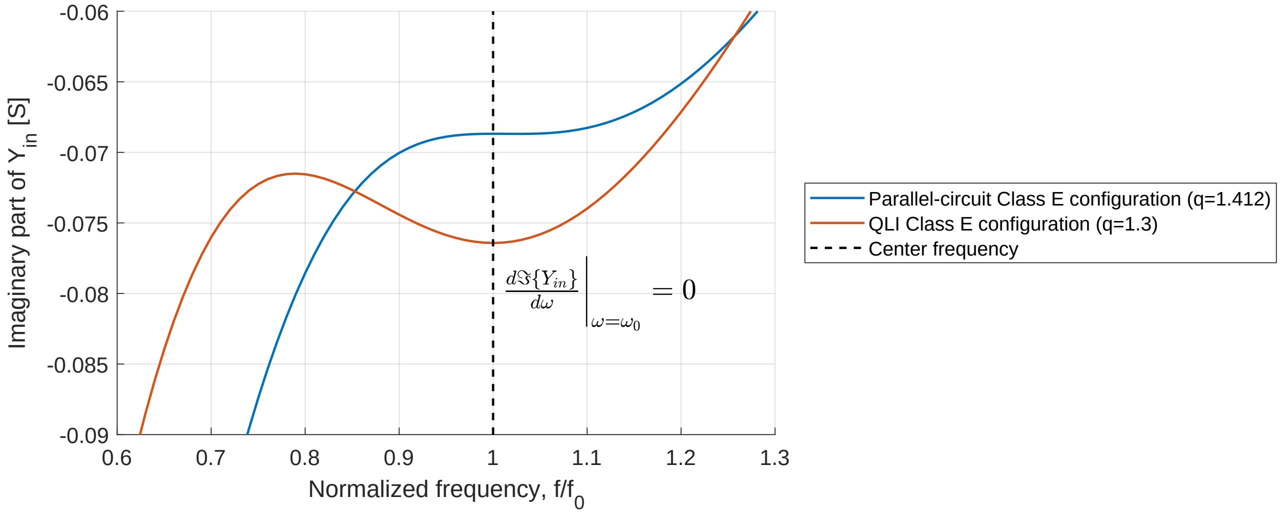

Figure 5.2: The imaginary part of the input Y-parameter is plotted versus the normalized frequency. One can quickly see that the parallel circuit produces a more flat Y-parameter response compared to QLI. This is the reason that this configuration is often used for wideband performance.

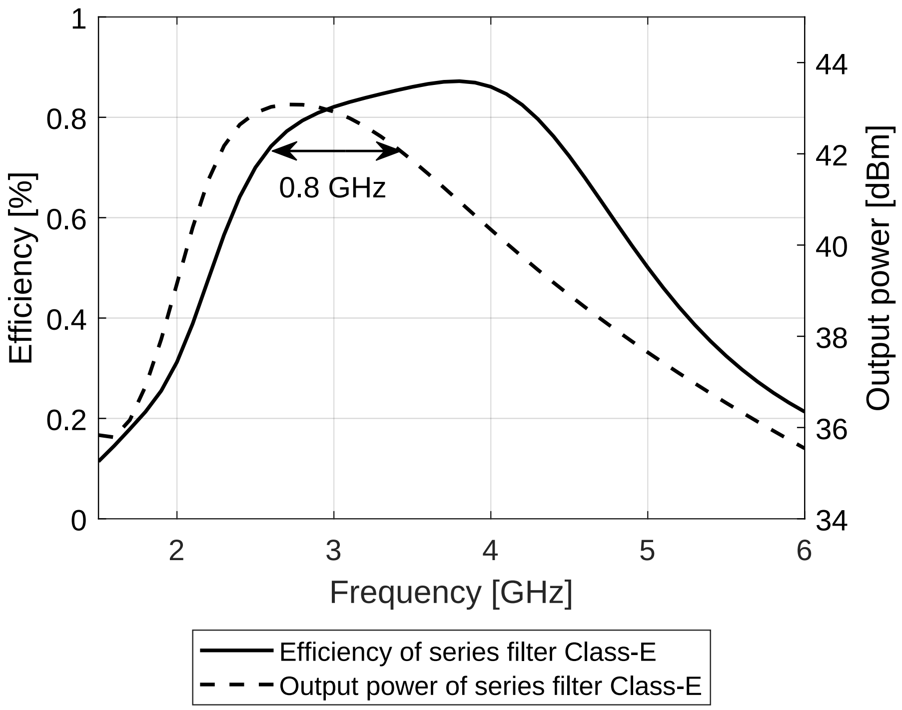

Figure 5.3: For a single-ended QLI Class E, the output power and drain efficiency are plotted. It is simulated using ADS Keysight using a linear model with an on-resistance of 1.33Ω and a drain-to-source capacitance of 1.26 pF. The matching elements are lossless. The bandwidth is determined based on a 10% drain efficiency drop and a 1 dB output power drop. In this case, the bandwidth can be approximated as around 0.8 GHz for a center frequency of 3.15 GHz.

chosen. This can be simulated using a linear model in ADS Keysight with finite on-resistance, as shown in Figure 5.3. When the bandwidth is defined as a 10% drain efficiency drop and a 1 dB output power drop, the bandwidth is around 0.8 GHz. This is well above the required bandwidth of 0.5 GHz.

The next step is to add a nonlinear transistor model with lossy components. The components used are from the UMS GH15 PDK, provided by TNO. The model used is the GH15; the width is 175 um, and the number of fingers is 24. This is around the size of a single peaking amplifier. The drain efficiency is calculated by dividing the fundamental output power on the load resistor by the DC power supplied by the voltage source. The result is Figure 5.4, where the bandwidth shifted a little

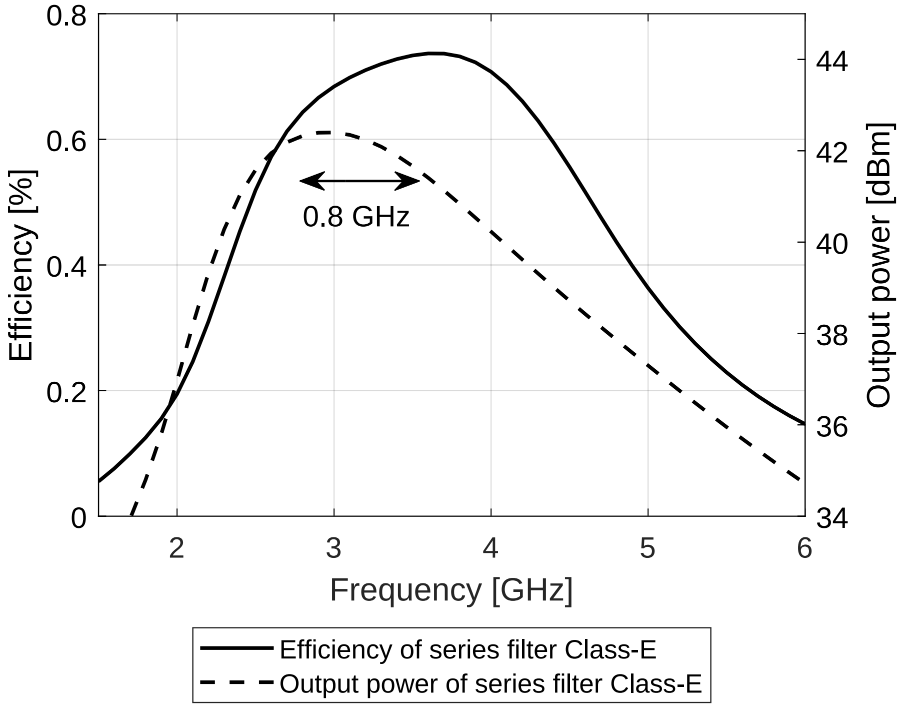

Figure 5.4: For a single-ended QLI Class E, the output power and drain efficiency are plotted. It is simulated using a nonlinear model from UMS. The model used is the GH15, the width is 175 um, and the number of fingers is 24. And the lumped components are lossy, implemented using the UMS PDK. The bandwidth of 0.8 GHz is larger than the required operating range that lays between 2.9 and 3.4 GHz, which results in a bandwidth of 0.5 GHz.

bit, but the bandwidth stayed the same around 0.8 GHz. A big downside of the lower Q-factor of the resonator is the higher second harmonic on the load, which results in power loss, and therefore in a lower drain efficiency. Therefore, it is important to know the value of the second harmonic with respect to the fundamental. This can be calculated as follows:

$$\Delta_{SD,dB} = P_{drain,f_0} - P_{drain,2f_0} = 44\ dBm - 33\ dBm = 11\ dB \tag{5.8}$$

$$\Delta_{SO,dB} = P_{load,f_0} - P_{load,2f_0} = 42\ dBm - 30\ dBm = 12\ dB \tag{5.9}$$

Therefore, the second harmonic's output power is around 12 dB lower than that of the fundamental frequency of operation. The attenuation at the second harmonic due to the series resonator is around 1 dB; this is very low and mainly results from a low Q-factor. Note, that these values are found by using a linear model, but the nonlinear model has around a 1 dB difference.

5.2. Wideband matching

Up until now, an ideal transformer has been used for the analysis. However, in practice, a matching network has losses and finite bandwidth. Implementing such a matching network could take many forms, but this project is restricted to integrated circuitry. This results in the limited use of transmission lines. The result is, ideally, a combination of lumped components. In this section, two solutions are discussed: using lumped components and transformers. The transformer should be avoided because of the additional losses; at high power, losses can become a cooling and current density issue. Nevertheless, both are discussed, and the design methodology is presented.

The goal is not just to have a constant impedance over the required bandwidth but also a correct response when the real load increase in power back-off. In this application, the load is modulated; ideally, the response stays on the real axis. In Figure 5.5, 50 Ω is matched to a far higher impedance (2000 Ω). In Figure 5.5a, the first design is a one-stage matching network using both an LC network. The input impedance shifts to the complex domain when the load impedance increases. In the next design, in Figure 5.5b, we can see that the input impedance moves down when the load impedance increases. Although the impedance stays on the real axis, the response differs from an ideal transformer's. The ideal transformer is shown in Figure 5.5c, where an increase in load impedance results in an equal increase in input impedance.

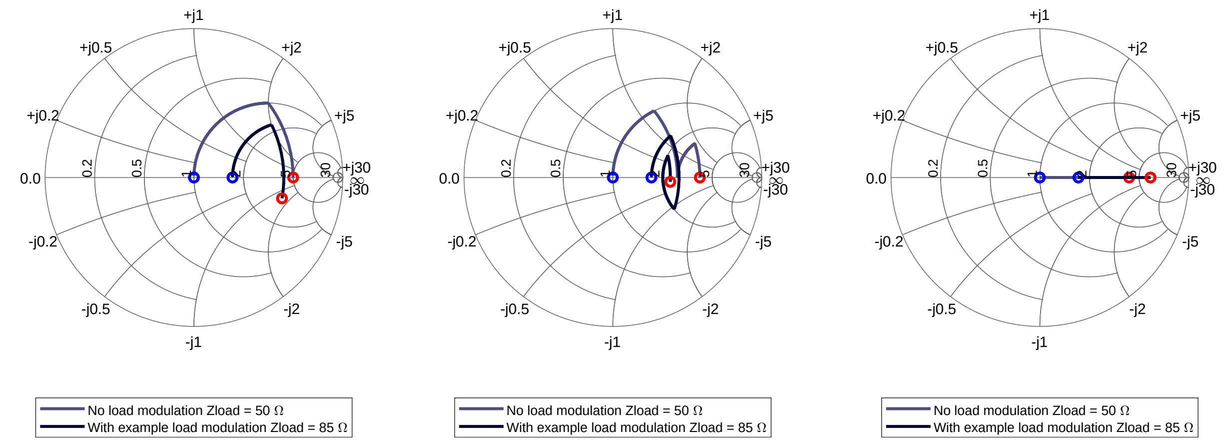

(a) Using a one-stage lumped component matching network.

(b) Using a two-stage lumped component matching network.

(c) Using a transformer as a matching network.

Figure 5.5: The three Smith charts show how the different matching networks depend on an increasing load: the one-stage LC network moves the input impedance to the complex domain, the two-stage LC network decreases the input impedance, and the ideal transformer increases the input impedance.

5.2.1. One stage matching network

A second order one-stage matching network uses capacitors or inductors as lumped components. Such a circuit is shown in Figure 5.6. One can design a low-pass or high-pass filter depending on the inductor's and capacitor's placement. To design a step-up impedance transformer instead of step-down (from left to right), the input and output ports must be exchanged. The imaginary part at the designed frequency needs to be zero to design a real impedance transformation.

$$\Im\{Z_{in}\} = 0 \tag{5.10}$$

The derivation is not given and can easily be derived, but the result for the variables is as follows:

$$X_C = \frac{\sqrt{(R_{in} - R_L)R_L}R_{in}}{R_{in} - R_L} \tag{5.11}$$

$$X_L = -\sqrt{(R_{in} - R_L)R_L} \tag{5.12}$$

When the impedance converter needs to be downstepped, the configuration changes slightly, but the math stays very similar. In this case, R_L and R_{in} need to be exchanged, and X_C and X_L are exchanged.

5.2.2. Two stage matching network

A two-stage network contains four elements, as shown in Figure 5.7, two single stages in series. This changes the impedance in two steps. For example, from 50–75–100. The goal is not to design an optimal filter; therefore, the single impedance must be chosen by hand. The improvement that the two stages bring is that the bandwidth is usually larger, and the response when the real load increases is that the input impedance stays close to the real axis. The resulting equations are similar to Equation 5.12 but generalized for N steps.

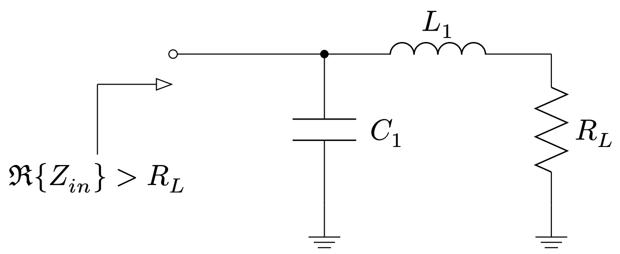

Figure 5.6: One stage low-pass LC impedance transformer using lumped components.

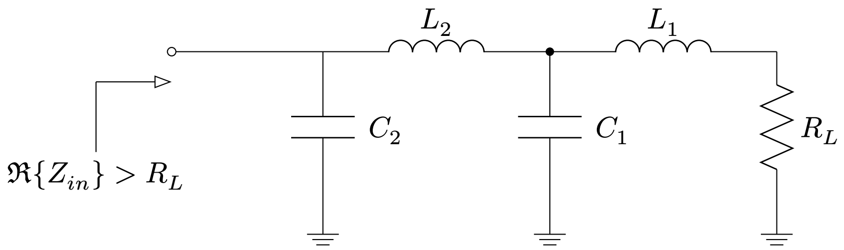

Figure 5.7: Two-stage low-pass LC impedance transformer using lumped components.

5.2.3. Resonating transformer matching network

The ideal transformer is not frequency-dependent; however, a transformer consists of two inductors coupled with a coupling factor of k. In the ideal case, the coupling factor is 1, but in practice, it is more like 0.7. The transformation ratio n describes the ratio of the two inductors; all in all, this equates to:

$$n^2 = \frac{L_1}{L_2} \tag{5.13}$$

According to [5], the equivalent circuit for a transformer is Figure 5.8. The capacitor C is added to resonate out the inductor kL_1. If this is not done, the circuit is a high-pass filter, requiring very high inductance values to operate at 2.9 GHz. When the inductance kL_2 is ignored, the resonating capacitance should equate to:

$$C = \frac{1}{\omega_0^2 k L_1 n^2} \tag{5.14}$$

And lastly, the required inductance value of the transformer depends on the required bandwidth. The Q-factor of the parallel RLC resonator is defined as follows:

$$Q_p = \frac{f_0}{\Delta f} \tag{5.15}$$

Using the Q-factor, we can find the size of L_1 as follows:

$$L_1 = \frac{R}{Q 2\pi f_0} = \frac{R \cdot \Delta f}{2\pi f_0^2} \tag{5.16}$$

Where Δf is the -3 dB bandwidth, which is not the required -1 dB bandwidth but around three times as much; this equates to around 1.5 GHz. In other words, the larger the required bandwidth, the larger the required inductance, and the higher the losses because an inductor has reasonably high losses.

When the inductor is lossy, it has a series resistor R_s associated with it. In this case, both the resonating frequency and the transformer ratio are off. The derivation is not presented here, but the new values are as follows:

$$R_s = \frac{kL_1\omega_0}{Q_l} \tag{5.17}$$

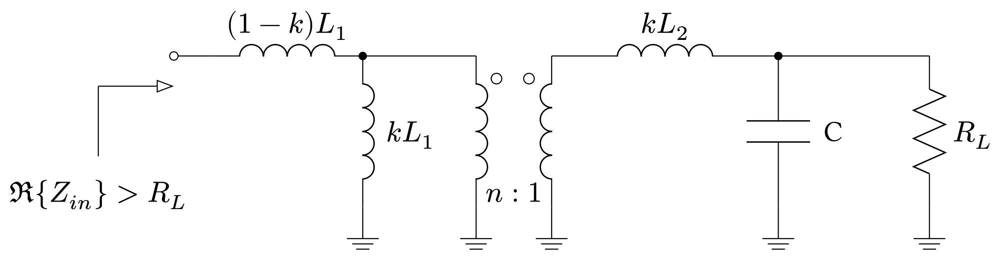

Figure 5.8: A resonating impedance matching transformer.

5.3. Wideband hybrid coupler

The hybrid coupler up until now was assumed to be ideal and described using the ideal Z-matrix from Equation 2.31. But in reality, a hybrid coupler can be realized with transmission lines or lumped components. Transmission lines are preferred because of lower losses and ease of implementation, but at lower GHz frequencies, the size can become too large. When transmission lines are used, there are still two main options to implement the hybrid coupler: using a branchline coupler or coupled lines. The branchline coupler is often used because it is easier to implement. In contrast, the coupled lines need precise manufacturing control over the spacing between the lines. However, an advantage of the coupled lines is that they generally have a higher bandwidth than the branchline coupler. Also, the total size of the design is smaller because it needs two 90-degree transmission lines instead of four. In Figure 5.10a and 5.9, both the branchline coupler setup and the coupled lines are shown. To compare the losses, we first need to design a basic transmission line, for that, the technology used is shown in Table 5.2. The substrate has a height of 70 um, which makes the lines very narrow. Besides that, the 90-degree line will be very long at 3.15 GHz. This makes the design of such a hybrid coupler unpractical, but nevertheless, we can still compare the results. Note that a better approach would be to implement the lumped equivalent. The chosen parameters are given in the Appendix E in Table 4.1. And in Appendix E, the results are plotted. One can see that the branchline coupler has higher losses (1.5 dB compared to 1 dB) and a lower bandwidth compared to coupled lines. However, coupled lines need a very small gap. In the end the coupled lines are implemented using lumped components, with inductors with a Q-factor of 10. The circuit can be found in Figure 5.9. In [37] it is explained how the values for such a lumped equivalent coupled line topology is found. The parameters can be found according to the following equations:

$$k = \frac{1}{\sqrt{2}} \tag{5.18}$$

Where k is the coupling factor for the two inductors. Altough other values are possible, for -3 dB hybrid coupler this is most often chosen. Next, the value of the inductor and capactiance need to be chosen for propper matching. This is done as follows:

$$L = \frac{\sqrt{2}Z_0}{\omega_0} \tag{5.19}$$

$$C = \frac{\sqrt{2}}{\omega_0 Z_0} \tag{5.20}$$

The values of the actual capacitances follow from this:

$$C_M = \frac{C}{\sqrt{2}} \tag{5.21}$$

$$C_G = C - \frac{C}{\sqrt{2}} \tag{5.22}$$

Parameter	Value
ε_r	10.43
tan δ	0.01
H	70 um
T	2 um
σ	3.7e7

Table 5.2: Layer description parameters

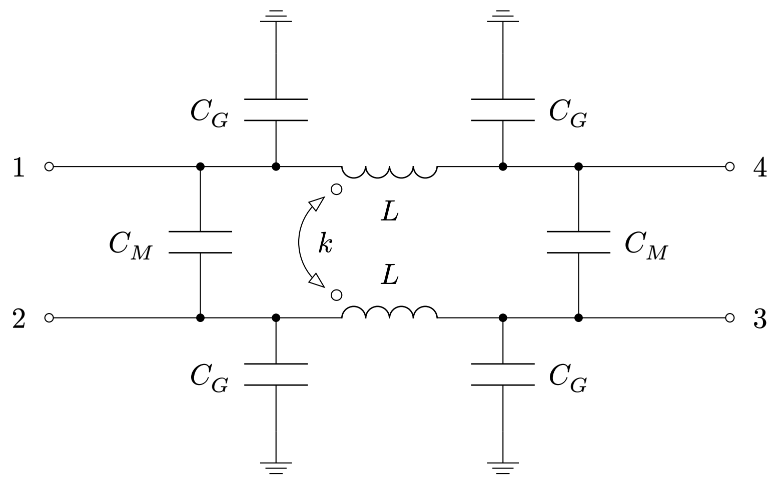

Figure 5.9: Lumped equivalent of the coupled lines.

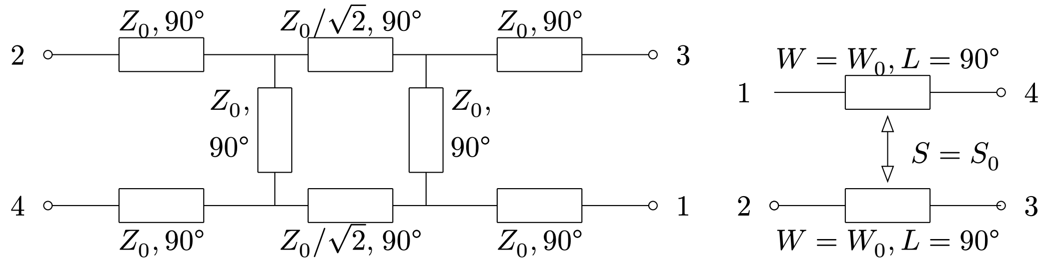

(a) Basic branchline coupler setup, the branches are not needed for matching but to get the correct Z-matrix that is used in Equation 4.37

(b) Basic coupled line setup. The value of W_0 and S_0 can be determined by using EM simulations or tools like ADS Keysight linecalc

5.4. Asymmetrical peaking amplifiers

Asymmetrical LMBA, also called ALMBA, has proven benefits, such as higher VSWR resilience and improved average drain efficiency in OPBO. However, a digital LMBA provides difficulties for implementing such a structure. The reason is that one can only turn one peaking amplifier on and, after that, the second one; this is because of the losses involved when switching the on-resistance becomes dominant. In the analog case, the two peaking amplifiers can be turned on together, and the voltage saturation is only at peak power. Instead, in the digital case, the voltage saturation for the first peaking amplifier is already in the middle.

To move the first peak in the middle, we need to decrease the power of the first peaking amplifier and increase the power of the second peaking amplifier. Ideally, the waves coming from the two peaking amplifiers cancel at the main amplifier (the isolation port of the hybrid coupler). But when they are asymmetric, they do not cancel, and there is load modulation for the main amplifier. This behavior could improve or worsen the performance of the main amplifier.

To improve the result, one can look at Figure 4.8b; this figure shows that the main amplifier's current first rises and thereafter falls back to its value at OPBO. To keep the main amplifier's output power (output current) high, the two peaking amplifiers must have different sizes. To achieve the load impedance for the main amplifier should stay lower compared to its initial value, when looking at Equation 4.53, we can see that the primary peaking amplifier current needs to stay larger compared to the secondary peaking amplifier, but this will move the middle peak to the left instead of to the right. The solution is to use a two-stage real impedance transformer for the main amplifier. The two-stage impedance transformer has a negative response to increase the load impedance. As a result, the middle peak moves to the left instead of the right; this greatly improves the result. However, this matching network limits the achievable bandwidth. The best case (this author found) with ideal components is shown in Figure 5.11. This implementation is more bandwidth-limited and, therefore, not chosen as the final design but can be found in Appendix G.

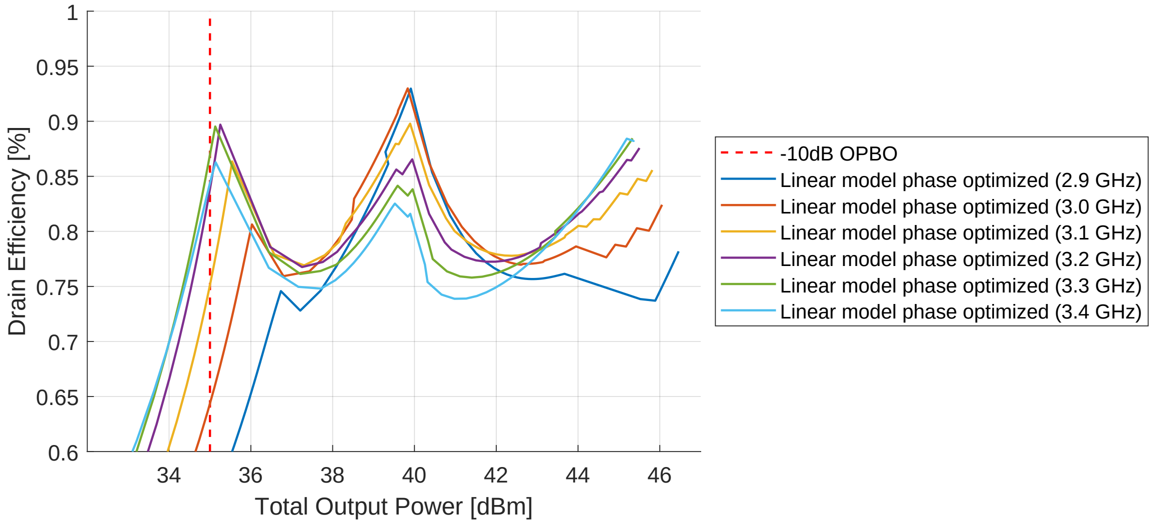

Figure 5.11: The drain efficiency is plotted versus total output power for an asymmetrical configuration, where the first turned-on peaking amplifier is twice as large as the other peaking amplifier. The simulation uses the linear model with realistic on-resistance, but the rest of the circuit is ideal and lossless. Phase optimization is applied to optimize the best drain efficiency.

5.5. Wideband Class E LMBA

The full chain is discussed in this section, from the chosen size of the transistors and the matching networks for a full design. The design is separated into multiple steps. First, the losses of the Class-E matching network are added. Thereafter, the non-ideal hybrid coupler is added. Next, the matching network is designed, together with the losses. In the end, a full design is presented. Note that in each step, the losses are very significant; in the end, there is not much left of the ideal performance. Also, some components, like a transformer, are likely not implementable at high power. The asymmetrical impedance transformer hybrid coupler is not discussed in this chapter. In this section, only the linear switching model is used; the non-linear one is very similar but has major convergence problems when phase-optimized.

5.5.1. The starting point

The starting parameters are similar to earlier, but in this case, the series resonator Q-factor is one, to fulfill the wideband requirement. This reduces the maximum drain efficiency attainable from 90% to 87% at PBO, at higher output powers. The second harmonics cancel using a wide bandwidth coupler, increasing the attainable drain efficiency. The results are in table 5.3, and the phase-optimized figure is Figure 5.12. Phase optimization is done by applying a phase compensation of $-45°$ — $45°$ with a delay for the main PA. All simulations are done in ADS Keysight, and the optimization is performed in MATLAB.

Parameters	PA_{peak1}	PA_{peak2}	PA_{main}	Unit
Number of transistors	6	6	3	-
q	1.3	1.3	1.3	-
Q_0	1	1	1	-
R_{on} single transistor	8	8	8	Ω
C_{ds} single transistor	0.21	0.21	0.21	pF
voltage switching (VS)	0	0	0	V
voltage slope switching (VSS)	0	0	-36	Vs/s

Table 5.3: The starting design parameters for a Class-E LMBA.

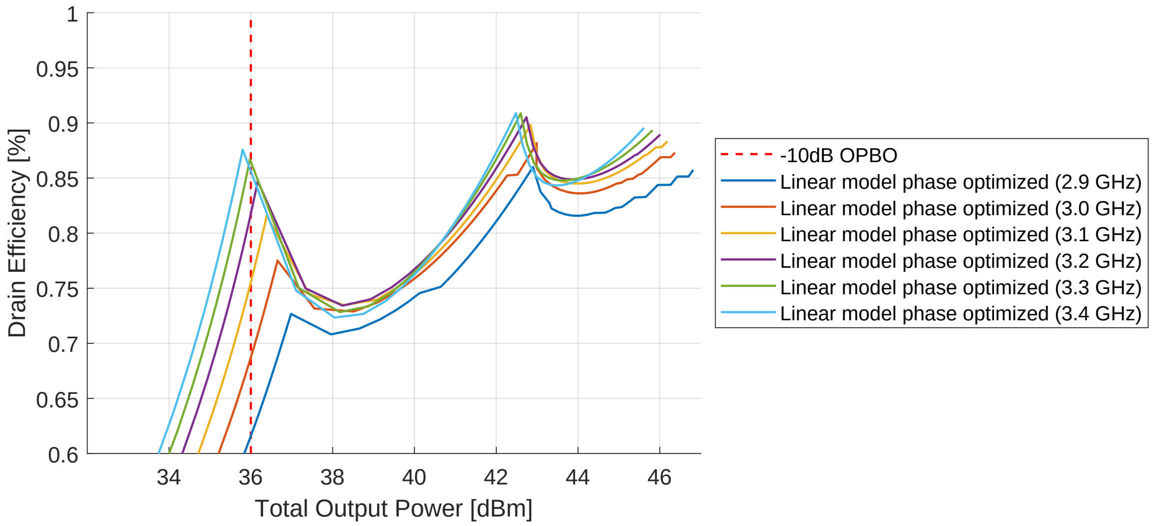

Figure 5.12: The drain efficiency is plotted versus total output power by using the parameters from Table 5.3. The simulation uses the linear model with realistic on-resistance, but the rest of the circuit is ideal and lossless. Phase optimization is applied to optimize the best drain efficiency. The main amplifier has a higher drain efficiency when the two peaking amplifiers are enabled, the reason is that second harmonic from the main amplifier is canceled by the second harmonics of the two peaking amplifiers. This is commonly seen in LMBAs.

5.5.2. A lossy single-ended QLI Class E

A Class-E configuration has two primary lossy components: the feed inductor and the resonator inductor. If they have a finite Q_l of 15, the new values can be found by adding these losses to the state-space and finding the new optimal design parameters. The drain-efficiencies are after this highly decreased. The result is shown in Figure 5.13.

5.5.3. Adding the lossy coupled lines

The next step is to add the lossy coupled lines discussed earlier. It is quite important to note that the losses could be lower, depending on the implementation. The implementation of Table E.1 is used for the coupled lines, and the result is Figure 5.14. When the OPBO point is not in the desired position, the VSS for the main PA can be made less or more negative. By changing the voltage slope we can change the output power of the main amplifier at power back-off.

5.5.4. Adding the matching networks

The next step is to replace the transformers with matching networks. The difficulty lies here with the high impedance transformations. The hybrid coupler is designed for 50 Ω, the two peaking amplifiers for 25 Ω, and the main amplifier for around 200 Ω, all in the ideal case. The main amplifier matching network is, therefore, the most important. Its implementation uses a two-stage low-pass filter, where the values are given in the Appendix F. The good thing about the two-stage filter is that it has lower losses compared to a wideband resonating transformer and is also implementable for high powers.

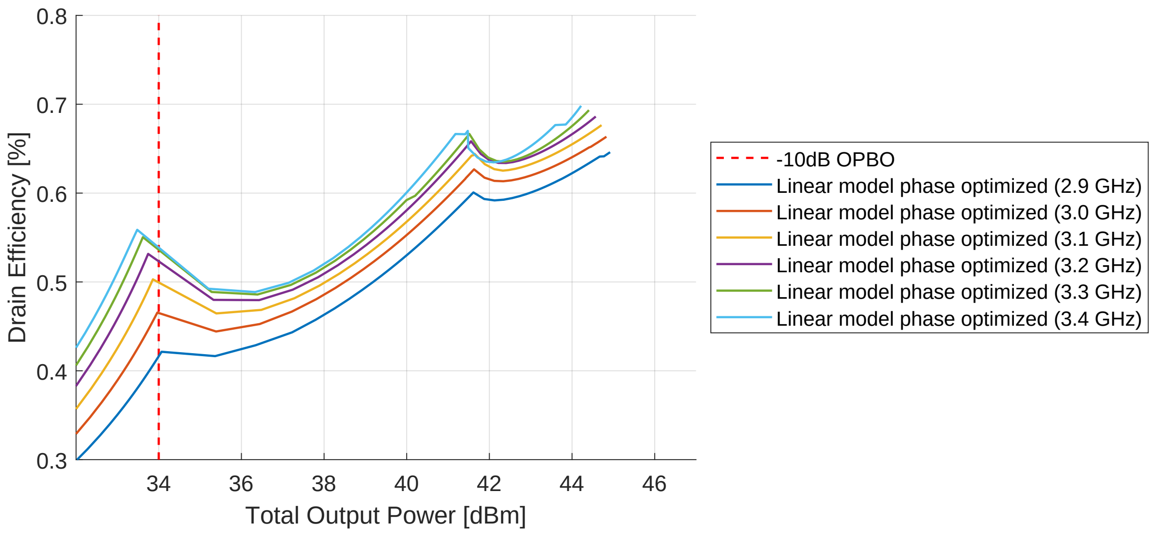

Figure 5.13: The drain efficiency is plotted versus total output power by using the parameters from Table 5.3. This time, the Class-E matching network is no longer ideal but has a Q_l of 15. Phase optimization is applied to optimize the best drain efficiency.

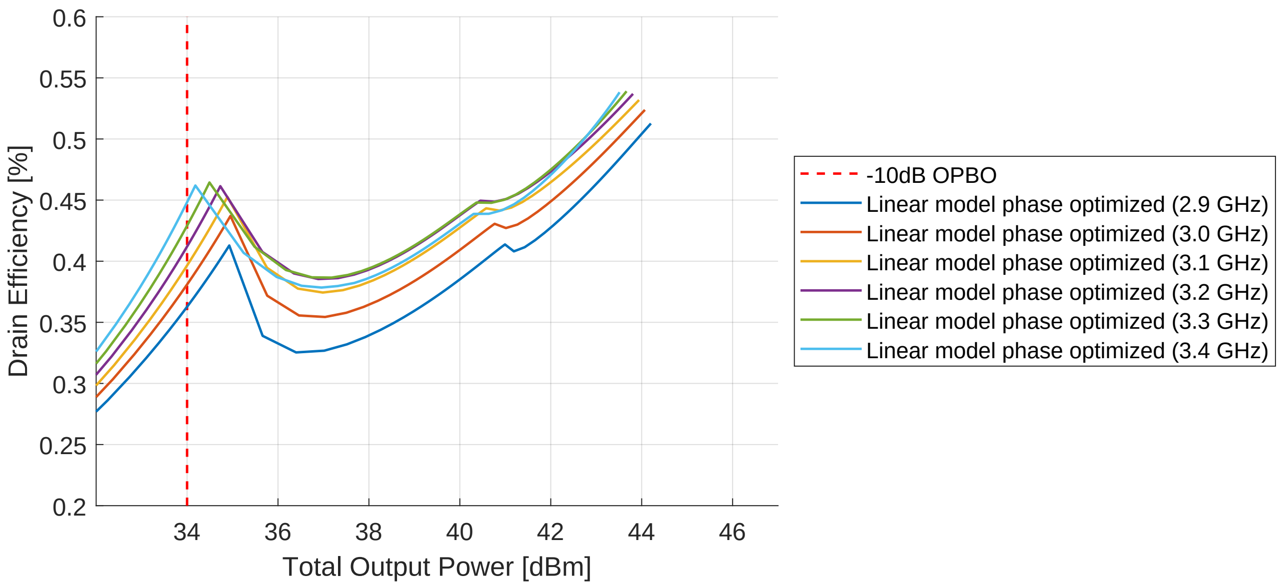

Figure 5.14: The drain-efficiency is plotted versus total output power by using the parameters from Table 5.3. This time, the hybrid coupler is added.

The bad thing is that the input impedance decreases with increased load impedance. This can be solved by changing the turn-on order for the peaking amplifiers. Instead of turning on the primary PA and then the secondary PA, we first turn on the secondary PA and then the primary PA. This problem is also present for the two peaking amplifiers in the matching network. However, we can design an asymmetrical hybrid coupler as an impedance transformer, but this is likely not implementable either, and this has not been implemented, a simple lossy ($Q_l = 15$) wideband resonating transformer is used for now. The ADS Keysight implementation can be found in Appendix F. The final result is a peak drain efficiency of 45% and a PBO drain efficiency of 25% at the lowest.

5.5.5. Dealing with peak drain voltage

One of the main downsides of using Class E is its high peak drain voltage. For this design, it is chosen to be out of scope; when the drain-to-source voltage is too high, the DC supply can be decreased from 25 V down to 20 V or even lower. Note that this will decrease the total output power, depending on the actual performance. However, the drain efficiency will not decrease, so the result

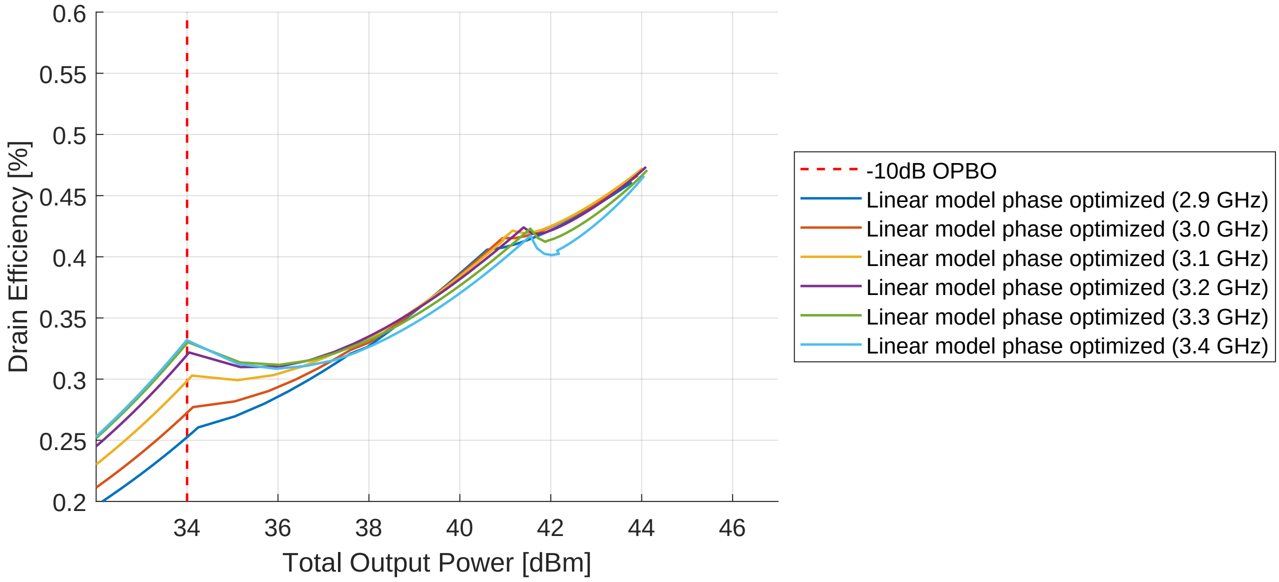

Figure 5.15: The drain efficiency is plotted versus total output power. This time, the lossy matching network, consisting of a two-stage lumped-component matching network and two transformers, is added.

will not significantly change. The PAE and the gain are out of scope and will be affected the most by a decrease in output power. An alternative is to design a Class E/F3, which limits the drain-to-source voltage. This seems to be the most promising solution. In the end, there was no time to research this further.

5.5.6. Final design

In the final design, an ALMBA configuration is chosen; here, the secondary peaking amplifier is first turned on and is larger than the primary peaking amplifier. The reverse order of turn-on is because of the matching network. The wrong sizing may be perceived as counter-intuitive, and it is, but the cause of this improvement needs more research. Note that one of the main problems of an LMBA is the low reflection for the main amplifier at the two peaking amplifiers' sides. The final improvement is made by changing the parameter q of the main amplifier. In the ideal case, all three PAs should be a quasi-load invariant (QLI) Class E, but by trial and error, it has been found that for the main amplifier, a q of 1.2 improves the result; in the case that losses are included. The final chosen parameters are in Table 5.4. The final component values are in Appendix J. The results are shown in Figure 5.16. It is clear that the middle peaking shifts to the right, but at 10 dB OPBO, the drain efficiency is between 33–43%. At peak power, the drain efficiency is between 53-57%, having a peak power of 45 dBm.

Parameters	PA_{peak1}	PA_{peak2}	PA_{main}	Unit
Number of transistors	4	8	3	-
q	1.3	1.3	1.2	-
Q_0	1	1	1	-
R_{on} single transistor	8	8	8	Ω
C_{ds} single transistor	0.21	0.21	0.21	pF
voltage switching (VS)	0	0	0	V
voltage slope switching (VSS)	0	0	-11	Vs/s

Table 5.4: The final design parameters for a Class-E LMBA.

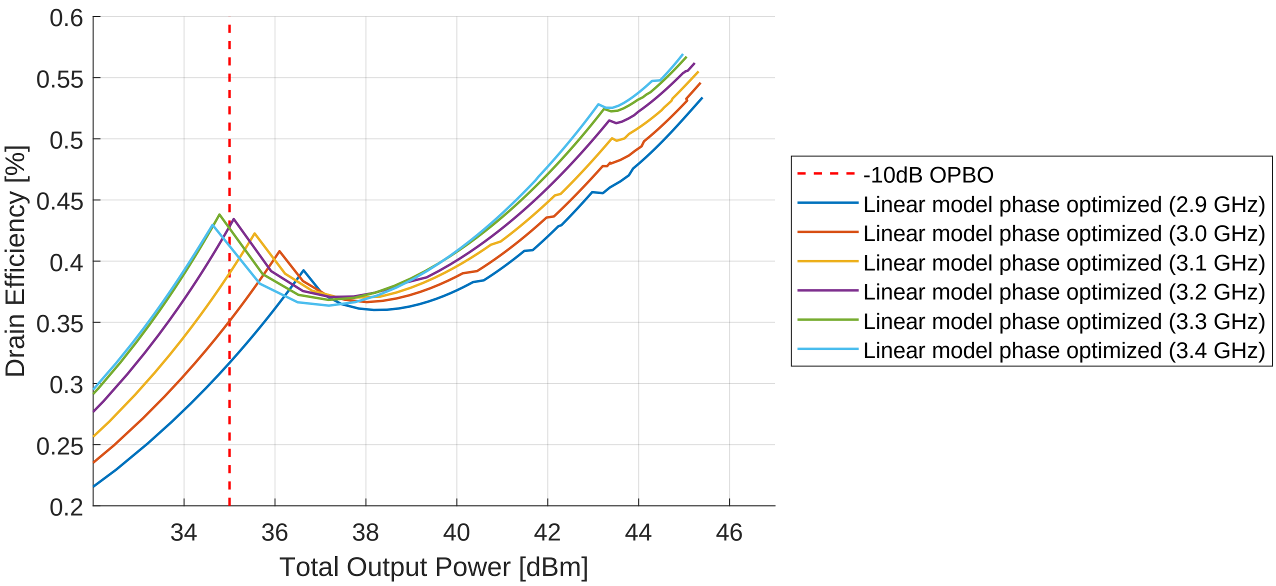

Figure 5.16: The drain-efficiency is plotted versus total output power by using the parameters from Table 5.4. This is the best design found until this point, improvements should be possible.

6 State-of-the-Art

Comparing this work to state-of-the-art is difficult. The main reason is that there are only a few integrated LMBAs designed. The integrated variants seem to have a significantly lower peak drain efficiency, but they are often also operating in higher frequency bands. This work has comparable drain efficiencies, output powers, and bandwidth ratios to these designs. The discrete designs could reach average drain efficiencies of 70%, which this design is not close to. But this design shows that there are lots of improvements to be made. The theoretical average drain efficiency of 82%, using lossless components but with a realistic transistor model, is not found in any paper about LMBAs to this date. The main reason is that there is no fully Class E LMBA designed yet.

Ref / Year	Architecture	Freq. (GHZ)	FBW (%)	P_{max} (dBm)	DE @ P_{max} (%)	DE @ 10 dB BO (%)	Technology
[28] 2020	2-way-Doherty, Class AB/C	2.8-3.5	24	42-43	66-78	50-61	GaN discrete
[35] 2014	3-way-Doherty, Class AB/C	1.9-2.4	23	40-44	60-75	60-69	GaN discrete
[11] 2021	H-ALMBA, Class F-1/C	1.7-3.0	55	42-43	63-81	50-66	GaN discrete
[29] 2022	PD-LMBA, Class AB/C	2.5-3.5	33	47-48	50-65	45-67	GaN discrete
[36] 2020	PD-LMBA, Class B/C	3.0-3.6	15	42-44	61-75	43-51	GaN discrete
[18] 2021	Outphasing LMBA, Class E	0.7	-	37	60	80	GaN discrete
[14] 2023	LMBA, Class AB/C	4.2-5.2	21	30-32	34-59	28-40	GaAs integrated
[44] 2021	LMBA	8.0-12.0	40	43	52-57	41-44	GaN integrated
This work	H-ALMBA, Class E	2.9-3.4	16	45-47	54-57	32-44	GaN integrated

Table 6.1: Comparison table where all the references are measured, while this work is a simulation with approximated losses. Another problem with comparing this work is that there is no work to compare it with. There is neither a full Class E LMBA nor an integrated LMBA using GaN in this frequency band.

7 Conclusion

In this thesis, research is done on different ways to implement digital power amplifiers. Starting with the digital Class AB and C, which provide the possibility for an increase in output power with the same drain efficiency, Next, a short discussion is done on Class D/D-1, which is promising in its differential configuration. There is Class F, which has the same promise compared to Class-E but with a more complicated implementation and lower drain efficiencies. Class E is the chosen design because of its simple typology and its promising drain efficiency. The Class-E/F topology has promises but is more difficult to implement, with one of the main improvements being a lower peak drain voltage and improved load modulation.

The goal of this thesis was to design a load-modulated balanced amplifier; therefore, a lot of research was done on different types of LMBAs. After that, the Hybrid Asymmetrical Load-Modulated Balanced Amplifier (H-ALMBA) was chosen for its high drain efficiency in the power back-off region.

Before starting the design, the GaN transistor was accurately modeled using a switch with finite on-resistance and a parallel drain-to-source voltage. This was done because it could be used for further mathematical modeling, and the model provided had significant convergence problems.

Next, a state-space model was used to find the required parameters for the matching network. Using these parameters, the total performance of a Class E LMBA could be calculated using a new semi-analytical mathematical model.

In the end, a final wideband design is presented first using a lossless matching network. This resulted in an H-LMBA with peak drain efficiencies of 88–85 % with 10 dB PBO and a minimum drain efficiency of 72 %. It was also shown that the H-ALMBA could have an average drain efficiency of 82 %, however, at the cost of bandwidth. The final design is also an H-ALMBA with an average drain efficiency of 45%, operating between 2.9—3.4 GHz with an output power of 45 dBm using GaN.

8 Future Work

The Class E LMBA could be improved further, especially since the losses in the matching network are currently very large. Therefore, more work should be put into having lower losses in the matching network. Also, the efficiency of the main amplifier at OPBO is decreased a lot by losses due to a low reflection coefficient at the peaking amplifiers. To solve this properly, more research is needed.

Next, a layout is not yet created; this could improve or worsen the result depending on the losses in the matching. Next, drivers for each transistor should be designed, preferably in CMOS. But in this case, an interface between GaN and CMOS is also required; this probably needs something like a flip-chip implementation, which is difficult to do.

Besides this, more work should be put into looking at the breakdown voltage of the GaN transistor, which is ignored in the current design. This would probably result in a Class E/F design that is more reliant on phase optimization for high efficiencies in output power back-off.

Lastly, one should start designing a fully digital Class B LMBA instead of starting at Class E. This will result in lower losses in the matching network and, therefore, a better overall result. A mix of classes is also proven to be useful.

References

[1] *A Wideband Four-Way Doherty Bits-In RF-Out CMOS Transmitter | IEEE Journals & Magazine | IEEE Xplore*. URL: https://ieeexplore.ieee.org/document/9526619 (visited on 11/13/2023).

[2] Mustafa Acar, Anne Johan Annema, and Bram Nauta. "Analytical Design Equations for Class-E Power Amplifiers with Finite DC-Feed Inductance and Switch On-Resistance". In: *2007 IEEE International Symposium on Circuits and Systems*. New Orleans, LA: IEEE, May 2007, pp. 2818–2821. ISBN: 978-1-4244-0920-4. DOI: 10.1109/ISCAS.2007.378758. URL: https://ieeexplore.ieee.org/document/4253264/ (visited on 12/01/2022).

[3] Mustafa Acar, Anne Johan Annema, and Bram Nauta. "Generalized Design Equations for Class-E Power Amplifiers with Finite DC Feed Inductance". In: *2006 European Microwave Conference*. Sept. 2006, pp. 1308–1311. DOI: 10.1109/EUMC.2006.281237. URL: https://ieeexplore.ieee.org/abstract/document/4058071 (visited on 01/16/2024).

[4] Mustafa Acar, Mark P. van der Heijden, and Domine M. W. Leenaerts. "0.75 Watt and 5 Watt drivers in standard 65nm CMOS technology for high power RF applications". In: *2012 IEEE Radio Frequency Integrated Circuits Symposium*. ISSN: 2375-0995. June 2012, pp. 283–286. DOI: 10.1109/RFIC.2012.6242282.

[5] Inder J. Bahl. *Lumped elements for RF and microwave circuits*. en. Second edition. Artech House microwave library. Boston London: ARTECH HOUSE, 2023. ISBN: 978-1-63081-932-3.

[6] R.J. Bootsman et al. "An 18.5 W Fully-Digital Transmitter with 60.4 % Peak System Efficiency". In: *2020 IEEE/MTT-S International Microwave Symposium (IMS)*. ISSN: 2576-7216. Aug. 2020, pp. 1113–1116. DOI: 10.1109/IMS30576.2020.9223942.

[7] Robert J. Bootsman et al. "High-Power Digital Transmitters for Wireless Infrastructure Applications (A Feasibility Study)". In: *IEEE Transactions on Microwave Theory and Techniques* 70.5 (May 2022). Conference Name: IEEE Transactions on Microwave Theory and Techniques, pp. 2835–2850. ISSN: 1557-9670. DOI: 10.1109/TMTT.2022.3153000. URL: https://ieeexplore.ieee.org/document/9733179 (visited on 02/16/2024).

[8] Yuchen Cao and Kenle Chen. "Dual-Octave-Bandwidth RF-Input Pseudo-Doherty Load Modulated Balanced Amplifier with ≥ 10-dB Power Back-off Range". en. In: *2020 IEEE/MTT-S International Microwave Symposium (IMS)*. Los Angeles, CA, USA: IEEE, Aug. 2020, pp. 703–706. ISBN: 978-1-72816-815-9. DOI: 10.1109/IMS30576.2020.9224026. URL: https://ieeexplore.ieee.org/document/9224026/ (visited on 11/02/2023).

[9] Yuchen Cao and Kenle Chen. "Hybrid Asymmetrical Load Modulated Balanced Amplifier With Wide Bandwidth and Three-Way-Doherty Efficiency Enhancement". In: *IEEE Microwave and Wireless Components Letters* 31.6 (June 2021). Conference Name: IEEE Microwave and Wireless Components Letters, pp. 721–724. ISSN: 1558-1764. DOI: 10.1109/LMWC.2021.3068613. URL: https://ieeexplore.ieee.org/document/9385139 (visited on 11/21/2023).

[10] Yuchen Cao and Kenle Chen. "Pseudo-Doherty Load-Modulated Balanced Amplifier With Wide Bandwidth and Extended Power Back-Off Range". en. In: *IEEE Transactions on Microwave Theory and Techniques* 68.7 (July 2020), pp. 3172–3183. ISSN: 0018-9480, 1557-9670. DOI: 10.1109/TMTT.2020.2983925. URL: https://ieeexplore.ieee.org/document/9072311/ (visited on 11/02/2023).

[11] Yuchen Cao, Haifeng Lyu, and Kenle Chen. “Asymmetrical Load Modulated Balanced Amplifier With Continuum of Modulation Ratio and Dual-Octave Bandwidth”. In: *IEEE Transactions on Microwave Theory and Techniques* 69.1 (Jan. 2021). Conference Name: IEEE Transactions on Microwave Theory and Techniques, pp. 682–696. ISSN: 1557-9670. DOI: 10.1109/TMTT.2020.3014616. URL: https://ieeexplore.ieee.org/document/9181485 (visited on 11/21/2023).

[12] Yuchen Cao, Haifeng Lyu, and Kenle Chen. “Continuous-Mode Hybrid Asymmetrical Load-Modulated Balanced Amplifier With Three-Way Modulation and Multi-Band Reconfigurability”. en. In: *IEEE Transactions on Circuits and Systems I: Regular Papers* 69.3 (Mar. 2022), pp. 1077–1090. ISSN: 1549-8328, 1558-0806. DOI: 10.1109/TCSI.2021.3129166. URL: https://ieeexplore.ieee.org/document/9629377/ (visited on 04/16/2024).

[13] Chi-Tsan Chen et al. “Design and linearization of Class-E power amplifier for non-constant envelope modulation”. In: *2008 IEEE Radio Frequency Integrated Circuits Symposium*. ISSN: 2375-0995. June 2008, pp. 145–148. DOI: 10.1109/RFIC.2008.4561405.

[14] Weijuan Chen et al. “Fully-Integrated Broadband GaAs MMIC Load Modulated Balanced Amplifier for Sub-6 GHz Applications”. en. In: *IEEE Transactions on Circuits and Systems II: Express Briefs* 70.8 (Aug. 2023), pp. 2834–2838. ISSN: 1549-7747, 1558-3791. DOI: 10.1109/TCSII.2023.3246042. URL: https://ieeexplore.ieee.org/document/10048493/ (visited on 06/19/2024).

[15] Steve C. Cripps. *RF Power Amplifiers for Wireless Communications*. en. Google-Books-ID: 3ntuQgAACAAJ. Artech House, 1999. ISBN: 978-0-89006-989-9.

[16] F. del-Aguila-Lopez et al. “A Discrete-Time Technique for the Steady-State Analysis of Nonlinear Class-E Amplifiers”. In: *IEEE Transactions on Circuits and Systems I: Regular Papers* 54.6 (June 2007). Conference Name: IEEE Transactions on Circuits and Systems I: Regular Papers, pp. 1358–1366. ISSN: 1558-0806. DOI: 10.1109/TCSI.2007.896741. URL: https://ieeexplore.ieee.org/document/4232581 (visited on 04/08/2024).

[17] Paul Dent. “Doherty amplifier”. US20050134377A1. June 2005. URL: https://patents.google.com/patent/US20050134377/en (visited on 11/14/2023).

[18] Jose A. Garcia et al. “Current-Injected Load-Modulated Outphasing Amplifier for Extended Power Range Operation”. en. In: *IEEE Microwave and Wireless Components Letters* 31.6 (June 2021), pp. 713–716. ISSN: 1531-1309, 1558-1764. DOI: 10.1109/LMWC.2021.3062150. URL: https://ieeexplore.ieee.org/document/9363158/ (visited on 10/09/2023).

[19] Ali Ghahremani, Anne-Johan Annema, and Bram Nauta. “Load Mismatch Sensitivity of Class-E Power Amplifiers”. en. In: *IEEE Transactions on Microwave Theory and Techniques* 67.1 (Jan. 2019), pp. 216–230. ISSN: 0018-9480, 1557-9670. DOI: 10.1109/TMTT.2018.2873702. URL: https://ieeexplore.ieee.org/document/8500354/ (visited on 01/09/2024).

[20] Ali Ghahremani, Anne-Johan Annema, and Bram Nauta. “Outphasing Class-E Power Amplifiers: From Theory to Back-Off Efficiency Improvement”. en. In: *IEEE Journal of Solid-State Circuits* 53.5 (May 2018), pp. 1374–1386. ISSN: 0018-9200, 1558-173X. DOI: 10.1109/JSSC.2017.2787759. URL: https://ieeexplore.ieee.org/document/8267479/ (visited on 10/11/2023).

[21] Andrei Grebennikov. “Class E high-efficiency power amplifiers: historical aspect and future prospect”. In: *Applied Microwave & Wireless* 14 (July 2002), 64–71(7), 64.

[22] Andrei Grebennikov and Marc J. Franco. *Switchmode RF and microwave power amplifiers*. en. Third edition. London [England] ; San Diego: Academic Press, 2021. ISBN: 978-0-12-821448-0.

[23] Andrei Grebennikov and Frederick H. Raab. “History of Class-F and Inverse Class-F Techniques: Developments in High-Efficiency Power Amplification from the 1910s to the 1980s”. In: *IEEE Microwave Magazine* 19.7 (Nov. 2018). Conference Name: IEEE Microwave Magazine, pp. 99–115. ISSN: 1557-9581. DOI: 10.1109/MMM.2018.2862838. URL: https://ieeexplore.ieee.org/document/8490268 (visited on 12/07/2023).

[24] M. Hashemi. “Energy Efficient and Intrinsically Linear Digital Polar Transmitters”. en. In: (2020). DOI: 10.4233/uuid:7ad707a5-2db6-4185-bd3a-7a97fcf74b23. URL: https://repository.tudelft.nl/islandora/object/uuid%3A7ad707a5-2db6-4185-bd3a-7a97fcf74b23 (visited on 05/17/2024).

[25] S.D. Kee et al. “The class-E/F family of ZVS switching amplifiers”. In: *IEEE Transactions on Microwave Theory and Techniques* 51.6 (June 2003). Conference Name: IEEE Transactions on Microwave Theory and Techniques, pp. 1677–1690. ISSN: 1557-9670. DOI: 10.1109/TMTT.2003.812564. URL: https://ieeexplore.ieee.org/document/1201800 (visited on 11/13/2023).

[26] Scott David Kee. “The Class E/F Family of Harmonic-Tuned Switching Power Amplifiers”. en. phd. California Institute of Technology, 2002. DOI: 10.7907/MD86-FX51. URL: https://resolver.caltech.edu/CaltechETD:etd-04262005-152703 (visited on 11/29/2023).

[27] N. Kumar et al. “High-Efficiency Broadband Parallel-Circuit Class E RF Power Amplifier With Reactance-Compensation Technique”. en. In: *IEEE Transactions on Microwave Theory and Techniques* 56.3 (Mar. 2008), pp. 604–612. ISSN: 0018-9480, 1557-9670. DOI: 10.1109/TMTT.2008.916906. URL: http://ieeexplore.ieee.org/document/4447389/ (visited on 05/03/2024).

[28] Meng Li et al. “Bandwidth Enhancement of Doherty Power Amplifier Using Modified Load Modulation Network”. en. In: *IEEE Transactions on Circuits and Systems I: Regular Papers* 67.6 (June 2020), pp. 1824–1834. ISSN: 1549-8328, 1558-0806. DOI: 10.1109/TCSI.2020.2972163. URL: https://ieeexplore.ieee.org/document/8995800/ (visited on 06/18/2024).

[29] Han Liu et al. “Simulated Annealing Particle Swarm Optimization for a Dual-Input Broadband GaN Doherty Like Load-Modulated Balance Amplifier Design”. en. In: *IEEE Transactions on Circuits and Systems II: Express Briefs* 69.9 (Sept. 2022), pp. 3734–3738. ISSN: 1549-7747, 1558-3791. DOI: 10.1109/TCSII.2022.3173608. URL: https://ieeexplore.ieee.org/document/9771178/ (visited on 06/18/2024).

[30] Haifeng Lyu and Kenle Chen. “Hybrid Load-Modulated Balanced Amplifier With High Linearity and Extended Dynamic Range”. en. In: *IEEE Microwave and Wireless Components Letters* 31.9 (Sept. 2021), pp. 1067–1070. ISSN: 1531-1309, 1558-1764. DOI: 10.1109/LMWC.2021.3083235. URL: https://ieeexplore.ieee.org/document/9439961/ (visited on 10/29/2023).

[31] Earl McCune. “A Technical Foundation for RF CMOS Power Amplifiers: Part 3: Power Amplifier 3-Port Characteristics”. In: *IEEE Solid-State Circuits Magazine* 8.1 (2016). Conference Name: IEEE Solid-State Circuits Magazine, pp. 44–50. ISSN: 1943-0590. DOI: 10.1109/MSSC.2015.2495664. URL: https://ieeexplore.ieee.org/document/7387885 (visited on 11/23/2023).

[32] Matteo Meneghini, Gaudenzio Meneghesso, and Enrico Zanoni, eds. *Power GaN Devices: Materials, Applications and Reliability*. en. Power Electronics and Power Systems. Cham: Springer International Publishing, 2017. ISBN: 978-3-319-43197-0 978-3-319-43199-4. DOI: 10.1007/978-3-319-43199-4. URL: http://link.springer.com/10.1007/978-3-319-43199-4 (visited on 09/21/2023).

[33] Dominic Mikrut et al. “A Comparison Study on the Broadband Performance of Load-Modulated Architectures using Nonlinear Embedding at 20 GHz”. en. In: *2023 IEEE Topical Conference on RF/Microwave Power Amplifiers for Radio and Wireless Applications*. Las Vegas, NV, USA: IEEE, Jan. 2023, pp. 32–35. ISBN: 978-1-66549-317-8. DOI: 10.1109/PAWR56957.2023.10046277. URL: https://ieeexplore.ieee.org/document/10046277/ (visited on 11/02/2023).

[34] Dieuwert P.N. Mul et al. “Efficiency and Linearity of Digital ”Class-C Like” Transmitters”. en. In: *2020 50th European Microwave Conference (EuMC)*. Utrecht, Netherlands: IEEE, Jan. 2021, pp. 1–4. ISBN: 978-2-87487-059-0. DOI: 10.23919/EuMC48046.2021.9338122. URL: https://ieeexplore.ieee.org/document/9338122/ (visited on 10/12/2023).

[35] Xuan Anh Nghiem, Junqing Guan, and Renato Negra. “Design of a broadband three-way sequential Doherty power amplifier for modern wireless communications”. en. In: *2014 IEEE MTT-S International Microwave Symposium (IMS2014)*. Tampa, FL, USA: IEEE, June 2014, pp. 1–4. ISBN: 978-1-4799-3869-8. DOI: 10.1109/MWSYM.2014.6848476. URL: http://ieeexplore.ieee.org/document/6848476/ (visited on 06/18/2024).

[36] Jingzhou Pang et al. “Analysis and Design of Highly Efficient Wideband RF-Input Sequential Load Modulated Balanced Power Amplifier”. en. In: *IEEE Transactions on Microwave Theory and Techniques* 68.5 (May 2020), pp. 1741–1753. ISSN: 0018-9480, 1557-9670. DOI: 10.1109/TMTT.2019.2963868. URL: https://ieeexplore.ieee.org/document/8966560/ (visited on 06/18/2024).

[37] Jong Seok Park and Hua Wang. “A Transformer-Based Poly-Phase Network for Ultra-Broadband Quadrature Signal Generation”. en. In: *IEEE Transactions on Microwave Theory and Techniques* 63.12 (Dec. 2015), pp. 4444–4457. ISSN: 0018-9480, 1557-9670. DOI: 10.1109/TMTT.2015.2496187. URL: http://ieeexplore.ieee.org/document/7331329/ (visited on 06/19/2024).

[38] Abdul R. Qureshi et al. “A 112W GaN dual input Doherty-Outphasing Power Amplifier”. en. In: *2016 IEEE MTT-S International Microwave Symposium (IMS)*. San Francisco, CA: IEEE, May 2016, pp. 1–4. ISBN: 978-1-5090-0698-4. DOI: 10.1109/MWSYM.2016.7540194. URL: http://ieeexplore.ieee.org/document/7540194/ (visited on 11/02/2023).

[39] P. Reynaert, K.L.R. Mertens, and M.S.J. Steyaert. “A state-space behavioral model for CMOS class E power amplifiers”. In: *IEEE Transactions on Computer-Aided Design of Integrated Circuits and Systems* 22.2 (Feb. 2003). Conference Name: IEEE Transactions on Computer-Aided Design of Integrated Circuits and Systems, pp. 132–138. ISSN: 1937-4151. DOI: 10.1109/TCAD.2002.806602. URL: https://ieeexplore.ieee.org/abstract/document/1174090 (visited on 01/31/2024).

[40] Daniel J. Shepphard, Jeffrey Powell, and Steve C. Cripps. “A Broadband Reconfigurable Load Modulated Balanced Amplifier (LMBA)”. In: *2017 IEEE MTT-S International Microwave Symposium (IMS)*. June 2017, pp. 947–949. DOI: 10.1109/MWSYM.2017.8058743. URL: https://ieeexplore.ieee.org/document/8058743 (visited on 11/02/2023).

[41] Daniel J. Shepphard, Jeffrey Powell, and Steve C. Cripps. “An Efficient Broadband Reconfigurable Power Amplifier Using Active Load Modulation”. en. In: *IEEE Microwave and Wireless Components Letters* 26.6 (June 2016), pp. 443–445. ISSN: 1531-1309, 1558-1764. DOI: 10.1109/LMWC.2016.2559503. URL: http://ieeexplore.ieee.org/document/7469815/ (visited on 10/09/2023).

[42] A. Sigg et al. “High efficiency GaN current-mode class-D amplifier at 2.6 GHz using pure differential transmission line filters”. en. In: *Electronics Letters* 49.1 (2013), pp. 47–49. ISSN: 1350-911X. DOI: 10.1049/el.2012.3984. URL: https://onlinelibrary.wiley.com/doi/abs/10.1049/el.2012.3984 (visited on 11/07/2023).

[43] David Vegas et al. “UHF Class E/F2 Outphasing Transmitter for 12 dB PAPR Signals”. In: *2019 IEEE MTT-S International Microwave Symposium (IMS)*. ISSN: 2576-7216. June 2019, pp. 71–74. DOI: 10.1109/MWSYM.2019.8700947. URL: https://ieeexplore.ieee.org/document/8700947 (visited on 12/04/2023).

[44] Zheng Yin et al. "8-12GHz Pre-matched Load Modulation Balanced Power Amplifier". en. In: *2021 7th International Conference on Computer and Communications (ICCC)*. Chengdu, China: IEEE, Dec. 2021, pp. 169–172. ISBN: 978-1-66540-950-6. DOI: 10.1109/ICCC54389.2021.9674439. URL: https://ieeexplore.ieee.org/document/9674439/ (visited on 06/19/2024).

A

A simple Switch Mode Power Amplifier

The most simple SMPA using an ideal switch is shown in Figure A.1. A perfect switch is either short or open and has either voltage-zero drop or zero current flow. As a result, the voltage or the current is never present simultaneously, resulting in zero power dissipation. All the power could be delivered to the load using a DC feed from the power supply. This results in a square wave on the load. The square wave is a combination of the fundamental harmonic and higher harmonics. The drain efficiency is defined as the power of the fundamental frequency f_0 divided by the DC power, shown in equation A.1. A time-domain square wave exists from odd frequency components and its fundamental frequency. The only frequency of interest is the fundamental frequency. The ratio of the fundamental frequency and odd multiples depends on the duty-cycle α.

$$\eta_d = \frac{P_{OUT,f_0}}{P_{DC}} = \frac{P_{load,f_0}}{P_{load,f_0} + P_{switch}} \tag{A.1}$$

In Figure A.1, the current and voltage waveforms over the switch can be seen. Changing the conduction angle α(can be seen as a variant on the duty cycle) would change the efficiency as given in A.2, where the maximum drain-efficiency achievable is $8/\pi^2$ or, in other words, 81%.

$$\eta_d = \frac{2 \cdot \sin(\alpha)^2}{\alpha \cdot (\pi - \alpha)} \tag{A.2}$$

It is essential to realize that the FET cannot be reduced down to an ideal switch. When the transistor behaves in its triode region, it can be simplified as a resistor with on-resistance R_{on}. This feature creates a current division from the base to the load, as shown here:

$$I_{sw}(0) = I_{pk} = \frac{V_{DC} + R_L \cdot I_{DC}}{R_L + R_{on}} \tag{A.3}$$

This reduces the SMPA's efficiency due to the extra power consumption of the on-resistance. Note that this on-resistance can also be changed by either changing the width of the transistor, the threshold voltage when possible, or the number of fingers enabled; this can then be used as a form of power modulation. When a non-zero on resistance is included in the drain-efficiency equation, the equation becomes:

$$\eta_d = \frac{2\sin(\alpha)^2}{\alpha \cdot (\pi - \alpha)} \cdot \frac{R_L}{R_L + 2 \cdot R_{on}} \tag{A.4}$$

Even with zero on-resistance will the drain effiency not be a 100%. This is caused by the additional higher harmonics still pressent on the load. The losses due to the higher harmonics can be removed by using a correct matching network, some possible matching networks are Class-E, Class-F and Class-D^{-1}

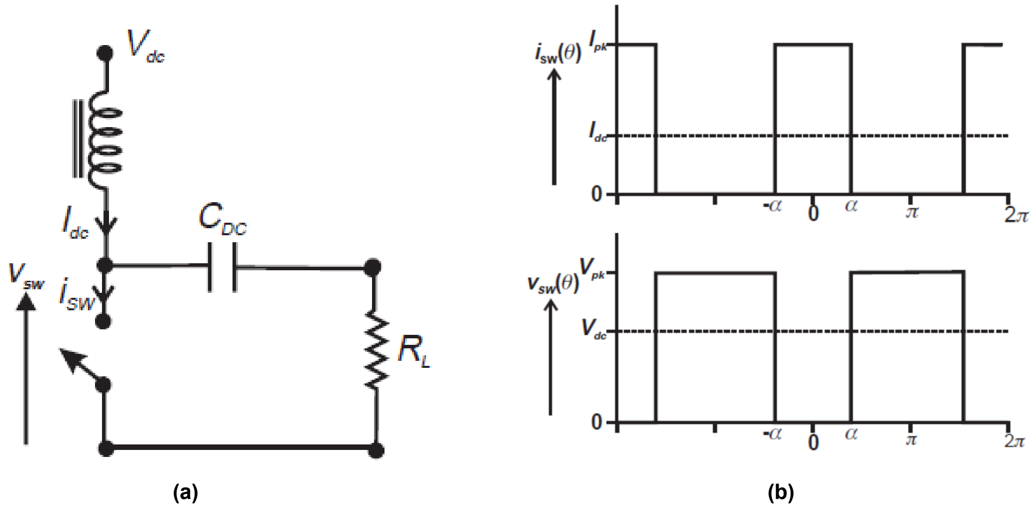

Figure A.1: The most simple SMPA with at its right the voltage and current waveforms from [15].

B

Derivation of Output Currents

First, the integral is taken:

$$\frac{d}{dt}\left(e^{-2\pi j\frac{t+t_n}{T}} \cdot \mathbf{q}_n(t)\right) = e^{-2\pi j\frac{t+t_n}{T}} \cdot \frac{d\mathbf{q}_n(t)}{dt} - \frac{2\pi j}{T} \cdot e^{-2\pi j\frac{t+t_n}{T}} \cdot \mathbf{q}_n(t) \tag{B.1}$$

Now, the general state space equation 4.1 is injected:

$$\frac{d}{dt}\left(e^{-2\pi j\frac{t+t_n}{T}} \cdot \mathbf{q}_n(t)\right) = e^{-2\pi j\frac{t+t_n}{T}} \cdot (\mathbf{A}_n \cdot \mathbf{q}_n(t) + \mathbf{B}_n) - \frac{2\pi j}{T} \cdot e^{-2\pi j\frac{t+t_n}{T}} \cdot \mathbf{q}_n(t) \tag{B.2}$$

Next, integrate both sides:

$$\int_0^{dtn} \frac{d}{dt}\left(e^{-2\pi j\frac{t+t_n}{T}} \cdot \mathbf{q}_n(t)\right)\, dt = \int_0^{dtn} e^{-2\pi j\frac{t+t_n}{T}} \cdot (\mathbf{A}_n \cdot \mathbf{q}_n(t) + \mathbf{B}_n)\, dt - \int_0^{dtn} \frac{2\pi j}{T} \cdot e^{-2\pi j\frac{t+t_n}{T}} \cdot \mathbf{q}_n(t)\, dt \tag{B.3}$$

$$= \int_0^{dtn} e^{-2\pi j\frac{t+t_n}{T}} \cdot \mathbf{q}_n(t)\, dt \cdot \left(\mathbf{A}_n - \frac{2\pi j}{T} \cdot \mathbf{I}\right) + \int_0^{dtn} e^{-2\pi j\frac{t+t_n}{T}} \cdot \mathbf{B}_n\, dt \tag{B.4}$$

$$\begin{aligned} &= \int_0^{dtn} e^{-2\pi j\frac{t+t_n}{T}} \cdot \mathbf{q}_n(t)\, dt \cdot \left(\mathbf{A}_n - \frac{2\pi j}{T} \cdot \mathbf{I}\right) \\ &\quad + \frac{jT\mathbf{B}_n}{2\pi}\left(e^{-2\pi j\frac{t_n}{T}} - e^{-2\pi j\frac{t_{n-1}}{T}}\right) \end{aligned} \tag{B.5}$$

On the left side, the following can be worked out:

$$\begin{aligned} \int_0^{dtn} \frac{d}{dt}\left(e^{-2\pi j\frac{t+t_n}{T}} \cdot \mathbf{q}_n(t)\right)\, dt &= \left[e^{-2\pi j\frac{t+t_n}{T}} \cdot \mathbf{q}_n(t)\right]_0^{dt_n} \\ &= e^{-2\pi j\frac{dtn+t_{n-1}}{T}} \cdot \mathbf{q}_n(dt_n) - e^{-2\pi j\frac{t_{n-1}}{T}} \cdot \mathbf{q}_n(0) \end{aligned} \tag{B.6}$$

Combining both B.5 and B.6:

$$\begin{aligned} \left(\mathbf{A}_n - \frac{2\pi j}{T} \cdot \mathbf{I}\right) \cdot \int_0^{dtn} e^{-2\pi j\frac{t+t_n}{T}} \cdot \mathbf{q}_n(t)\, dt + \frac{jT\mathbf{B}_n}{2\pi}\left(e^{-2\pi j\frac{t_n}{T}} - e^{-2\pi j\frac{t_{n-1}}{T}}\right) = \\ e^{-2\pi j\frac{dtn+t_{n-1}}{T}} \cdot \mathbf{q}_n(dt_n) - e^{-2\pi j\frac{t_{n-1}}{T}} \cdot \mathbf{q}_n(0) \end{aligned} \tag{B.7}$$

$$\begin{aligned} \int_0^{dtn} e^{-2\pi j\frac{t+t_n}{T}} \cdot \mathbf{q}_n(t)\, dt = \\ \left(\mathbf{A}_n - \frac{2\pi j}{T} \cdot \mathbf{I}\right)^{-1} \cdot \left(e^{-2\pi j\frac{t_n}{T}} \cdot \mathbf{q}_n(dt_n) - e^{-2\pi j\frac{t_{n-1}}{T}} \cdot \mathbf{q}_n(0) - \frac{jT\mathbf{B}_n}{2\pi}\left(e^{-2\pi j\frac{t_n}{T}} - e^{-2\pi j\frac{t_{n-1}}{T}}\right)\right) \end{aligned} \tag{B.8}$$

First, we know that the state space variable is defined as: $\mathbf{q} = \begin{bmatrix} i_l & i_x & v_C & v_0 \end{bmatrix}$, where i_x is the current that flows through the hybrid coupler. To determine the fundamental current component, we can set up the following equations:

$$\begin{aligned}
\hat{\mathbf{q}}(1) &= \frac{2}{T}\int_0^T e^{-2\pi j \frac{t}{T}} \cdot \mathbf{q}(t)\,dt \\
&= \frac{2}{T}\left(\int_{t_0}^{t_1} e^{-2\pi j \frac{t}{T}} \cdot \mathbf{q}_1(t)\,dt + \int_{t_1}^{t_2} e^{-2\pi j \frac{t}{T}} \cdot \mathbf{q}_2(t)\,dt + \dots\right) \\
&= \frac{2}{T}\left(\int_0^{dt_1} e^{-2\pi j \frac{t+t_0}{T}} \cdot \mathbf{q}_1(t)\,dt + \int_0^{dt_2} e^{-2\pi j \frac{t+t_1}{T}} \cdot \mathbf{q}_2(t)\,dt + \dots\right) \\
&= \frac{2}{T}\sum_{n=1}^{N}\left(\int_0^{dt_n} e^{-2\pi j \frac{t+t_{n-1}}{T}} \cdot \mathbf{q}_n(t)\,dt\right)
\end{aligned} \tag{B.9}$$

Where $T = t_0 + t_1 + \ldots + t_N = \sum_{n=0}^{N} t_n$ and $dt_n = t_n - t_{n-1}$

C

Matching derivations

Start with the basic LMBA equations:

$$\begin{bmatrix} v_1 \\ v_2 \\ v_3 \end{bmatrix} = \begin{bmatrix} 0 & Z_0 & \sqrt{2}Z_0 \\ -Z_0 & 2Z_0 & \sqrt{2}Z_0 \\ -\sqrt{2}Z_0 & \sqrt{2}Z_0 & Z_0 \end{bmatrix} \begin{bmatrix} i_1 \\ i_2 \\ i_3 \end{bmatrix} \tag{C.1}$$

When the transformers are added, both the voltages and the currents are changed. The relationship of a transformer is as follows:

$$\begin{aligned} v_{x,new} &= \frac{v_x}{n_x} \\ i_{x,new} &= n_x i_x \end{aligned} \tag{C.2}$$

Implementing this in the complete equation is as follows:

$$\begin{bmatrix} n_1 & 0 & 0 \\ 0 & n_2 & 0 \\ 0 & 0 & n_3 \end{bmatrix} \begin{bmatrix} v_{1new} \\ v_{2new} \\ v_{3new} \end{bmatrix} = \begin{bmatrix} 0 & Z_0 & \sqrt{2}Z_0 \\ -Z_0 & 2Z_0 & \sqrt{2}Z_0 \\ -\sqrt{2}Z_0 & \sqrt{2}Z_0 & Z_0 \end{bmatrix} \begin{bmatrix} 1/n_1 & 0 & 0 \\ 0 & 1/n_2 & 0 \\ 0 & 0 & 1/n_3 \end{bmatrix} \begin{bmatrix} i_{1new} \\ i_{2new} \\ i_{3new} \end{bmatrix} \tag{C.3}$$

$$\begin{bmatrix} v_{1new} \\ v_{2new} \\ v_{3new} \end{bmatrix} = \begin{bmatrix} n_1 & 0 & 0 \\ 0 & n_2 & 0 \\ 0 & 0 & n_3 \end{bmatrix}^{-1} \begin{bmatrix} 0 & Z_0 & \sqrt{2}Z_0 \\ -Z_0 & 2Z_0 & \sqrt{2}Z_0 \\ -\sqrt{2}Z_0 & \sqrt{2}Z_0 & Z_0 \end{bmatrix} \begin{bmatrix} 1/n_1 & 0 & 0 \\ 0 & 1/n_2 & 0 \\ 0 & 0 & 1/n_3 \end{bmatrix} \begin{bmatrix} i_{1new} \\ i_{2new} \\ i_{3new} \end{bmatrix} \tag{C.4}$$

$$\begin{bmatrix} v_{1new} \\ v_{2new} \\ v_{3new} \end{bmatrix} = \begin{bmatrix} 0 & \frac{Z_0}{n_2 n_1} & \frac{\sqrt{2}Z_0}{n_1 n_3} \\ -\frac{Z_0}{n_2 n_1} & 2\frac{Z_0}{n_2^2} & \frac{\sqrt{2}Z_0}{n_2 n_3} \\ -\frac{\sqrt{2}Z_0}{n_3 n_1} & \frac{\sqrt{2}Z_0}{n_3 n_2} & \frac{Z_0}{n_3^2} \end{bmatrix} \begin{bmatrix} i_{1new} \\ i_{2new} \\ i_{3new} \end{bmatrix} \tag{C.5}$$

This can be rewritten into the impedance matrix as follows:

$$\begin{bmatrix} 1/i_{1new} & 0 & 0 \\ 0 & 1/i_{3new} & 0 \\ 0 & 0 & 1/i_{2new} \end{bmatrix} \begin{bmatrix} v_{1new} \\ v_{2new} \\ v_{3new} \end{bmatrix} = \begin{bmatrix} 1/i_{1new} & 0 & 0 \\ 0 & 1/i_{2new} & 0 \\ 0 & 0 & 1/i_{3new} \end{bmatrix} \begin{bmatrix} 0 & \frac{Z_0}{n_2 n_1} & \frac{\sqrt{2}Z_0}{n_1 n_3} \\ -\frac{Z_0}{n_2 n_1} & 2\frac{Z_0}{n_2^2} & \frac{\sqrt{2}Z_0}{n_2 n_3} \\ -\frac{\sqrt{2}Z_0}{n_3 n_1} & \frac{\sqrt{2}Z_0}{n_3 n_2} & \frac{Z_0}{n_3^2} \end{bmatrix} \begin{bmatrix} i_{1new} \\ i_{2new} \\ i_{3new} \end{bmatrix} \tag{C.6}$$

$$\begin{bmatrix} Z_{1new} \\ Z_{2new} \\ Z_{3new} \end{bmatrix} = \begin{bmatrix} 1/i_{1new} & 0 & 0 \\ 0 & 1/i_{2new} & 0 \\ 0 & 0 & 1/i_{3new} \end{bmatrix} \begin{bmatrix} 0 & \frac{Z_0}{n_2 n_1} & \frac{\sqrt{2} Z_0}{n_1 n_3} \\ -\frac{Z_0}{n_2 n_1} & 2\frac{Z_0}{n_2^2} & \frac{\sqrt{2} Z_0}{n_2 n_3} \\ -\frac{\sqrt{2} Z_0}{n_3 n_1} & \frac{\sqrt{2} Z_0}{n_3 n_2} & \frac{Z_0}{n_3^2} \end{bmatrix} \begin{bmatrix} i_{1new} \\ i_{2new} \\ i_{3new} \end{bmatrix} \tag{C.7}$$

$$\begin{aligned} Z_{1new} &= Z_0 \left(\frac{i_{2new}}{i_{1new} n_1 n_2} + \frac{\sqrt{2} i_{3new}}{i_{1new} n_1 n_3} \right) \\ Z_{2new} &= Z_0 \left(\frac{2}{n_2^2} + \frac{\sqrt{2} i_{3new}}{i_{2new} n_2 n_3} - \frac{i_{1new}}{i_{2new} n_1 n_2} \right) \\ Z_{3new} &= Z_0 \left(\frac{1}{n_3^2} + \frac{\sqrt{2} i_{2new}}{i_{3new} n_2 n_3} - \frac{\sqrt{2} i_{1new}}{i_{3new} n_1 n_3} \right) \end{aligned} \tag{C.8}$$

D

The Fourier transform of a square wave with a delay

The square wave can be described by adding odd harmonics, as follows:

$$\frac{4}{\pi}\sum_{k=1}^{\infty}\left(\frac{\sin((2k-1)\cdot\omega_0 t+\pi)}{2k-1}\right) \tag{D.1}$$

When we look at only the fundamental and its first harmonic, we have the following:

$$\frac{4}{\pi}\sum_{k=1}^{2}\left(\frac{\sin((2k-1)\cdot\omega_0 t+\pi)}{2k-1}\right)=-\frac{4}{\pi}\sin(\omega_0 t)-\frac{4}{3\pi}\sin(3\omega_0 t) \tag{D.2}$$

Therefore, there is no phase rotation at the fundamental and third-order harmonics. Next, we can add a delay of t_d to the input as follows:

$$\frac{4}{\pi}\sum_{k=1}^{2}\left(\frac{\sin((2k-1)\cdot\omega_0 (t-t_d)+\pi)}{2k-1}\right)=-\frac{4}{\pi}\sin(\omega_0 (t-t_d))-\frac{4}{3\pi}\sin(3\omega_0 (t-t_d)) \tag{D.3}$$

We can apply the Fourier time delay property:

$$\mathfrak{F}\{x(t-t_d)\}=\mathfrak{F}\{x(t)\}e^{-j\omega t_d} \tag{D.4}$$

Next, we want to compensate for the phase shift (ϕ_{shift}) at the fundamental frequency by applying a time delay to the input:

$$\omega_0 t_d=\phi_{shift} \tag{D.5}$$

$$\begin{aligned}\frac{4}{\pi}\sum_{k=1}^{2}\left(\frac{\sin((2k-1)\cdot\omega_0 (t-t_d+\frac{\phi_{shift}}{\omega_0})+\pi)}{2k-1}\right)&=-\frac{4}{\pi}\sin(\omega_0 (t-t_d)+\phi_{shift})-\frac{4}{3\pi}\sin(3\omega_0 (t-t_d)+\phi_{shift})\\&=-\frac{4}{\pi}\sin(\omega_0 t)-\frac{4}{3\pi}\sin(3\omega_0 t-2\omega_0 t_d)\end{aligned} \tag{D.6}$$

In this equation, we see that at the fundamental frequency, the phase shift is properly compensated, but at the third harmonic, this is not the case; therefore, the simplification of 4.37 can only be applied to the fundamental frequency.

E

Coupler designs

Parameter	Value
W	18 um
S	2 um
L	10^4 um

Table E.1: Design parameters for a -3dB coupled line.

Parameter	Value
$W_{50\Omega}$	64 um
$L_{50\Omega}$	9152 um
$W_{35\Omega}$	122 um
$L_{35\Omega}$	8834 um

Table E.2: Design parameters for a 90 degrees branchline coupler.

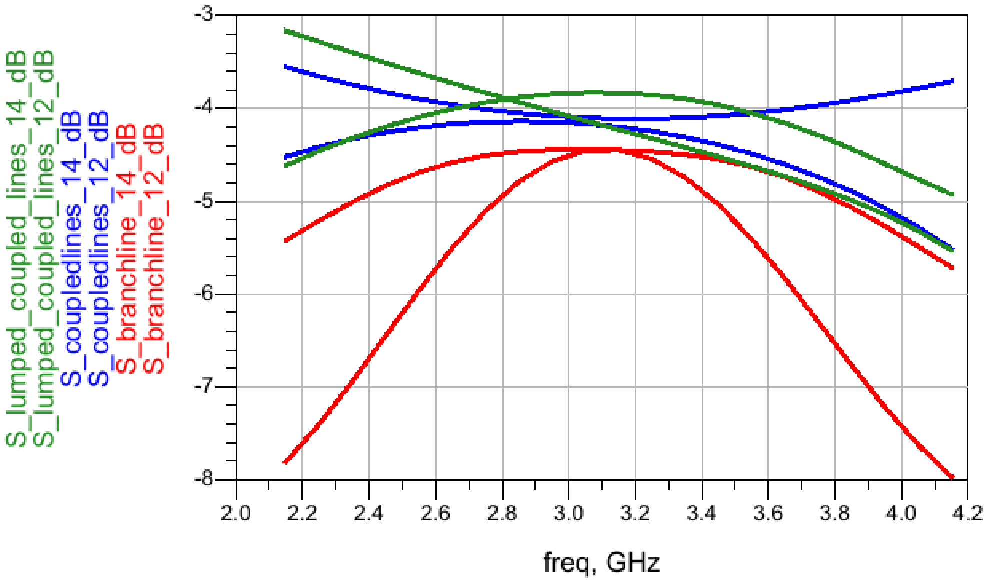

Figure E.1: The input reflection S-parameters, where all are properly matched to 50 Ω. However, the branchline coupler is more narrowband.

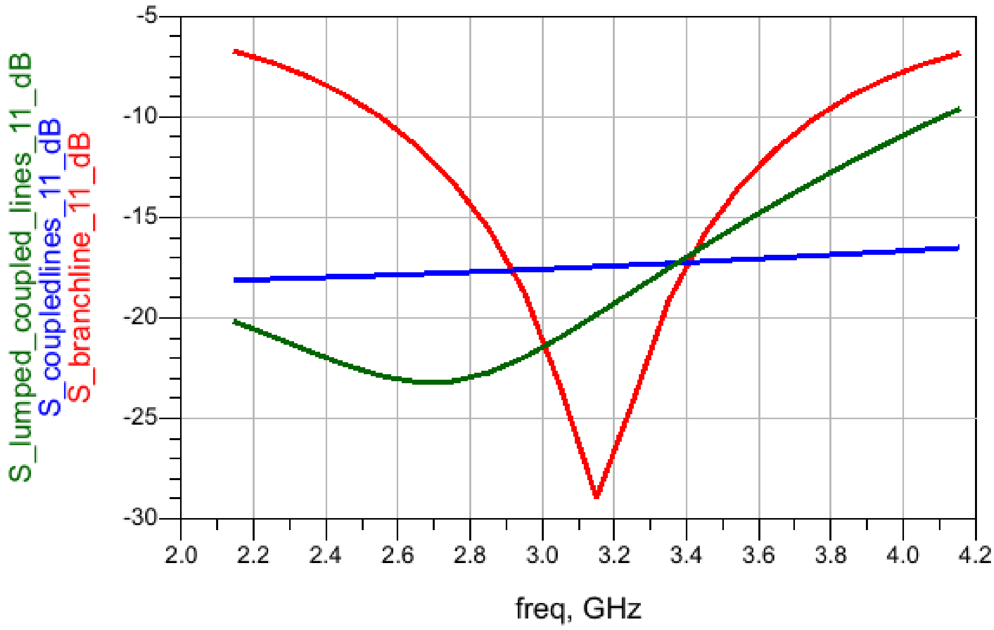

Figure E.2: The transmission S-parameters, where all split the input. But the coupled lines are less lossy compared to the branchline coupler. The coupled lines are also wide bandwidth.

F
Matching network

The implementation of the matching network, consists out of three matching networks:

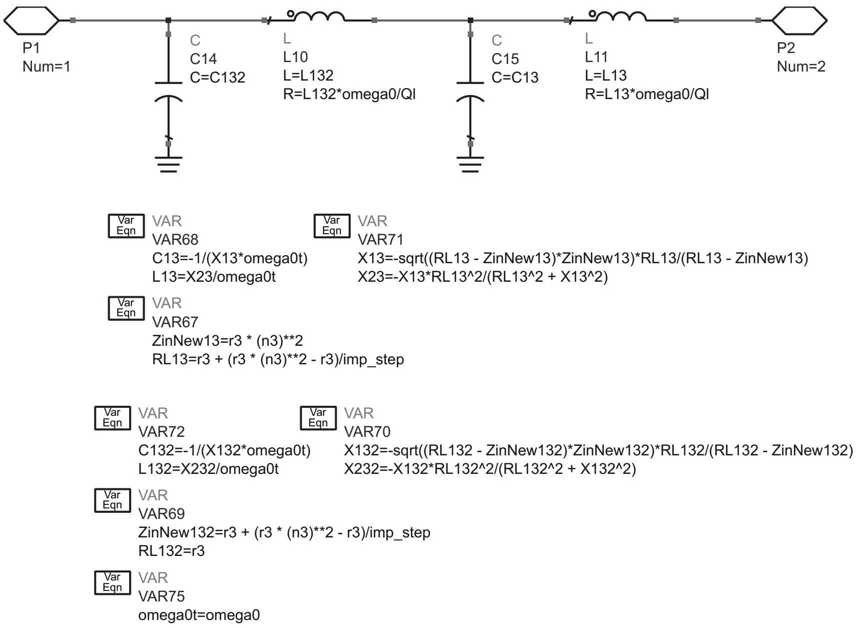

Figure F.1: The two stage matching network consists out of two low-pass filters which keeps the load modulation on the real-axis.

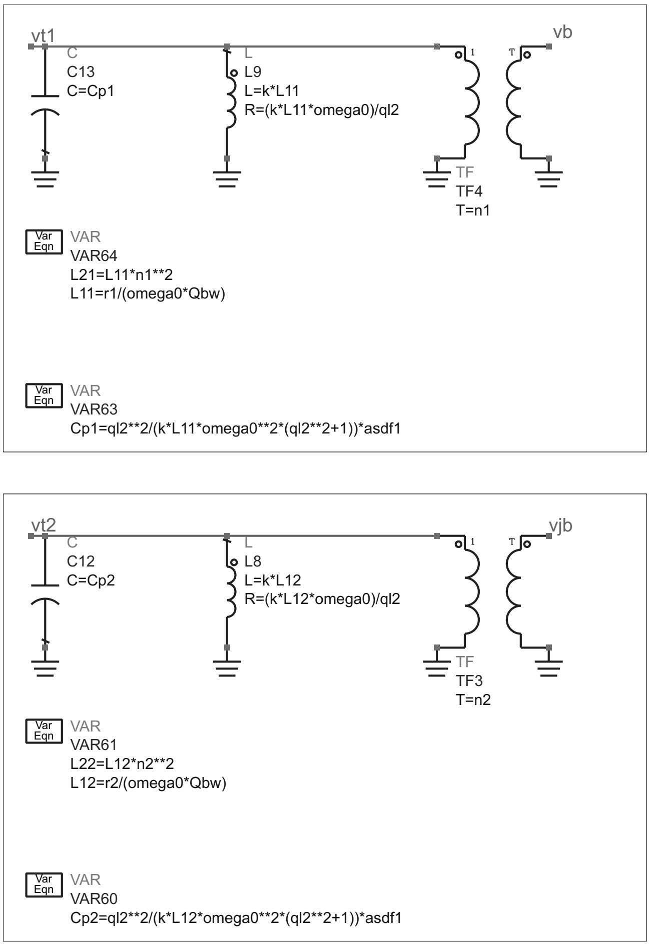

Figure F.2: The transformer based matching network is simplified, but the main important part is the resonating behaviour, the bandwidth of the resonator is chosen to be 2 GHz.

G

Alternative Design

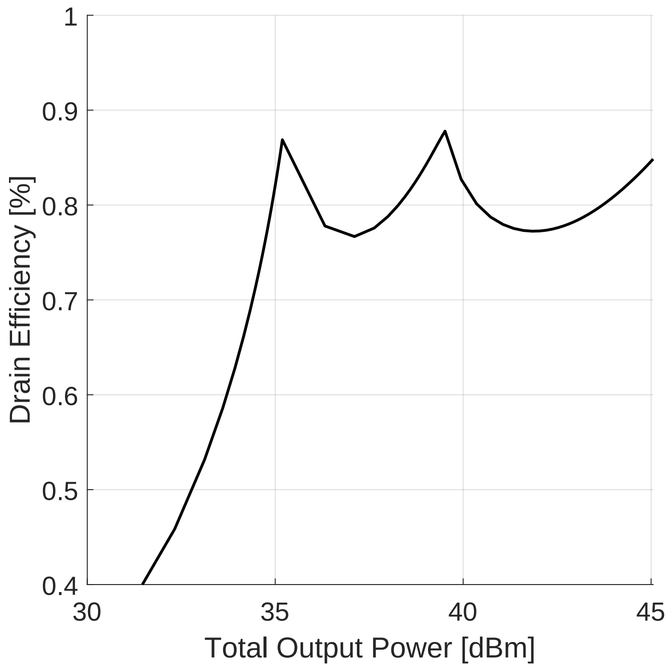

(a)

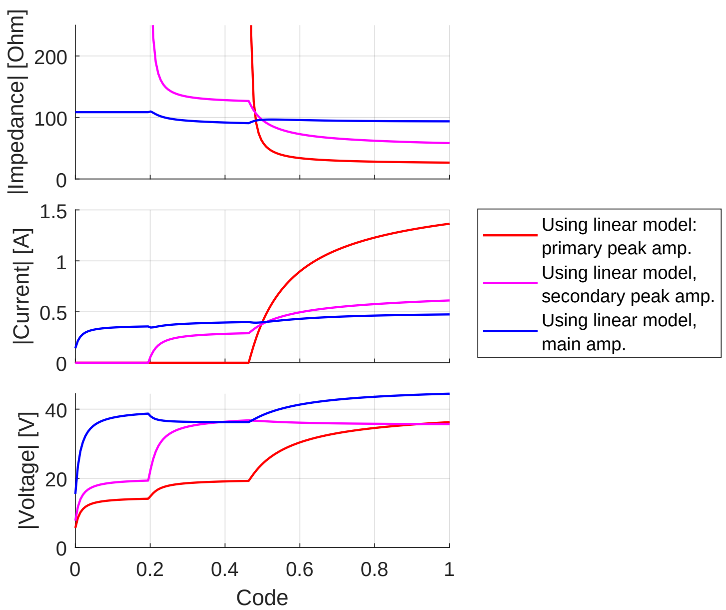

(b)

Figure G.1: Using lossless components, an almost ideal response can be found. This is simulated using linear model and nonlinear models give equivalent results.

Parameters	PA_{peak1}	PA_{peak2}	PA_{main}	Unit
Number of transistors	8	4	3	-
q	1.3	1.3	1.3	-
Q_0	1	1	1	-
R_{on} single transistor	8	8	8	Ω
C_{ds} single transistor	0.21	0.21	0.21	pF
voltage switching (VS)	0	0	0	V
voltage slope switching (VSS)	0	0	-27	Vs/s

Table G.1: The alternative design parameters for a Class-E LMBA.

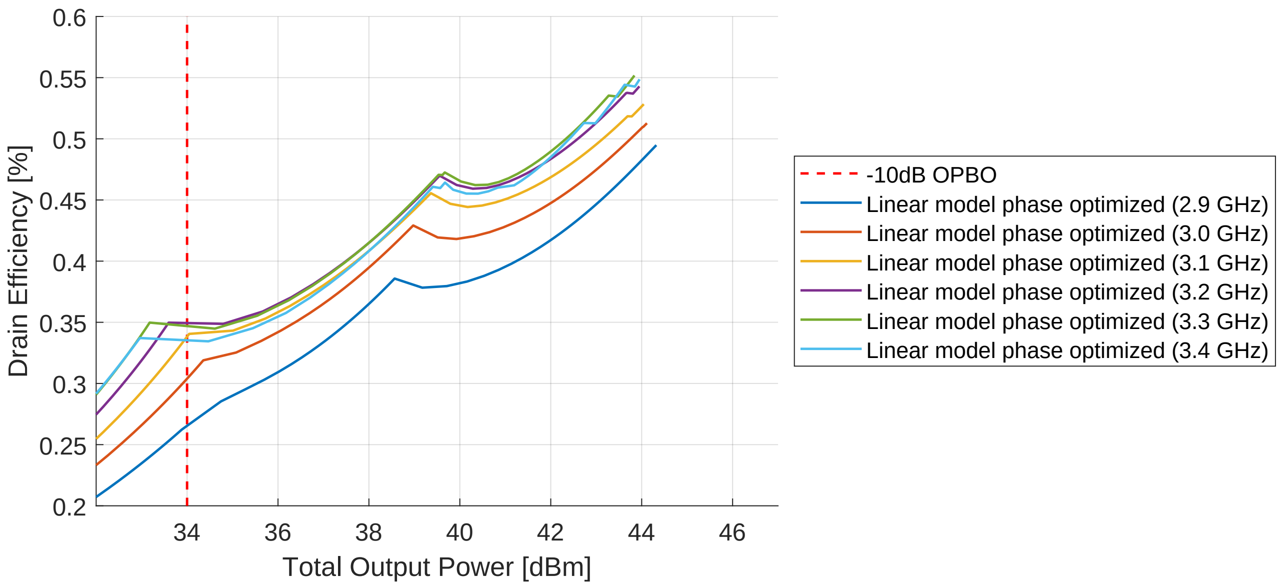

Figure G.2: The drain-efficiency is plotted versus total output power by using the parameters from Table G.1. This is an alternative design.

H

MATLAB code

```
%% Main script to find the solution for a single Class E

clear all
clc
close all

% Chosen parameters
omega3 = 2*pi*3.15e9;    % The center frequency
vdd3 = 25;               % The supply voltage
ql = 15;                 % The q-factor of the inductors
roff3 = 1e9;             % The transistor off impedance

nscale3 = 3;             % The number of transistors parallel
pdrive03 = 0.3;          % The driving power for one transistor
ron03 = 8;               % The on-resistance for one transistor
cds03 = 2.1e-13;         % The drain-to-source capacitance for one
   transistor
q3 = 1.3;                % The parameter q for finite Class E
q03 = 1;                 % The q-factor for the series resonator
isf23 = 0;               % Enabling this finds a solution for E/F2 (not
   recommended)
xx3 = 0;                 % Not used
vs3 = 0;                 % The voltage at the time of switching
vss3 = 0;                % The voltage-slope at the time of switching
ronlin3 = 1;             % Apply non-linear on-resistance (not
   recommended)

lambda3 = [ron03, cds03, omega3, vdd3, nscale3, q3, isf23, xx3, vs3,
   vss3, ronlin3,pdrive03,roff3,1, q03, ql];

% Solving for the required vs and vss
alpha0 = [0, 0];
xunc3 = [2.9549    1.1553];
vd = @(x) Class_E_ss_matrix(x,lambda3,alpha0,xunc3,0);
options = optimoptions('lsqnonlin','Display','off','Algorithm','
   levenberg-marquardt');
x0 = [50, 0];
```

```
[x3, ~] = lsqnonlin(vd,x0,[10,-300],[300,300],[],[],[],[],[], options);

[vd, Pout, Pdc, Pdrive, ix] = Class_E_ss_matrix(x3,lambda3,alpha0,xunc3
   ,0);

% Printing the values
r3 = x3(1);
x3 = x3(2);
angle03 = rad2deg(-angle(ix));

fprintf('Rx: %.1f \n',r3)
fprintf('Xx: %.1f \n\n',x3)

fprintf('Pout: %.1f W \n',Pout)
fprintf('Pdc: %.1f W \n',Pdc)
fprintf('Pdrive: %.1f W \n',Pdrive)
fprintf('Drain efficiency: %.1f %% \n',(Pout/Pdc)*100)
```

```
function [vd, Pout, Pdc, Pdrive, ix] = Class_E_ss_matrix(x,lambda,alpha,
   xunc,plott)
    % ##########################################################
    % Code to solve finite inductance Class-E(/F2)
    %
    % ###### Input:
    % x
    %   Rload    = load impedance
    %   Xload    = load reactance
    %
    % lambda
    %   ron0        = on-resistance when nonlin initial guess
    %   cds0        = drain-source capacitance of one transistor
    %   omega       = operating angular frequency
    %   vdd         = supply-voltage
    %   nscale      = number of parallel transistors
    %   q           = resonating factor of cds: omega*q=1/(sqrt(lfeed*
       cds))
    %   isf2        = if '1' cds is resonated out at the second harmonic
    %   xx          = added reactance in series with the load can be
       either...
    %                 positive and negative
    %   vs          = required voltage switching when closed
    %   vss         = required voltage-slope switching when closed
    %   isronlin    = '0' if on-resistance should be evaluated non-
       linearly
    %   pdrive0     = power to drive one transistor
    %   roff        = off-resistance
    %   xresolution = resolution of simulation
    %   qo          = q-factor of series resonator
    %   ql          = q-loss-factor of each inductor
    %
    % alpha
    %   phimod   = adding phase delay at the gate
    %   foff     = ratio of transistors being off is between 0 and 1
```

```
%               where 1 is all on and 0 is all off
%
% ######  Output:
%   Pout      = output power at the load in Watt
%   Pdc       = DC power supplied in watt
%   ix        = complex current flowing through the load
%   vd       =  difference betweeb required and resulting ...
%               switching conditions
% ########################################################

% Initialize default parameters
q20 = 100;


% Initialize parameters given by the user
ron0 = lambda(1);
cds0 = lambda(2);
omega = lambda(3);
vdd = lambda(4);
nscale = lambda(5);
q = lambda(6);
isf2 = lambda(7);
xx = lambda(8);
vs = lambda(9);
vss = lambda(10);
isronlin = lambda(11);
pdrive0 = lambda(12);
roff = lambda(13);
xresolution = lambda(14);
q0 = lambda(15);
ql = lambda(16);

% Parameters for controll
phimod = alpha(1);
foff = alpha(2);

% Deriving the functional parameters
cds = cds0*nscale;
ron_actual = 0;
ron_actual_n = ron0/nscale/(1-foff);

%------------------------------------------------------------
% Lomegaooping over the non-linear on-resistance
q02(3) = 0;
while (abs(ron_actual-ron_actual_n)>0.03 || q02(3)==0)
    ron_actual = ron_actual_n;
    rx = x(1);


    l00 = (rx*q0)/(omega);
    c0 = 1/(omega^2*l00);
    lx = (x(2)+xx)/omega;
    l0 = lx+l00;
```

```
        lf = 1/(omega^2*q^2*cds);

        rf = omega*lf/ql;
        rl0 = omega*l0/ql;
        rc0 = 0;

        c20 = 1/(2*omega*50*q20);
        l200 = 1/c20/(2*omega)^2;
        lc20 = 1/cds/(2*omega)^2;
        l20 = l200+lc20;

        % The differential matrices are defined as follows:
        if(isf2==1)
            A1 = [[-rf/lf, 0, -1/lf, 0, 0, 0]; ...
                  [0, -(rx+rc0+rl0)/l0, 1/l0, -1/l0, 0, 0]; ...
                  [1/cds, -1/cds, -1/ron_actual/cds, 0, -1/cds, 0];...
                  [0, 1/c0, 0, 0, 0, 0];...
                  [0, 0, 1/l20, 0, 0, -1/l20];...
                  [0, 0, 0, 0, 1/c20, 0]];
            A2 = [[-rf/lf,          0,        -1/lf,     0,      0,
               0]; ...
                  [0,     -(rx+rc0+rl0)/l0,        1/l0, -1/l0,      0,
                          0]; ...
                  [1/cds, -1/cds, -1/roff/cds,     0, -1/cds,      0];...
                  [0,       1/c0,            0,     0,      0,      0];...
                  [0,          0,        1/l20,     0,      0, -1/l20];...
                  [0,          0,            0,     0,  1/c20,      0]];
            B1 = [vdd/lf; 0; 0; 0; 0; 0];
            B2 = [vdd/lf; 0; 0; 0; 0; 0];
        else
            A1 = [[-rf/lf, 0, -1/lf, 0]; ...
                  [0, -(rx+rc0+rl0)/l0, 1/l0, -1/l0]; ...
                  [1/cds, -1/cds, -1/ron_actual/cds, 0];...
                  [0, 1/c0, 0, 0]];
            A2 = [[-rf/lf, 0, -1/lf, 0]; ...
                  [0, -(rx+rc0+rl0)/l0, 1/l0, -1/l0]; ...
                  [1/cds, -1/cds, -1/roff/cds, 0];...
                  [0, 1/c0, 0, 0]];
            B1 = [vdd/lf; 0; 0; 0];
            B2 = [vdd/lf; 0; 0; 0];
        end

        % Initializing the switch time
        N = length(A1);
        T = 2*pi/omega;
        t1 = 0.5*T;
        t2 = (1-0.5)*T;

        % Calculating the solution of the State-Space
        A2e = expm(A2*t2);
        B2e = A2\(expm(A2*t2)-eye(N,N))*B2;
        A1e = expm(A1*t1);
        B1e = A1\(expm(A1*t1)-eye(N,N))*B1;
```

```
        q01 = linsolve(A2e*A1e-eye(N,N),-B2e-A2e*B1e);
        q02 = A1e*q01+B1e;

        % The on resistance at the time the switch opens
        xdata = q02(3);
        xunc = [2.9549    1.1553]*(xresolution/nscale/(1-foff));
        nl = xunc(1) + xunc(2).*xdata;
        ron_actual_n = nl;

        % In the case that the resistance should be evaluated linearly
        if(isronlin)
                break;
        end

    end
    %
       -----------------------------------------------------------------------



    % The resulting waveforms for both when the switch is closed and
       open
    q1 = @(t) expm(A1*t)*q01+A1\(expm(A1*t)-eye(N,N))*B1;
    q2 = @(t) expm(A2*t)*q02+A2\(expm(A2*t)-eye(N,N))*B2;

    % To determine the output and input power we can derive the
       following:
    G1 = (A1^(-1))*(q1(t1)-q1(0)-B1*t1)*B1.'...
         + B1*(q1(t1).'-q1(0).'-B1.'*t1)/A1.'...
         -(q1(t1)*q1(t1).'-q1(0)*q1(0).');
    G2 = (A2^(-1))*(q2(t2)-q2(0)-B2*t2)*B2.'....
         + B2*(q2(t2).'-q2(0).'-B2.'*t2)/A2.'...
         -(q2(t2)*q2(t2).'-q2(0)*q2(0).');

    W1 = lyap(A1,G1);
    W2 = lyap(A2,G2);

    iq1 = (A1^(-1))*(q1(t1)-q1(0)-B1*t1);
    iq2 = (A2^(-1))*(q2(t2)-q2(0)-B2*t2);

    CDC = [sqrt(vdd) zeros(1,N-1)];

    % Deriving the input current (copy pase from the lmba script)
    n = 2;
    A_N = length(A1);
    c1 = zeros(A_N,1);
    A(:,:,1) = A1;
    A(:,:,2) = A2;
    B(:,1) = B1;
    B(:,2) = B2;
    X0(:,1) = q01;
    X0(:,2) = q02;
```

```
    tn(1) = 0;
    tn(2) = t1;
    tn(3) = (t1+t2);
    dt(1) = t1;
    dt(2) = (t1+t2)-t1;
    for ni = 1:n
        X_t = @(t) Function_X_t(t, X0(:,ni), A(:,:,ni), B(:,ni));
        c1 = c1 + (A(:,:,ni)-2*pi*1j*eye(A_N)/T)^-1 * (exp(-2*pi*1j*tn(
           ni+1)/T)*X_t(dt(ni)) - (exp( -2*pi*1j*tn(ni)/T ) *X_t(0)) -
           (1j*T*B(:,ni)/(2*pi))*( exp(-2*pi*1j*tn(ni+1)/T)-exp(-2*pi*1j
           *tn(ni)/T) ) );
    end
    ix = 2*c1(2)/T;

    % Resulting output power
    Pout = real(rx).*(abs(ix).^2/2);
    Pdc = (1/T)*CDC*(iq1+iq2)*sqrt(vdd);
    Pdrive = nscale*(1-foff)*pdrive0;



    % Voltage switching points
    vsr = q2(t1)-vs;
    vssr = (A2*q2(t1)+B2)/omega-vss;
    vd = sqrt(vsr(3)^2+vssr(3)^2);

    % Plotting the time domain wave forms
    if (plott)
        clf(figure(1))
        tx=linspace(0,t1,100);
        q1sol=zeros(length(B1),length(tx));
        q2sol=zeros(length(B1),length(tx));

        for i=1:length(tx)
            q1sol(:,i) = q1(tx(i));
            q2sol(:,i) = q2(tx(i));
        end

        figure(1)
        yyaxis right
        hold on
        plot(tx,q1sol(3,:),'r-')
        hold on
        plot(tx+tx(end),q2sol(3,:),'r-')
        xlabel('Conduction angle (\theta)')
        ylabel('Voltage [V]')
        % hold off


        yyaxis left
        plot(tx,q1sol(3,:)/ron_actual_n(1),'b-')
        hold on
        plot(tx+tx(end),(q1sol(3,end)/ron_actual_n(1))*exp(-tx*1e16),'b-
```

```
            ')
        ylabel('Current [A]')
        xticks(0:tx(end):tx(end)*2)
        xticklabels({'0','\pi','2\pi'})
        hold off

        title("Output power: " + num2str(Pout) + " W", " Drain
            efficiency: " + num2str((Pout/Pdc)*100) + " %")

        set(gcf,'color','w');
    end
end

function X = Function_X_t(t, X0, A, B)
    % Function to derive the states versus a time matrix t
    Ate_add = zeros(size(A));
    Bte_add = zeros(size(B));
    for m = 1:length(t)
        Ate_add(:,:,m) = expm(A(:,:,m)*t(m));
        Bte_add(:,m) = A(:,:,m) \ (Ate_add(:,:,m)-eye(size(A))) * B(:,m)
            ;
        X(:,m) = Ate_add(:,:,m)*X0(:,m)+Bte_add(:,m);
    end
end
```

```
%% Main script to find the solution to a Class E LMBA
clear
close all
clc

% Set the global parameters
omega = 2*pi*3.15e9;        % The center frequency
vdd = 25;                   % The supply voltage
xresolution = 10;           % The extra resolution added
ql = 1e23;                  % The q-factor of the inductors

% Set the parameter for the first peaking amplifier
xresolution1 = xresolution;
roff1 = 1e12;
nscale1 = 6*xresolution1;
pdrive01 = 0.3/xresolution1;
ron01 = 8*xresolution1;
cds01 = 2.1e-13/xresolution1;
q1 = 1.3;
q01 = 10;
isf21 = 0;
xx1 = 0;
vs1 = 0;
vss1 = 0;
ronlin1 = 1;
lambda1 = [ron01, cds01, omega, vdd, nscale1, q1, isf21, xx1, vs1, vss1,
    ronlin1, pdrive01, roff1, xresolution1, q01, ql];
```

```
% Set the parameter for the secondary peaking amplifier
xresolution2 = xresolution;
roff2 = 1e12;
nscale2 = 6*xresolution2;
pdrive02 = 0.3/xresolution2;
ron02 = 8*xresolution2;
cds02 = 2.1e-13/xresolution2;
q2 = 1.3;
q02 = 10;
isf22 = 0;
xx2 = 0;
vs2 = 0;
vss2 = 0;
ronlin2 = 1;
lambda2 = [ron02, cds02, omega, vdd, nscale2, q2, isf22, xx2, vs2, vss2,
    ronlin2,pdrive02,roff2,xresolution2, q02, ql];

% Set the parameter for the main amplifier
xresolution3 = xresolution;
roff3 = 1e12;
nscale3 = 3*xresolution3;
pdrive03 = 0.3/xresolution3;
ron03 = 8*xresolution3;
cds03 = 2.1e-13/xresolution3;
q3 = 1.3;
q03 = 10;
isf23 = 0;
xx3 = 0;
vs3 = 0;
vss3 = -38;
ronlin3 = 1;
lambda3 = [ron03, cds03, omega, vdd, nscale3, q3, isf23, xx3, vs3, vss3,
    ronlin3,pdrive03,roff3,xresolution3, q03, ql];

% Set the asymmetrical hybrid coupler parameters
Z1 = 50;
Z2 = 50;
zeta = [Z1, Z2];

% Find the transformer ratios, reactance compensation, and required
   delays
alpha0 = [0, 0];
[beta, ~] = Class_E_find_beta(lambda1, lambda2, lambda3, alpha0, alpha0,
    alpha0, zeta);
lambda = [lambda1; lambda2; lambda3].';

% Find the resulting powers, voltages, currents and impedances at peak
% power
alpha = zeros(3,2);
[vd, Pout, Pdc, Pdrive, ix, zload, ids] =
   Class_E_LMBA_ss_matrix_phase_shift(beta, lambda, alpha, zeta, Plot=0)
   ;
```

```
% Find all the resulting powers, voltages, currents and impedances
[p_opbo, zload_opbo, ix_opbo, ids_opbo] = Class_E_ss_asym_OPBO(beta,
   lambda, zeta, Phiopt=0);

NON3 = 1:nscale3;
% NON1 = [zeros(1,nscale3), 1:nscale1];
% NON2 = [zeros(1,nscale3), zeros(1,nscale1), 1:nscale2];
NON1 = [zeros(1,nscale3), zeros(1,nscale2), 1:nscale1];
NON2 = [zeros(1,nscale3), 1:nscale2];

% The design parameters:
% disp(beta)
%% Plot either the resulting waveforms either from imported data or
   MATLAB
logplotefftotADSMATLAB(p_opbo,drain_efficiency=1,adsmatpath="")

%% Plot the impedance, voltage and current curves vesus code
plotzloadixADSMATLAB(zload_opbo, ids_opbo,adsmatpath="")

%% Function to find the optimal design parameters
function [beta, xsol] = Class_E_find_beta(lambda1, lambda2, lambda3,
   alpha1, alpha2, alpha3, zeta)

    % For PA1:
    % Function to determine the maximum output power x value
    xunc1 = [2.9549    1.1553];
    vd = @(x) Class_E_ss_matrix(x,lambda1,alpha1,xunc1,0);
    options = optimoptions('lsqnonlin','Display','off','Algorithm','
       levenberg-marquardt');
    x0 = [50, 0];
    [x1, ~] = lsqnonlin(vd,x0,[5,-300],[300,300],[],[],[],[],[], options
       );

    % For PA2:
    % Function to determine the maximum output power x values
    xunc2 = [2.9549    1.1553];
    vd = @(x) Class_E_ss_matrix(x,lambda2,alpha2,xunc2,0);
    options = optimoptions('lsqnonlin','Display','off','Algorithm','
       levenberg-marquardt');
    x0 = [50, 0];
    [x2, ~] = lsqnonlin(vd,x0,[5,-300],[300,300],[],[],[],[],[], options
       );

    % For PA3:
    % Function to determine the maximum output power x values
    xunc3 = [2.9549    1.1553];
    vd = @(x) Class_E_ss_matrix(x,lambda3,alpha3,xunc3,0);
    options = optimoptions('lsqnonlin','Display','off','Algorithm','
       levenberg-marquardt');
    x0 = [100, 0];
    [x3, ~] = lsqnonlin(vd,x0,[5,-300],[300,300],[],[],[],[],[], options
       );
```

```
    [~, ~, ~, ~, ix1] = Class_E_ss_matrix(x1, lambda1, alpha1, xunc1,0);
    [~, ~, ~, ~, ix2] = Class_E_ss_matrix(x2, lambda2, alpha2, xunc2,0);
    [~, PB0, PDC, ~, ix3] = Class_E_ss_matrix(x3, lambda3, alpha3, xunc3
       ,0);

    xsol = [x1, x2, x3];

    % Compensate the angles like as also done in simulation
    beta(10) = angle(ix1);
    beta(11) = angle(ix2);
    beta(12) = angle(ix3);

    % The currents are now equal to the absolute values
    ix1 = (ix1)*exp(-1j*angle(ix1));
    ix2 = (ix2)*exp(-1j*angle(ix2));
    ix3 = (ix3)*exp(-1j*angle(ix3));

    % Solving the Z-matrix equations with the particle swarm algorithm
    fun = @(xz) find_nx(xz, x1, x2, x3, ix1, ix2, ix3, zeta);
    options = optimoptions('particleswarm','Display','off');
    [xzsol, ~] = particleswarm(fun
       ,6,[0.3,0.3,0.3,-400,-400,-400],[2,2,2,400,400,400],options);

    beta(1) = sqrt(zeta(1)*zeta(2));
    beta(2) = zeta(1);
    beta(3) = zeta(2);

    beta(7:9) = xzsol(1:3);
    beta(4:6) = xzsol(4:6);

    beta(13:15) = [x1(1), x2(1), x3(1)];
end

function feval = find_nx(xz, x1, x2, x3, ix1, ix2, ix3, zeta)
    % Function to be minized
    % The input are currents and the required input impedances

    n(1:3) = xz(1:3);

    % Z-matrix equations written inside a function
    Z1 = zeta(1);
    Z2 = zeta(2);
    ZB = [[0, Z2/(n(1)*n(2)), sqrt(2*Z1*Z2)/(n(1)*n(3))];...
    [-Z2/(n(1)*n(2)), 2*Z2/n(2)^2, sqrt(2*Z1*Z2)/(n(3)*n(2))];...
    [-sqrt(2*Z1*Z2)/(n(1)*n(3)), sqrt(2*Z1*Z2)/(n(3)*n(2)), Z1/n(3)^2]];

    % First setup: match at maximum output power
    ZBsol = [x1; x2; x3];
    ix = [ix1; ix2; ix3];

    Zin = ZB*ix./ix;

    ZinImDiff1 = xz(4:6).' + imag(Zin) - ZBsol(:,2);
```

```
    ZinReDiff1 = real(Zin)-ZBsol(:,1);

    feval1 = [abs(ZinImDiff1).', abs(ZinReDiff1).'];



     % Third setup
    ZBsol = x3;
    ix = [0; 0; ix3];

    Zin = ZB*ix./ix;

    ZinImDiff3 = xz(6).' + imag(Zin(3)) - ZBsol(2);
    ZinReDiff3 = real(Zin(3))-ZBsol(1);

    feval3 = [abs(ZinImDiff3).', abs(ZinReDiff3).'];

    feval = rms([feval1(1:2),feval1(4:5), feval3]);
end
```

```
function [vd, Pout, Pdc, Pdrive, ixt, vds, ids, angle0] =
   Class_E_LMBA_ss_matrix_phase_shift(beta, lambda, alpha, zeta, options
   )
    % #################################################################
    % Code to solve finite inductance Class-E(/F2)
    %
    % ###### Input:
    % x:
    %   Rload        = load impedance
    %   Xload        = load reactance
    % beta:
    %   Z0           = charasteristic impedance
    %   n(1:3)       = transformer ratios
    %   x(1:3)       = reactance compensation
    %   angle(1:3)   = delay compensation
    %   x1, x2, x3   = optimum loads for PAs
    %
    %
    %
    %
    % lambda:
    %   ron0         = on-resistance when nonlin initial guess
    %   cds0         = drain-source capacitance of one transistor
    %   omega        = operating angular frequency
    %   vdd          = supply-voltage
    %   nscale       = number of parallel transistors
    %   q            = resonating factor of cds: omega*q=1/(sqrt(lfeed*
      cds))
    %   isf2         = if '1' cds is resonated out at the second harmonic
    %   xx           = added reactance in series with the load can be
      either...
    %                  positive and negative
    %   vs           = required voltage switching when closed
```

```
%   vss          = required voltage-slope switching when closed
%   isronlin     = '0' if on-resistance should be evaluated non-
   linearly
%   pdrive0      = power to drive one transistor
%   roff         = off-resistance
%   xresolution = resolution of simulation
%   qo           = q-factor of series resonator
%   ql           = q-loss-factor of each inductor
%
% alpha:
%   phimod       = adding phase delay at the gate
%   foff         = ratio of transistors being off is between 0 and 1
%                where 1 is all on and 0 is all off
%
% ######  Output:
%   vd           =  difference between required and resulting ...
%                switching conditions
%   Pout         = output power at the load in Watt
%   Pdc          = DC power supplied in watt
%   Pdrive       = Total drive power depending on fon
%   ixt          = complex current flowing through the load
%   vds          = drain-to-source voltage
%   ids          = drain-to-source current
%   angle0       = output current angle
% ##################################################################

arguments
    beta (1,15) double
    lambda (16,3) double
    alpha (3,2) double
    zeta (1,2) double
    options.Plot (1,1) {mustBeNumericOrLogical} = 1
end

% Design specified
n = beta(1,7:9);
xx = beta(1,4:6);

% Initialize default parameters
q20 = 1e3;

% Initialize parameters given by the user
ron0 = lambda(1,:);
cds0 = lambda(2,:);
omega = lambda(3,:);
vdd = lambda(4,:);
nscale = lambda(5,:);
q = lambda(6,:);
isf2 = lambda(7,:);
vs = lambda(9,:);
vss = lambda(10,:);
isronlin = lambda(11,:);
pdrive0 = lambda(12,:);
```

```
    roff = lambda(13,:);
    xresolution = lambda(14,:);
    q0 = lambda(15,:);
    rx = beta(13:15);
    ql = lambda(16,:);

    % Parameters for controll
    phimod = alpha(:,1).' + beta(10:12);
    foff = alpha(:,2).';

    % Deriving the functional parameters
    cds = cds0.*nscale;
    ron_actual_n = ron0./nscale./(1-foff);

    ron_actual = ron_actual_n;

    l00 = (rx.*q0)./(omega);
    c0 = 1./(omega.^2.*l00);
    lx = (xx)./omega;
    l0 = lx+l00;
    lf = 1./(omega.^2.*q.^2.*cds);

    c20 = 1./(2.*omega.*5.*q20);
    l200 = 1./c20./(2.*omega).^2;
    lc20 = 1./cds./(2*omega).^2;
    l20 = l200+lc20;

    % Define the LMBA matrix
    Z1 = zeta(1);
    Z2 = zeta(2);
    A2cctn = [[0, Z2/(n(1)*n(2)), sqrt(2*Z1*Z2)/(n(1)*n(3))];...
    [-Z2/(n(1)*n(2)), 2*Z2/n(2)^2, sqrt(2*Z1*Z2)/(n(3)*n(2))];...
    [-sqrt(2*Z1*Z2)/(n(1)*n(3)), sqrt(2*Z1*Z2)/(n(3)*n(2)), Z1/n(3)^2]];
    A2cc = A2cctn./l0.';

    % Add zero rows and collumns for propper addition
    A2c = [zeros(1,3);A2cc(1,:);zeros(3+2*(isf2(1)==1),3);A2cc(2,:);
       zeros(3+2*(isf2(2)==1),3);A2cc(3,:);zeros(2+2*(isf2(3)==1),3);];
    H_A2c = size(A2c,1);
    As = -[zeros(H_A2c,1),A2c(:,1),zeros(H_A2c,3+2*(isf2(1)==1)),A2c
       (:,2),zeros(H_A2c,3+2*(isf2(2)==1)),A2c(:,3),zeros(H_A2c,2+2*(
       isf2(3)==1));];

    % Define the state-space for three PAs with or without F2
    for k = 1:3
        if(isf2(k)==1)
            rf = omega.*lf(k)./ql;
            rl0 = omega.*l0(k)./ql;
            funA{k} = [[-rf/lf(k), 0, -1./lf(k), 0, 0, 0]; ...
                  [0, -(rl0(k))/l0(k), 1./l0(k), -1./l0(k), 0, 0]; ...
                  [1./cds(k), -1./cds(k), 0, 0, -1./cds(k), 0];...
                  [0, 1./c0(k), 0, 0, 0, 0];...
                  [0, 0, 1./l20(k), 0, 0, -1./l20(k)];
```

```
                [0, 0, 0, 0, 1/c20(k), 0]];
            funB{k} = [vdd(k)/lf(k); 0; 0; 0; 0; 0];
        else
            rf = omega.*lf(k)./ql;
            rl0 = omega.*l0(k)./ql;
            funA{k} = [[-rf(k)/lf(k), 0, -1./lf(k), 0]; ...
              [0, -(rl0(k))/l0(k), 1./l0(k), -1./l0(k)]; ...
              [1./cds(k), -1./cds(k), 0, 0];...
              [0, 1./c0(k), 0, 0]];
            funB{k} = [vdd(k)/lf(k); 0; 0; 0];
        end
    end

    Af = blkdiag(funA{1},funA{2},funA{3});

    % Add the state-spaces and the hybrid coupler z-matrix
    At(:,:) = As+Af;
    Bt(:,:) = [funB{1};funB{2};funB{3}];

    phi_delay = phimod.';
    duty_cycle = [0.5;0.5;0.5];

    % ---------------------------------------------------------------
    amount_runs = 0;
    while (any(abs(ron_actual-ron_actual_n)>0.03) || amount_runs==0)
        % Create the Ron-Roff matrix
        ron_actual = ron_actual_n;
        [Aron, phimodsort_diff, phimodsort_LU, ronm, ronmv] = find_Aron(
           ron_actual,cds,phi_delay, duty_cycle, roff, isf2);

        for i_ron = 1:size(Aron,3)
            Aron(:,:,i_ron) = Aron(:,:,i_ron)+At;
        end
        A = Aron;
        A_N = size(Aron,1);

        n_steps = length(phimodsort_diff);
        B = repmat(Bt,[1, n_steps]);

        T = 2*pi/omega(1);
        t = T*phimodsort_diff/2/pi;
        tn = T*phimodsort_LU/2/pi;

        % Find the expm matrices
        Ate = zeros(size(A));
        Bte = zeros(size(B));
        for i = 1:n_steps
            Ate(:,:,i) = expm(A(:,:,i)*t(i));
            Bte(:,i) = A(:,:,i) \ (Ate(:,:,i)-eye(A_N)) * B(:,i);
        end


        % Just for clearity redefine n
```

```
n = n_steps;

% Initialize the solution variable
X = zeros([A_N,n]);

% Initialize product and sum variables
product1_A = eye(A_N);

sum_term = zeros(A_N, 1);

% Compute the product and sum terms
for i_p = 1:(n-1)
    product1_A = Ate(:,:,i_p) * product1_A;
end

for i_s = 1:(n-2)
    product2_A = eye(A_N);
    for j_p = 1:(n-1-i_s)
        product2_A = product2_A * Ate(:,:,n-j_p);
    end
    sum_term = sum_term + product2_A * Bte(:,i_s);
end

% Compute xn using the formula
X0(:,n) = (eye(A_N) - product1_A * Ate(:,:,n)) \ (product1_A *
   Bte(:,n) + sum_term + Bte(:,n-1));

X0(:,1) = Ate(:,:,n) * X0(:,n) + Bte(:,n);

% Compute xn-1 iteratively knowing xn
j=0;
for j = 2:n-1
    X0(:,j) = Ate(:,:,j-1) * X0(:,j-1) + Bte(:,j-1);
end


% In case the non-linear on-resistance is badly approximated
   quit
amount_runs = amount_runs+1;
if(amount_runs==30 || (anynan(X0)))
    vd = 1e4;
    Pout = zeros(3,1);
    Pdc = zeros(3,1);
    Pdrive = zeros(3,1);
    return;
end

tswitch = T*phi_delay/2/pi;
tswitch_moved = [tswitch+duty_cycle*T; tswitch+duty_cycle*T-T];
[t_index, ~] = find(abs(tn-tswitch_moved.')<1e-14);
% The on resistance at the time the switch opens
if(isronlin(1) ~= 1 )
    xdata = X0(3,t_index(1));
```

```
            % Non-linear apprximation of the on-resistance
            xunc = [2.9549    1.1553]*(xresolution(1)/nscale(1)/(1-foff
               (1)));
            nl = xunc(1) + xunc(2).*abs(xdata);
            ron_actual_n(1) = nl;
        else
            ron_actual_n(1) = ron_actual(1);
        end

        if(isronlin(2) ~= 1 )
            xdata = X0(3+4,t_index(2));
            xunc = [2.9549    1.1553]*(xresolution(2)/nscale(2)/(1-foff
               (2)));
            nl = xunc(1) + xunc(2).*abs(xdata);
            ron_actual_n(2) = nl;
        else
            ron_actual_n(2) = ron_actual(2);
        end

        if(isronlin(3) ~= 1 )
            xdata = X0(3+8,t_index(3));
            xunc = [2.9549    1.1553]*(xresolution(3)/nscale(3)/(1-foff
               (3)));
            nl = xunc(1) + xunc(2).*abs(xdata);
            ron_actual_n(3) = nl;
        else
            ron_actual_n(3) = ron_actual(3);
        end
    end

    % ----------------------------------------------------------------
    % The on-resistance is correctly approximated now
    % derive the waves and output powers

    dt = t;
    tn = tn;

    % First the output load current is derived
    c1 = zeros(A_N,1);
    for ni = 1:n
        X_t = @(t) Function_X_t(t, X0(:,ni), A(:,:,ni), B(:,ni));
        c1 = c1 + (A(:,:,ni)-2*pi*1j*eye(A_N)/T)^-1 * (exp(-2*pi*1j*tn(
           ni+1)/T)*X_t(dt(ni)) - (exp( -2*pi*1j*tn(ni)/T ) *X_t(0)) -
           (1j*T*B(:,ni)/(2*pi))*( exp(-2*pi*1j*tn(ni+1)/T)-exp(-2*pi*1j
           *tn(ni)/T) ) );
    end

    select_matrix_ix = [2, 6+2*isf2(1), 10+2*isf2(1)+2*isf2(2)];
    ix = 2*c1(select_matrix_ix)/T;
    ixt = ix;

    % The angle that is extracted from the derived current
    angle0 = angle(ix.*(foff~=1).');
```

```
% Next step is to determine the DC current
X_t = @(t) Function_X_t(t, X0, A, B);
Btemp = X_t(t)-X_t(zeros(size(t)))-B.*t.';
Btempn(:,1,:) = (Btemp);
idct = pagemtimes(pageinv(A),Btempn);
idc = sum(idct(select_matrix_ix-1,1,:),[2,3])/T;

% The drain-to-source voltage is a readout of the state-space
   solution
select_matrix = [3, 7+2*isf2(1), 11+2*isf2(1)+2*isf2(2)];
vds = 2*c1(select_matrix)/T;

% The load impedance can be derived as follows
Zload = (A2cctn*ix./ix) + 1j*xx.';

% And finally the resulting output powers
Pout = real(Zload).*(abs(ix).^2/2);
Pdc = abs(idc)*vdd(1);
Pdrive = (nscale.*(1-foff).*pdrive0).';

[t_index, ~] = find(abs(tn-tswitch.')<1e-14);

% Next step is deriving the voltage slope and voltage switching
   moment
for l=1:3
    vsrt = X0(:,t_index(l));
    vsr(l) = vsrt((l-1)*4+3)-vs(l);
    vssrt = real(A(:,:,t_index(l))*X0(:,t_index(l))+B(:,t_index(l)))
       ./omega(1);
    vssr(l) = vssrt((l-1)*4+3)-vss(l);
end
vd = sum(abs(sqrt(vsr.^2+vssr.^2)));

% And lastly the drain-to-source current
c1 = zeros(3,1);
select_matrix = [3, 7+2*isf2(1), 11+2*isf2(1)+2*isf2(2)];
for ni = 1:n
    X_t = @(t) Function_X_t(t, X0(:,ni), A(:,:,ni), B(:,ni));
    temp = ((A(:,:,ni)-2*pi*1j*eye(A_N)/T)^-1 * (exp(-2*pi*1j*tn(ni
       +1)/T)*X_t(dt(ni)) - (exp( -2*pi*1j*tn(ni)/T ) *X_t(0)) - (1j
       *T*B(:,ni)/(2*pi))*( exp(-2*pi*1j*tn(ni+1)/T)-exp(-2*pi*1j*tn
       (ni)/T) ) ) );
    c1 = c1 - temp(select_matrix) ./ ronmv(:,ni);
end
ids = 2*c1/T;

% ---------------------------------------------------------------
% The last part is just plotting the voltage and current waves
if(options.Plot)
    t_resolution = 100;
    span_t = linspace(0,1,t_resolution);
    tx = span_t.*t;
```

```
    X_t = @(t) Function_X_t(t, X0, A, B);
    Xsol = zeros(A_N,n,t_resolution);
    for j = 1:size(tx,2)
        Xsol(:,:,j) = X_t(tx(:,j));
    end


    clf(figure(2))
    tiledlayout("vertical")
    fig2 = figure(2);
    for l = 1:3

        nexttile
        hold on
        tstep = 0;
        for p = 1:n

            plot(tx(p,:)+tstep,real(reshape(Xsol(2+4*(l-1),p,:),[1,
                t_resolution])),'r-','Linewidth',1.2);
            tstep = tstep + tx(p,end);
        end
        ylabel('Current [A]')
        xlabel('Conduction angle (\theta)')
        xticks(linspace(0,tstep,5))
        xticklabels({'0','1\pi/4','\pi/2','3\pi/4','\pi'})
    end



    fig2.Position = [100,100,500,450];
    fontsize(fig2, scale=1.2)
    exportgraphics(fig2,'qsol_il.pdf')

    clf(figure(1))
    tiledlayout("vertical")
    fig1 = figure(1);
    set(fig1,'defaultAxesColorOrder',[[1,0,0]; [0,0,1]])
    for l = 1:3

        nexttile
        yyaxis right
        hold on
        tstep = 0;
        for p = 1:n
            plot(tx(p,:)+tstep,real(reshape(Xsol(3+4*(l-1),p,:),[1,
                t_resolution])),'r-','Linewidth',1.2)
            tstep = tstep + tx(p,end);
        end
        ylim([0 100])
        xlabel('Conduction angle (\theta)')
        ylabel('Voltage [V]')

        yyaxis left
```

```
        tstep = 0;
        for p = 1:n
            plot(tx(p,:)+tstep,real(reshape(Xsol(3+4*(l-1),p,:),[1,
               t_resolution]))*ronm(l,p)/ron_actual_n(l),'b-','
               Linewidth',1.2)
            tstep = tstep + tx(p,end);
        end
        ylabel('Current [A]')
        ylim([0 7])
        hold off
        xticks(linspace(0,tstep,5))
        xticklabels({'0','1\pi/4','\pi/2','3\pi/4','\pi'})
    end

    fig1.Position = [700,100,500,450];
    fontsize(fig1, scale=1.2)
    exportgraphics(fig1,'qsol_vdsids.pdf')
end


function [A, phimodsort_diff, phimodsort_LU, ronm, ronmv] =
   find_Aron(ron, cds, phi_delay, duty_cycle, roff, isf2)
    % Function to derive the Ron-Roff matrix
    N = 3;
    A_N = 12+2*sum(isf2);

    phimod_tot = [phi_delay; phi_delay+2*pi*duty_cycle; phi_delay+2*
       pi; phi_delay - 2*pi; phi_delay+2*pi*duty_cycle - 2*pi];

    phimodsort = sort([0; phimod_tot; 2*pi]);
    phimodsort_unique = (uniquetol(phimodsort,1e-5));
    phimodsort_LU = phimodsort_unique(phimodsort_unique >= 0 &
       phimodsort_unique <= 2*pi);
    phimodsort_diff = diff(phimodsort_LU);

    angle_c=0;

    ronm = zeros(N,length(phimodsort_diff));
    for i = 1:length(phimodsort_diff)
        ronm(:,i) = fsquare(round(angle_c-phi_delay(:),4),duty_cycle
           );
        angled = phimodsort_diff(i);
        angle_c = angle_c + angled;
    end

    n_steps = length(phimodsort_diff);

    % The Ron-Roff matrix is there after determined at each step
    A = zeros(A_N,A_N,n_steps);
    for k = 1:n_steps
        ronmn =  @(i) [zeros(4+isf2(i)*2,2),[zeros(2,1); ronm(i,k);
           zeros(1+isf2(i)*2,1)], zeros(4+isf2(i)*2,1+isf2(i)*2)];
        A(:,:,k) = -blkdiag(ronmn(1)/ron(1)/cds(1),ronmn(2)/ron(2)/
```

```
                cds(2),ronmn(3)/ron(3)/cds(3));
            ronmv(:,k) = [ronm(1,k)*ron(1);ronm(2,k)*ron(2);ronm(3,k)*
                ron(3)];
        end

        for k = 1:n_steps
            ronmn =  @(i) [zeros(4+isf2(i)*2,2),[zeros(2,1); not(ronm(i,
                k)); zeros(1+isf2(i)*2,1)], zeros(4+isf2(i)*2,1+isf2(i)
                *2)];
            A(:,:,k) = A(:,:,k)-blkdiag(ronmn(1)/roff(1)/cds(1),ronmn(2)
                /roff(2)/cds(2),ronmn(3)/roff(3)/cds(3));
            ronmv(:,k) = ronmv(:,k) + [not(ronm(1,k))*roff(1);not(ronm
                (2,k))*roff(2);not(ronm(3,k))*roff(3)];
        end
    end

    function s = fsquare(t,duty)
        % Editted square() function

        % Compute values of t normalized to (0,2*pi)
        tmp = mod(t,2*pi);

        % Compute normalized frequency for breaking up the interval
            (0,2*pi)
        w0 = 2*pi*duty;

        % Assign 1 values to normalized t between (0,w0), 0 elsewhere
        s = (tmp+1e-3 < w0);
    end

    function X = Function_X_t(t, X0, A, B)
        % Function to derive the states versus a time matrix t
        Ate_add = zeros(size(A));
        Bte_add = zeros(size(B));
        for m = 1:length(t)
            Ate_add(:,:,m) = expm(A(:,:,m)*t(m));
            Bte_add(:,m) = A(:,:,m) \ (Ate_add(:,:,m)-eye(A_N)) * B(:,m)
                ;
            X(:,m) = Ate_add(:,:,m)*X0(:,m)+Bte_add(:,m);
        end
    end
end
```

```
function [xopt, ymin] = bruteforce(fun,lb,ub,n)
    % function to find brute force the optimal phase

    nm = (lb~=0 | ub~=0)*n + (lb==0 & ub==0)*1;
    x1 = linspace(lb(1), ub(1),nm(1));
    x2 = linspace(lb(2), ub(2),nm(2));
    x3 = linspace(lb(3), ub(3),nm(3));

    for x1i = 1:length(x1)
        for x2i = 1:length(x2)
```

```
            for x3i = 1:length(x3)
                y(x1i,x2i,x3i) = fun([x1(x1i) x2(x2i) x3(x3i)]);
            end
        end
    end

    y= y.*(y>-1);
    [ymin, index] = min(y,[],"all");
    [i, j, k] = ind2sub([nm,nm,nm],index);
    xopt = [x1(i), x2(j), x3(k)];
end
```

I

Final schematic

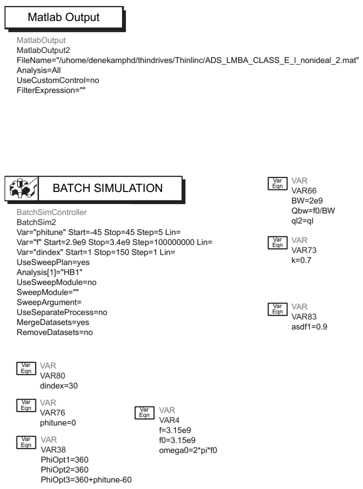

Figure I.1: Simulation setup

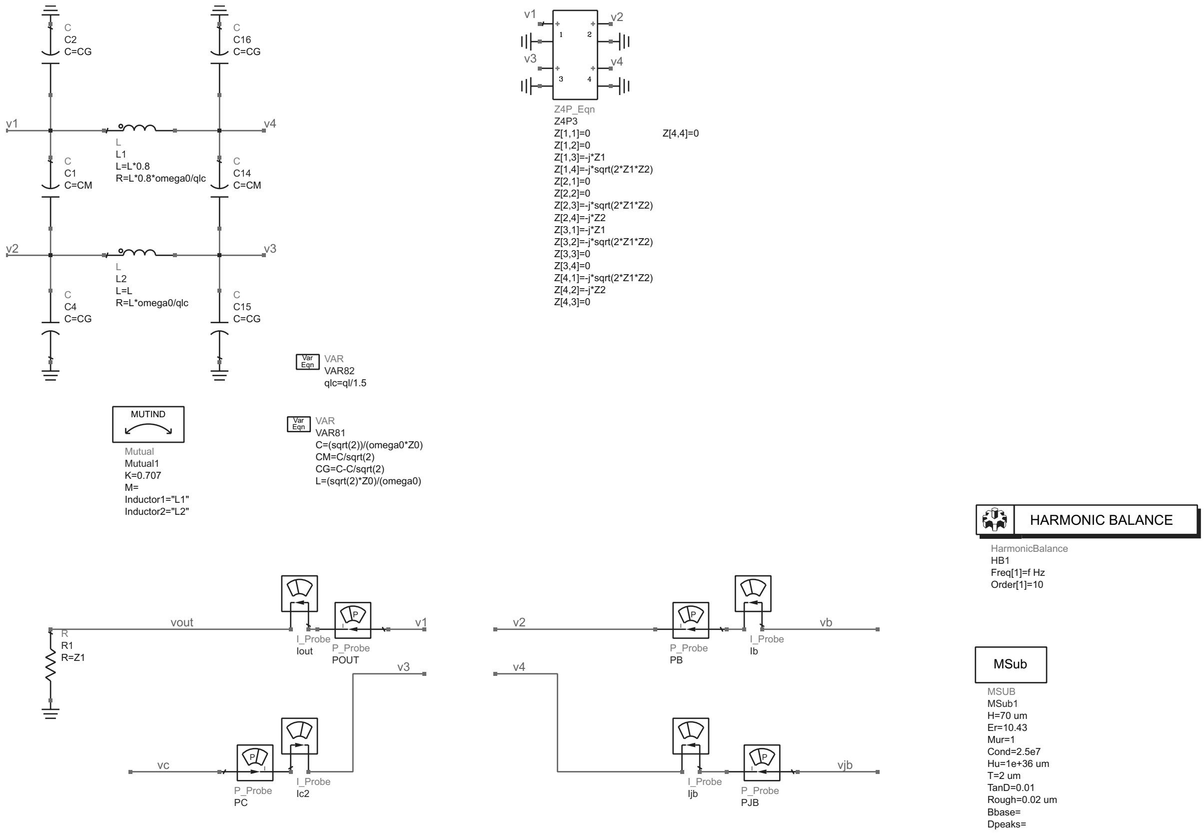

Figure I.2: The ideal and non-indeal hybrid coupler.

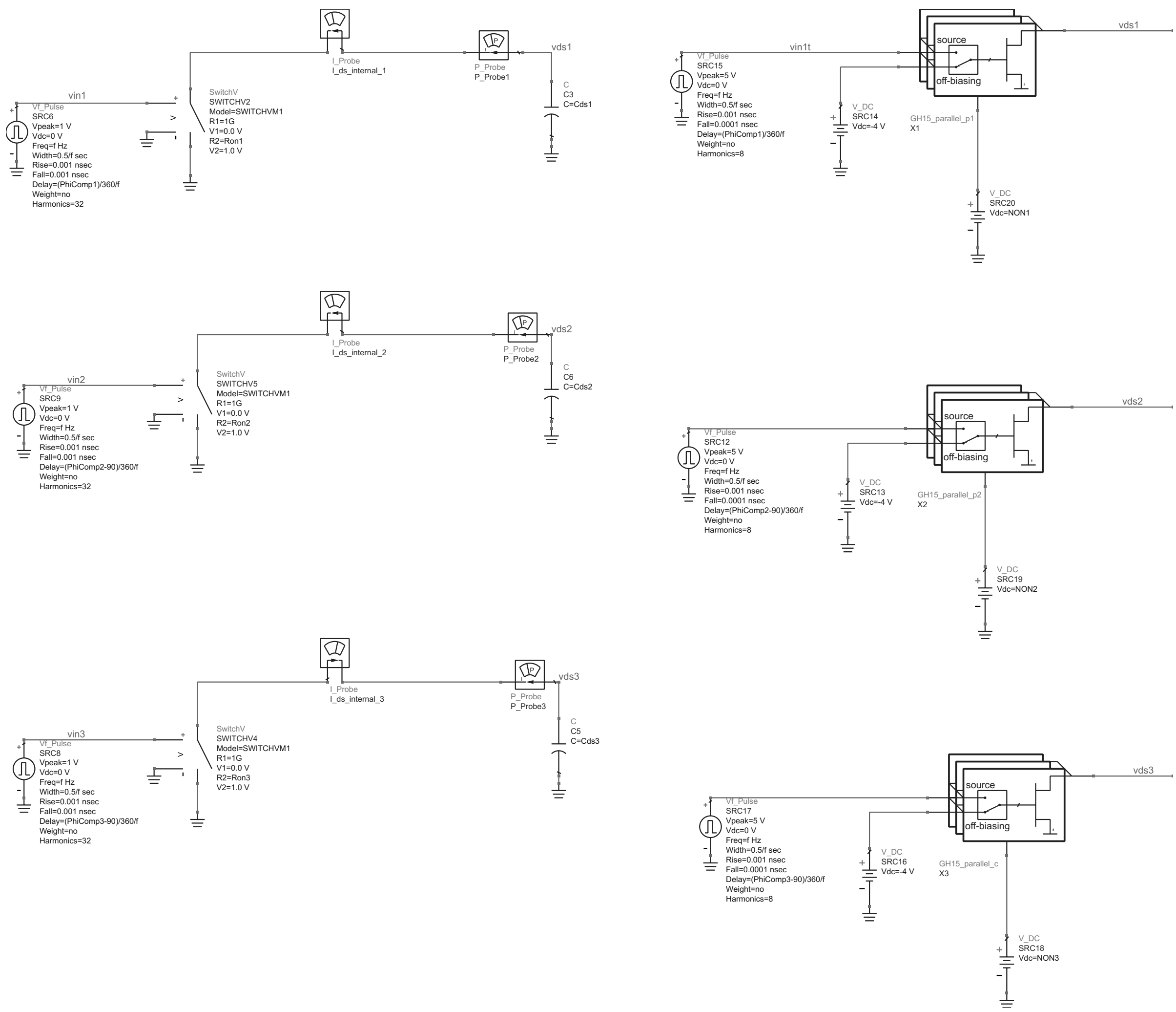

Figure I.3: The linear model at the left and nonlinear model at the right.

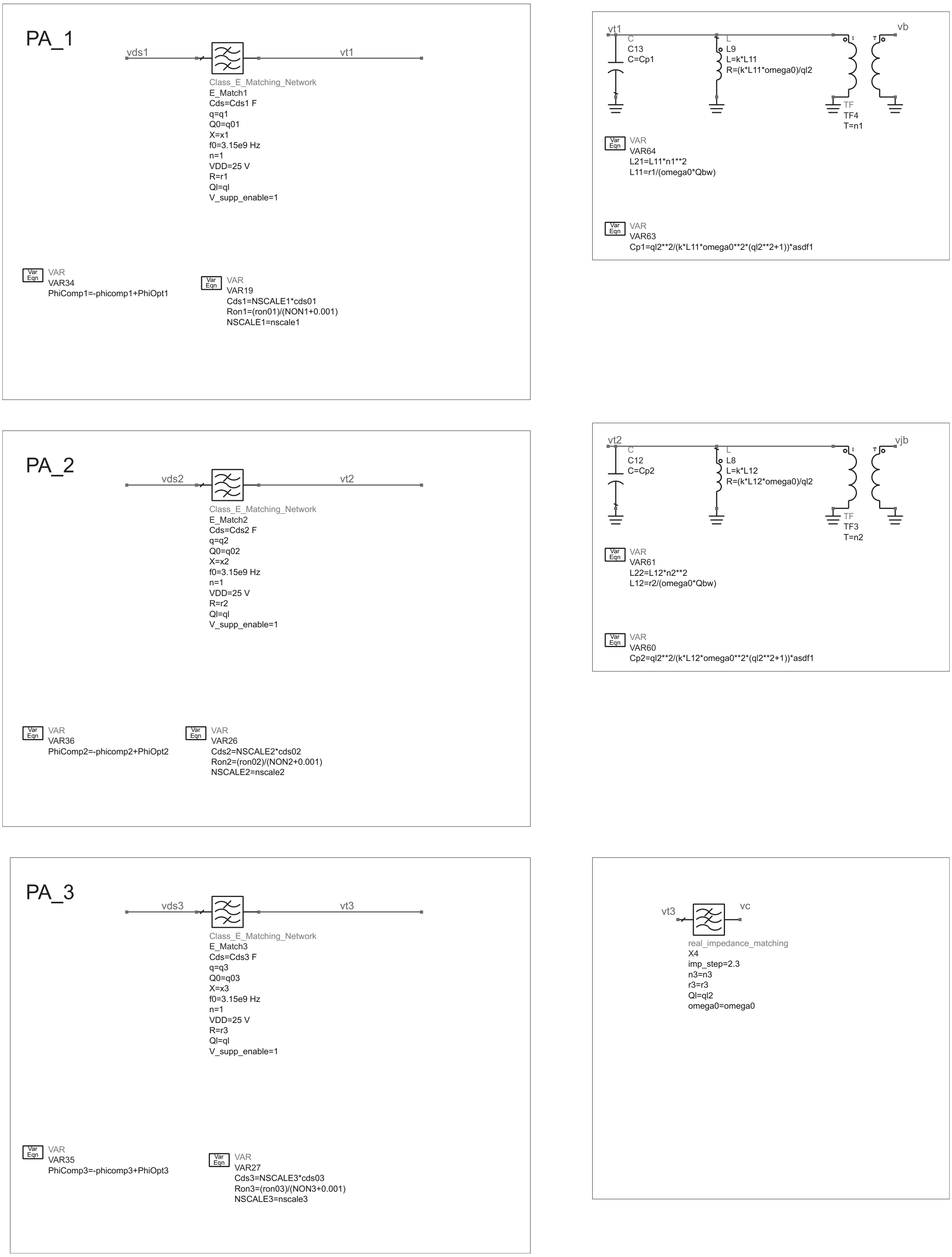

Figure I.4: The linear model at the left and nonlinear model at the right.

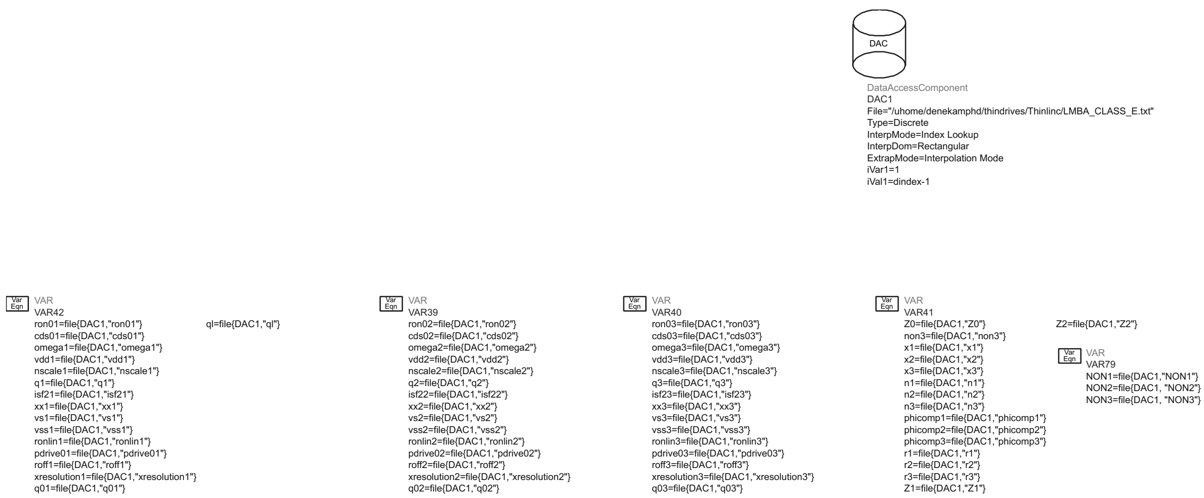

Figure I.5: The input parameters are given by MATLAB.

J

Final Design Component List

First it is important to note that the design is not made with directly the achievable components in mind, by reducing some inductors, the design could even improve. But because of limited time additional tuning is ignored and a simple design method was preferred. All inductors have a Q-factor of 15, independent of their size. Only the coupled lines have a lower Q-factor of 10, because this seemed more reasonable compared to the losses in the transmission line equivalent. The losses in the capacitors were ignored because its losses were found to be negligible compared to the losses in the inductors. The resulting table is Table J.1.

sub-part	which amplifier	Component	Value	Unit
Class E matching network	main amplifier			
		min R_{on}	2.66	Ω
		C_{ds}	0.63	pF
		L_f	2.8	nH
		L_0	3.419	nH
		C_x	-	F
		L_x	1.926	nH
Class E matching network	primary peaking amplifier			
		min R_{on}	2	Ω
		C_{ds}	0.84	pF
		L_f	1.798	nH
		L_0	2.39	nH
		C_x	-	F
		L_x	0.878	nH
Class E matching network	secondary peaking amplifier			
		min R_{on}	1	Ω
		C_{ds}	1.68	pF
		L_f	0.9	nH
		L_0	1.195	nH
		C_x	-	F
		L_x	0.439	nH
Two-stage matching network	main amplifier			
		C_{13}	0.380	pF
		C_{132}	0.271	pF
		L_{13}	1.155	nH
		L_{132}	1.106	nH
Transformer matching network	primary peaking amplifier			
		$k \cdot L_{11}$	1.265	nH
		C_p	2.001	pF
		n	1.95	
Transformer matching network	secondary peaking amplifier			
		$k \cdot L_{12}$	0.6327	nH
		C_p	4.017	pF
		n	2	
Coupled lines lumped network	-			
		L	0.224	nH
		C_M	1.011	pF
		C_G	0.4186	pF

Table J.1: Component values for the final design